

DTIC FILE COPY

4

AFGL-TR-87-0319  
ENVIRONMENTAL RESEARCH PAPERS, NO. 989

AD-A205 046

An Advanced System for Measurement of Transionospheric  
Radio Propagation Effects Using GPS Signals

G.J. BISHOP  
D.J. JACAVANCO  
D.S. COCO  
C.E. COKER  
J.A. KLOBUCHAR  
E.J. WEBER  
P.H. DOHERTY



13 November 1987



Approved for public release; distribution unlimited.



IONOSPHERIC PHYSICS DIVISION

**AIR FORCE GEOPHYSICS LABORATORY**

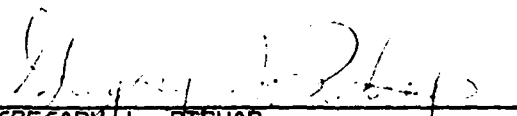
PROJECT LCDP

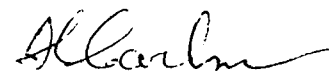
HANSCOM AFB, MA 01731

DTIC  
ELECTE  
FEB 17 1989  
S  $\alpha$  H D

89 2 16 192

"This technical report has been reviewed and is approved for publication."

  
GREGORY J. BISHOP  
Contract Manager

  
HERBERT C. CARLSON  
Branch Chief

FOR THE COMMANDER

  
ROBERT A. SKRIVANEK  
Division Director

This document has been reviewed by the ESD Public Affairs Office (PA) and is releasable to the National Technical Information Service (NTIS).

Qualified requestors may obtain additional copies from the Defense Technical Information Center. All others should apply to the National Technical Information Service.

If your address has changed, or if you wish to be removed from the mailing list, or if the addressee is no longer employed by your organization, please notify AFGL/DAA, Hanscom AFB, MA 01731. This will assist us in maintaining a current mailing list.

Do not return copies of this report unless contractual obligations or notices on a specific document requires that it be returned.

UNCLASSIFIED

SECURITY CLASSIFICATION OF THIS PAGE

## REPORT DOCUMENTATION PAGE

Form Approved  
OMB No. 0704-0188

1a. REPORT SECURITY CLASSIFICATION Unclassified			1b. RESTRICTIVE MARKINGS		
2a. SECURITY CLASSIFICATION AUTHORITY			3. DISTRIBUTION / AVAILABILITY OF REPORT Approved for public release; Distribution unlimited		
2b. DECLASSIFICATION / DOWNGRADING SCHEDULE			5. MONITORING ORGANIZATION REPORT NUMBER(S)		
4. PERFORMING ORGANIZATION REPORT NUMBER(S) AFGL-TR-87-0319 ERP, No. 989			7a. NAME OF MONITORING ORGANIZATION		
6a. NAME OF PERFORMING ORGANIZATION Air Force Geophysics Laboratory		6b. OFFICE SYMBOL (If applicable) LIS	7b. ADDRESS (City, State, and ZIP Code)		
6c. ADDRESS (City, State, and ZIP Code) Hanscom AFB Massachusetts 01731-5000			9. PROCUREMENT INSTRUMENT IDENTIFICATION NUMBER		
8a. NAME OF FUNDING / SPONSORING ORGANIZATION		8b. OFFICE SYMBOL (If applicable)	10. SOURCE OF FUNDING NUMBERS		
8c. ADDRESS (City, State, and ZIP Code)			PROGRAM ELEMENT NO. 62101F	PROJECT NO. LCDP	TASK NO. 6D
			WORK UNIT ACCESSION NO. 01		
11. TITLE (Include Security Classification) An Advanced System for Measurement of Transionospheric Radio Propagation Effects Using GPS Signals					
12. PERSONAL AUTHOR(S) Bishop, G.J., Jacavano, D.J., Coco, D.S.*, Coker, C.E.*, Klobuchar, J.A., Weber, E.J., and Doherty, P.H.**					
13a. TYPE OF REPORT Scientific Interim		13b. TIME COVERED FROM _____ TO _____	14. DATE OF REPORT (Year, Month, Day) 1987 November 13		15. PAGE COUNT 138
16. SUPPLEMENTARY NOTATION *Applied Research Laboratories The University of Texas at Austin, TX 78713-8029 **Physics Research Division Emmanuel College, 400 The Fenway Boston, MA 02115					
17. COSATI CODES			18. SUBJECT TERMS (Continue on reverse if necessary and identify by block number)		
FIELD	GROUP	SUB-GROUP	Ionospheric scintillation		
			Total electron content		
			Global positioning system		
19. ABSTRACT (Continue on reverse if necessary and identify by block number) An advanced sysytem for measurement of transionospheric radio propagation effects was developed, utilizing the TI-4100 four-channel Global Positioning System (GPS) receiver. During AFGL's Polar ARCS campaign at Sondrestrom, Greenland in February-March 1987, the system successfully measured ionospheric total electron content (TEC), phase scintillation, and amplitude scintillation on both GPS carrier frequencies, from up to four satellites simultaneously. This was the first time it has been possible to measure these parameters simultaneously, in multiple directions, in the high-latitude regions. Coupled with the simultaneous optical and incoherent scatter radar diagnostics obtained during the Polar ARCS campaign, these measurements significantly improve our capability to characterize high latitude ionospheric structures, particularly their temporal and spatial variation. Additionally, the development of this advanced system has contributed significantly to the technology base for specification of the Transionospheric Sensing System (TISS) for the Air Weather Service. The system can also be software upgraded to perform special navigation in addition to ionospheric measurements in airborne applications. — (12-1)					
20. DISTRIBUTION/AVAILABILITY OF ABSTRACT <input type="checkbox"/> UNCLASSIFIED/UNLIMITED <input checked="" type="checkbox"/> SAME AS RPT. <input type="checkbox"/> DTIC USERS			21. ABSTRACT SECURITY CLASSIFICATION Unclassified		
22a. NAME OF RESPONSIBLE INDIVIDUAL Gregory J. Bishop			22b. TELEPHONE (Include Area Code) (617) 377-3036		22c. OFFICE SYMBOL AFGL/LIS

## Preface

The authors would like to thank Dr. Herbert C. Carlson and Mr. W.K. Vickery who managed the Polar ARCS Campaign; SSgt Doug Carter and Sgt Terry Elthon for their assistance in installing and operating the instruments; and Mr. Al Bailey and MSgt Tony Coriaty for the use of their site facilities.

The research was partially funded by the AFGL Laboratory Commander's Discretionary Program IHWU LCDP6D01. ARL tasking was carried out under Naval Sea Systems Command Contract N00024-86-C-6134. Their final report, ARL:UT Ionospheric Monitoring System Performance Analysis, is included as the Appendix.



Accession For	
NTIS GRA&I	<input checked="" type="checkbox"/>
DTIC TAB	<input type="checkbox"/>
Unannounced	<input type="checkbox"/>
Justification	
By	
Distribution/	
Availability Codes	
Dist	Avail and/or Special
A-1	

## Contents

1. INTRODUCTION	1
2. APPROACH	2
3. SYSTEM MEASUREMENT CAPABILITIES AND LIMITATIONS	4
4. OBSERVATIONS	5
5. CONCLUSIONS	9
REFERENCES	11
APPENDIX	13
I Introduction	23
II AIMS Design Considerations	26
III Description of Hardware Components	35
IV System Operation	42
V Calculation of Derived Ionospheric Parameters	49
VI Mainframe Processing Software	61
VII AIMS Performance Evaluation	67
VIII Evaluation of Potential Aircraft Applications for AIMS	97
IX Summary	106

## Illustrations

- |    |  |   |
|----|--|---|
| 1. | All-Sky Images Illustrating Ionospheric Structures Observed During Sondrestrom Observations, with Symbols Marking Raypaths to GPS Satellites | 6 |
| 2. | Four Channel Relative TEC Measurement and Raypath Location During Four Hour Period Bracketing Optical Images                                 | 7 |
| 3. | Expanded Plot of Four Channel Relative TEC Measurement During Times of Optical Images  | 8 |

## Tables

- |    |  |   |
|----|--|---|
| 1. | Summarized AIMS Measurement Capability   | 4 |
| 2. | GPS Observations of Relative TEC Characteristic on Four Channels During Optical Observations | 5 |

# **An Advanced System for Measurement Of Transionospheric Radio Propagation Effects Using GPS Signals**

## **1. INTRODUCTION**

For over two decades, measurements of transionospheric radio propagation effects have been obtained from ground-based reception of satellite signals. Diurnal measurement of total electron content (TEC) has been obtained at middle and low latitudes by Air Weather Service (AWS) polarimeters monitoring geosynchronous communication satellites.<sup>1</sup> Amplitude scintillation has also been measured by monitoring the signal strength of such satellites. Phase and amplitude scintillation in high latitudes has been obtained by special phase-lock receiver monitoring of communication satellites in near-polar orbit.<sup>2,3,4,5</sup> Special satellites have been launched to facilitate

---

(Received for publication 29 October 1987)

1. Von Flotow, C.S. (1978) Ionospheric Forecasting at Global Weather Central, Proc. Ionospheric Effects Symposium: Effect of the Ionosphere on Space and Terrestrial Systems, 24-26 Jan, Arlington, VA.
2. Basu, S., MacKenzie, E., Basu, Su., Costa, E., Fougere, P.F., Carlson H.C., and Whitney, H.E. (1986) *250 MHz/GHz Scintillation Parameters in the Equatorial, Polar and Auroral Environments*, AFGL-TR-86-0070, ADA172211.
3. Basu, Su., Basu, S., Livingston, R.C., MacKenzie E., and Whitney, H.E. (1982) *Phase and Amplitude Scintillation Statistics at 244 MHz from Goose Bay Using a Geostationary Satellite*, AFGL-TR-82-0222, ADA124291.
4. Basu, Su., Basu, S., Livingston, R.C., Whitney, H.E., and MacKenzie, E. (1981) *Comparison of Ionospheric Scintillation Statistics from the North Atlantic and Alaskan Sectors of the Auroral Oval Using the WIDEBAND Satellite*, AFGL-TR-81-0266, ADA11187.
5. Mullen, J.P., MacKenzie, E., Basu, S., and Whitney, H.E. (1985) VHF/GHz scintillation observed at Ascension Island from 1980 through 1982, *Radio Sci.* **20**:357-365.

measurement to transionospheric propagation as well as acquire in-situ data.<sup>6,7</sup> The broadcast by these satellites of several coherent signals, widely spaced in frequency, has allowed phase and amplitude scintillation, as well as TEC to be measured. Navigation satellites, such as the Navy Navigation Satellite System (NNSS) and most recently Global Positioning System (GPS) have also been used for these measurements.<sup>8</sup>

Each of these major sources of measurements has its shortcomings: Polarimeter measurement of geosynchronous satellites is ineffective in the high latitudes since the ionospheric penetration point (if the satellite can be seen at all) is far south of the observation point. In addition the number of satellites with beacons usable for these measurements is dwindling. Phase scintillation measurements from the polar-orbit communication satellites lacking two-frequency coherent signals can not be made continuously and TEC is not available. The special satellites (WIDEBAND, HILAT, Polar BEAR) and the TRANSIT satellites are only visible for about ten minutes per pass every 2 or 3 hours, and thus cannot give full diurnal coverage.

The GPS satellites, however, will provide a fuller combination of capability and coverage for transionospheric measurements than any system previously available. With the full constellation in place, TEC, phase scintillation and amplitude scintillation will be obtainable anywhere in the world at all times, simultaneously from at least three and usually four satellites. For this reason, AWS has selected GPS technology as the basis of a new world-wide monitoring network, the Transionospheric Sensing System (TISS), to replace its polarimeters. The first systems utilizing GPS for these transionospheric measurements have been able to monitor one satellite at a time. The system described in this report is the first designed and built specifically for simultaneous monitoring of four GPS satellites for transionospheric measurements.

## 2. APPROACH

The objective of this effort was to significantly improve capability to measure ionospheric scintillation and TEC, and to apply that capability to characterizing the high latitude ionosphere. The advanced measurement system developed was based on state-of-the-art Global Positioning System (GPS) receiver, capable of monitoring signals from up to four GPS satellites simultaneously. A joint high latitude campaign was conducted with AFGL's Airborne Ionospheric Observatory (AIO) where measurements could be made in conjunction with diagnostics on the AIO, particularly the all-sky imaging system. The initial benefits sought from this campaign were the first high-latitude measurements of spatial distribution and variation of scintillation and TEC, the first

- 
6. Fremouw, E.J., Leadabrand, R.L., Livingston, R.C., Cousins, M.D., Rino, C.L., Fair, B.C., and Long, R.A. (1978) Early results from the DNA wideband satellite experiment-complex signal scintillation, *Radio Sci.* **13**:(No.1)167-187.
  7. Davies, K. (1980) Recent progress in satellite radio beacon studies with particular emphasis on the ATS-6 radio beacon experiment, *Space Sci. Reviews* **25**:357-430.
  8. Klobuchar, J.A., Bishop, G.J., and Doherty, P.H. (1985) Total Electron Content and L-Band Amplitude and Phase Scintillation Measurements in the Polar Cap Ionosphere, Proc. NATO AGARD Electromagnetic Wave Panel Symp: Propagation Effects on Military Systems in High Latitude Regions, paper 2-2, 3-7 Jun, Fairbanks, AK.



multidirectional comparison of transionospheric radio propagation effects with simultaneous optical measurements, and an initial experiment evaluating the multi-directional measurement capability as a means of detecting large scale plasma drift.

The GPS receiver acquired for this Advanced Ionospheric Measurement System (AIMS) was the Texas Instruments TI-4100 receiver. This receiver allowed four channel monitoring at more moderate cost compared to other multichannel receivers. Additionally, many of these receivers had already been successfully used in navigation and geodetic applications resulting in a significant body of experience with the technology and good assurance of capability. However, the more moderate cost of the receiver was at least partly due to the fact that its four channel capability was achieved via millisecond-scale time multiplexing of a single receiver channel. This time multiplexing ultimately made the control and data acquisition software more difficult as time shifts between the satellite signals varied with satellite position.

The TI-4100 receiver, unlike earlier receivers (such as the STI 5010 from Stanford Telecommunications Inc.) is entirely digitally controlled with all control inputs and data outputs travelling through one digital port. This structure enabled implementation of ionospheric measurements in software within the receiver, utilizing the digitally maintained satellite parameters therein. Thus, specialized external circuits were not required, but additional software functions were required.

Applied Research Laboratories (ARL) at the University of Texas at Austin was tasked to develop and evaluate AIMS. ARL had previously applied the TI-4100 to navigation applications, and had also made ionospheric measurements using the Navy Navigation Satellite System (NNSS) satellites. With their experience base ARL has a library of control and display software for the TI-4100 system, both for the receiver and its external processor. Design tradeoffs arrived at jointly by AFGL and ARL were necessary to arrive at data sampling rates and formats compatible with ionospheric measurement needs, TI 4100 capability, data port limitations, and potential future applications for airborne operation on the AIO. Considerable effort was required by ARL to develop data acquisition software that would maximally sample the receiver signals and not result in data losses due to the complexity of the TI-4100 time multiplexing scheme.

Working closely with AFGL, ARL developed the AIMS software, integrated software and hardware, and bench tested and calibrated the system at ARL. (A detailed description of the AIMS System and performance evaluation is given in the Appendix.) The system was shipped to AFGL for final testing, shakedown and operator training prior to the campaign in Greenland. Subsequently the AIMS was operated at Sondrestrom, Greenland for one month in February - March 1987 as part of AFGL's Polar ARCS campaign.

ARL developed AIMS bearing in mind the potential of using the system on the AIO. In this airborne application, precise navigation outputs would be desired, in addition to the ionospheric measurement, for proper alignment and interpretation of many experiments. ARL has evaluated the potential of AIMS for airborne use (Appendix) and concludes that operation without navigation outputs is feasible. However, to add the navigation outputs a significant rebuild of both receiver and external processor software would be required, in addition to a 33 percent reduction in data sampling rates. The impact and cost of this effort require further evaluation.

### 3. SYSTEM MEASUREMENT CAPABILITIES AND LIMITATIONS

Table 1 summarizes the bandwidths, sample rates and resolution of the measurements made by AIMS. Reconfiguring the receiver can change the bandwidth somewhat. Also, the sample rates could be significantly higher, but the limiting factor is the transmission of data across the TI 4100 digital port.

Table 1. Summarized AIMS Measurement Capability

Parameter	Bandwidth	Sample Rate	Data Resolution
Relative TEC (Phase)	6.0 Hz	8 1/3 Hz	0.04 to 0.11 TECU*
Absolute TEC	0.05 Hz	4 1/6 Hz	1.3 to 3.5 TECU*
Amplitude-L1	1 Hz	4 Hz	0.2 dB
Amplitude-L2	1 Hz	4 Hz	0.2dB

\*Variation linked to signal strength.

An evaluation of AIMS performance is presented in the Appendix. The system exhibits higher noise levels, slower sample rates and lower precision than the AFGL single channel system built around an STI-5010 receiver. These limitations are due primarily to the time multiplexed design and the limited data port of the TI-4100 receiver. A completely parallel four-channel system should exhibit performance as good as or better than the AFGL single-channel system.

Measurements of absolute TEC are impacted by two major error sources. Multipath<sup>9</sup> from the local environment of the antenna can cause cyclical errors of as much as  $\pm 20$  TEC units with periods of up to 10 to 15 minutes. (See data in the Appendix.) This error can be reduced by judicious antenna siting and using a mean absolute TEC from a time with limited multipath to reference concurrent relative TEC data.

A more serious error source is onboard offset in relative group delay (TEC) at the space vehicles. This offset is unique to each satellite and requires careful processing of several TEC data sets to define.<sup>10,11</sup> As these offsets are not firmly determined by the GPS community at this time, this report will give examples of only relative TEC measurements.

- 
9. Bishop, G.J., Klobuchar, J.A., and Doherty, P.H., (1985) Multipath effects on the determination of absolute ionospheric time delay from GPS signals, *Radio Sci.* **20**:388-396.
  10. Lanyi, G. E. (1986) Ionospheric Electron Content Prediction from SERIES/GPS Data, Proc. International Beacon Satellite Symposium, 9-14 June, Oulu, Finland.
  11. Lanyi, G.E. (1986) *Total Ionospheric Electron Content Calibration Using SERIES Global Positioning Satellite Data*, TDA Progress Report 42-85, pp. 1-12, Jet Propulsion Laboratory (JPL/NASA), Pasadena, CA.

#### 4. OBSERVATIONS

The Polar ARCS campaign more than met the objective of combining AIO optical diagnostics with high-latitude field test of AIMS. In addition to the AIO, the Sondestrom incoherent scatter radar and ground-based optical systems were simultaneously operated during several periods. As a result data was acquired which fulfilled the goals of obtaining the first high-latitude measurements of spatial distribution of scintillation and TEC, and the goal of multidirectional comparison of transionospheric radio propagation effects with simultaneous optical measurements. In many instances there was simultaneous radar data as well. The initial experiment evaluating the AIMS multidirectional measurement capability as a means of detecting large scale plasma drift was inconclusive due to lack of significant occurrence of the large scale plasma "patches" during the experiment period.

To illustrate the data obtained during Polar ARCS, Figure 1 shows all-sky images of ionospheric "auroral arc" structure obtained coincident with AIMS measurement. Table 2 gives the key to the symbols for the satellites tracked by the four AIMS channels, and a brief description of the observation on the relative TEC (phase scintillation) channel. Figure 2 shows relative TEC behavior

Table 2. GPS Observations of Relative TEC Characteristic  
on Four Channels During Optical Observations

Symbol	AIMS Tracking Channel	Observation on GPS Relative TEC Measurement
Triangle	1	Raypath is away from arc, TEC data is quiet but rises as satellite sets.
Circle	2	Arc moves through raypath, data shows small TEC variation about 1 TEC unit peak-to-peak.
Square	3	Raypath remains way from arc, data shows essentially no TEC variation.
Star	4	Raypath is within arc as satellite sets, data shows larger TEC variation: about 2 units peak-to-peak and a rise of 4 to 5 units from 'background'.

observed on the AIMS channels during the four hour period bracketing the optical measurements, while Figure 3 expands the same data during the key half hour. As summarized in Table 2, the observations show significant variation in ionospheric effect according to the region of observation. The two channels (1 and 3) observing in a position away from the region giving optical signature show quiet behavior and increasing TEC at low elevation angles, which would be more typical of mid-latitudes. The two channels observing in the "arc" signature region (2 and 4) show disturbed TEC conditions with variation of about one TEC unit ( $= 1 \times 10^{16}$  electrons/m<sup>2</sup>) peak to peak at high

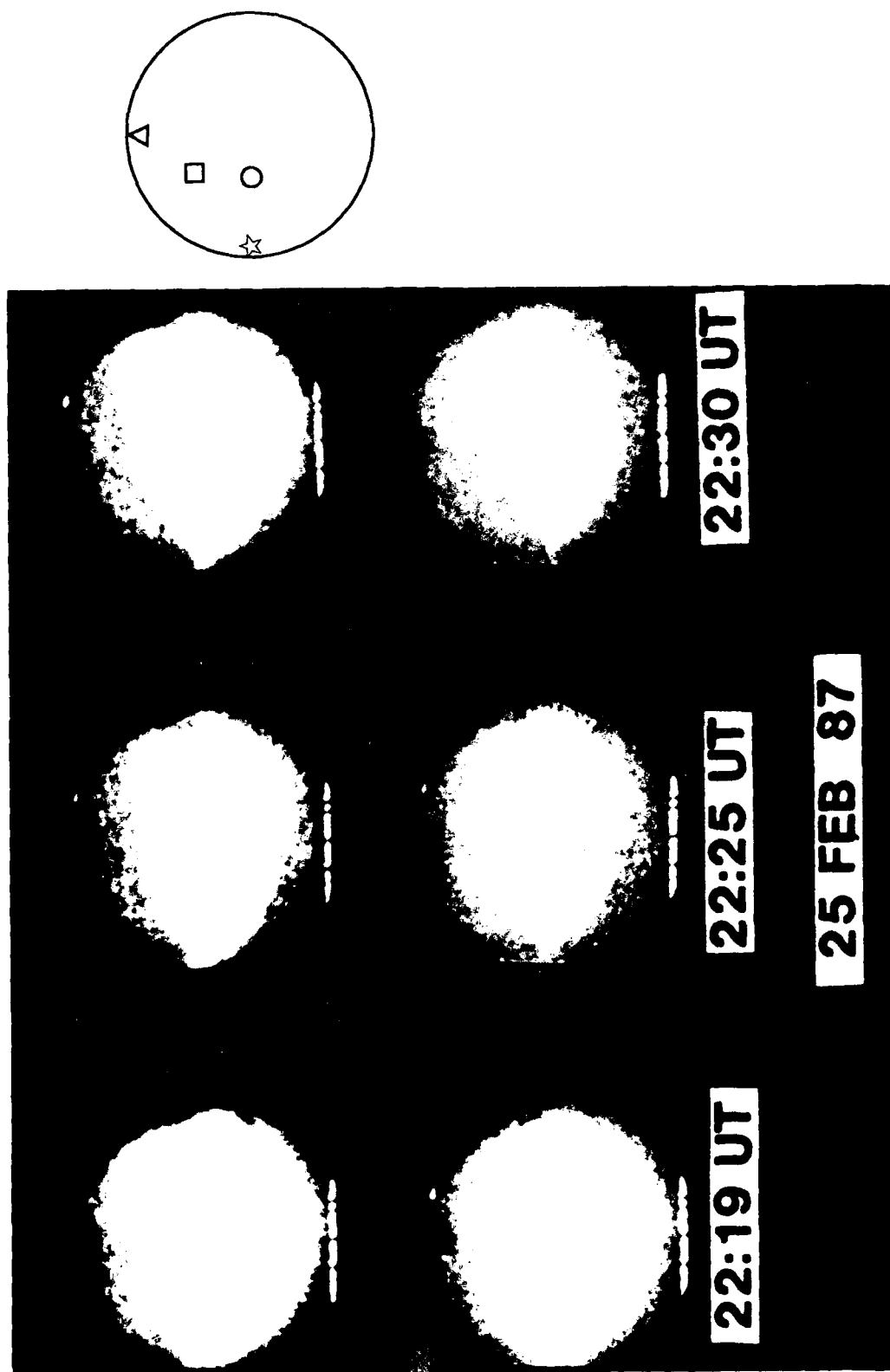


Figure 1. All-Sky Images Illustrating Ionospheric Structures Observed at Sondrestrom, with Symbols Marking Raypaths to GPS Satellites.

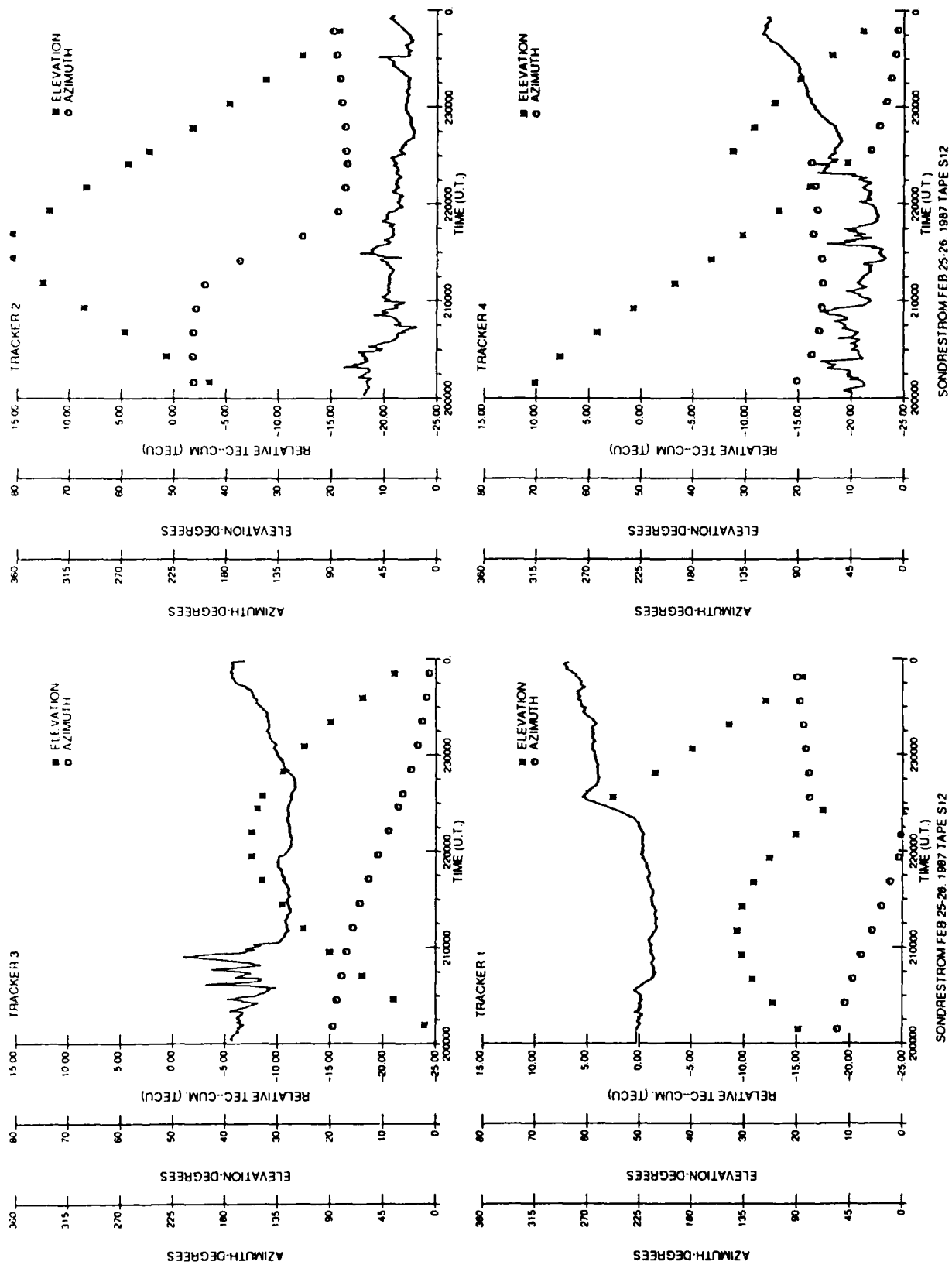
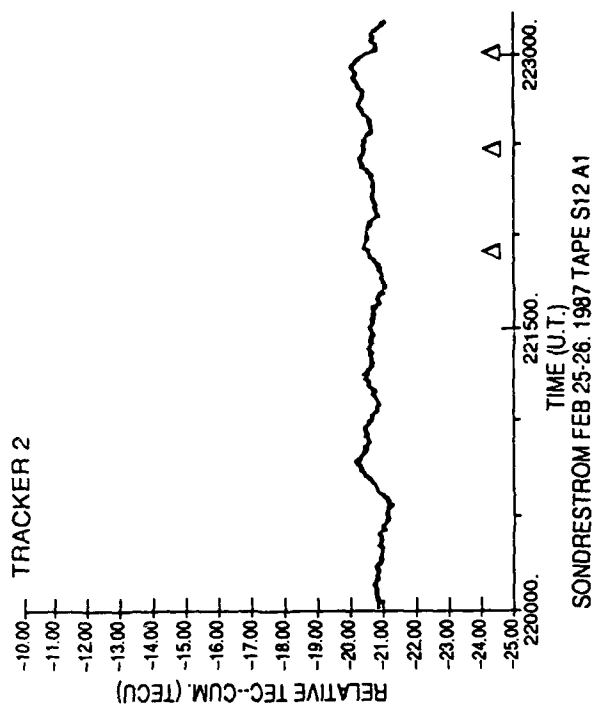
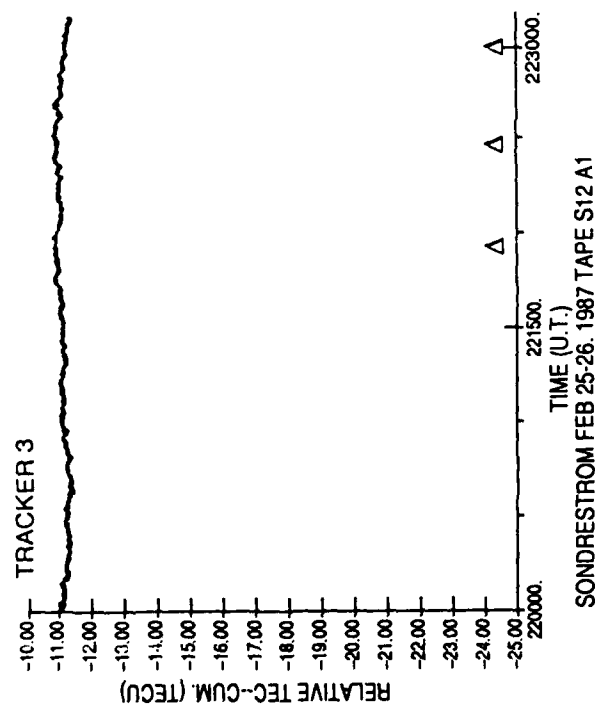
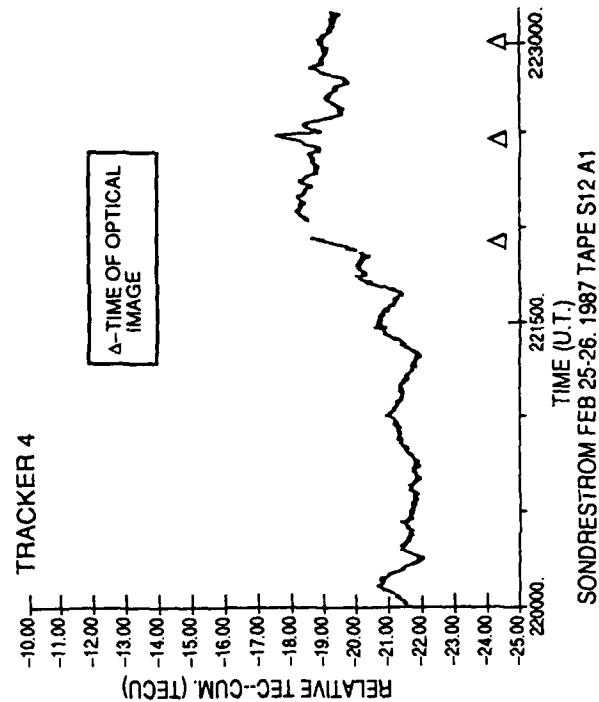


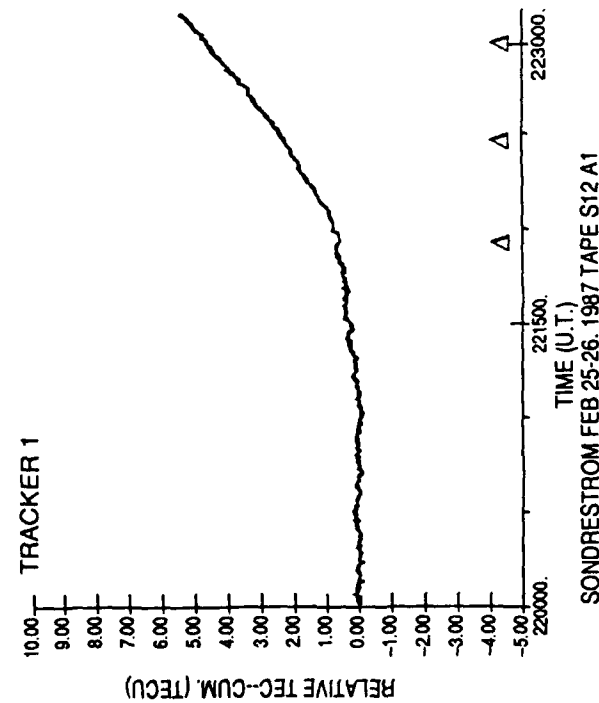
Figure 2. Four Channel Relative TEC Measurement and Raypath Locations During Four Hour Period Bracketing Optical Images.



### INSIDE OPTICAL FEATURE



### OUTSIDE OPTICAL FEATURE



HIGH  
ELEVATION

LOW  
ELEVATION

Figure 3. Expanded Plot of Four Channel Relative TEC Measurement During Times of Optical Images.

elevation angle ( $67^\circ$ ), and greater disturbance of up to 5 TEC units at low elevation angle ( $11^\circ$ ).

## 5. CONCLUSIONS

Development of the Advanced Ionospheric Monitoring System based on a four channel GPS receiver represents a major advance in capability to measure transionospheric scintillation and TEC. The four channel simultaneous measurement channels provide a new capability to characterize the spatial distribution and variation of scintillation effects.

Initial results obtained during the AFGL Polar ARCS campaign show the first high latitude measurements of spatial variation of TEC and scintillation and the first comparison of such data with all-sky optical diagnostics. The potential capability of this new system to measure large scale plasma drift could not be conclusively tested by the Polar ARCS data due to lack of occurrence of large scale plasma patches. For application to airborne operations, this new system can be applied to ionospheric measurement with only little modification but addition of navigation outputs will require significant software changes and sample rate reductions which may prove undesirable.

The difficulties in obtaining error free data with this receiver suggest that time multiplexed multichannel GPS receivers will be less attractive candidate technologies for supporting the Air Weather Service's Transionospheric Sensing System (TISS) development. Such receivers will probably deliver lower ionospheric data rates and will have significantly more complex software timing problems which can lead to data loss.

## References

1. Von Flotow, C.S. (1978) Ionospheric Forecasting at Global Weather Central, Proc. Ionospheric Effects Symposium: Effect of the Ionosphere on Space and Terrestrial Systems, 24-26 Jan, Arlington, VA.
2. Basu, S., MacKenzie, E., Basu, Su., Costa, E., Fougere, P.F., Carlson H.C., and Whitney, H.E. (1986) *250 MHz/GHz Scintillation Parameters in the Equatorial, Polar and Auroral Environments*, AFGL-TR-86-0070, ADA172211.
3. Basu, Su., Basu, S., Livingston, R.C., MacKenzie E., and Whitney, H.E. (1982) *Phase and Amplitude Scintillation Statistics at 244 MHz from Goose Bay Using a Geostationary Satellite*, AFGL-TR-82-0222, ADA124291.
4. Basu, Su., Basu, S., Livingston, R.C., Whitney, H.E., and MacKenzie, E. (1981) *Comparison of Ionospheric Scintillation Statistics from the North Atlantic and Alaskan Sectors of the Auroral Oval Using the WIDEBAND Satellite*, AFGL-TR-81-0266, ADA11187.
5. Mullen, J.P., MacKenzie, E., Basu, S., and Whitney, H.E. (1985) VHF/GHz scintillation observed at Ascension Island from 1980 through 1982, *Radio Sci.* **20**:357-365.
6. Fremouw, E.J., Leadabrand, R.L., Livingston, R.C., Cousins, M.D., Rino, C.L., Fair, B.C., and Long, R.A. (1978) Early results from the DNA wideband satellite experiment-complex signal scintillation, *Radio Sci.* **13**:(No.1)167-187.
7. Davies, K. (1980) Recent progress in satellite radio beacon studies with particular emphasis on the ATS-6 radio beacon experiment, *Space Sci. Reviews* **25**:357-430.
8. Klobuchar, J.A., Bishop, G.J., and Doherty, P.H. (1985) Total Electron Content and L-Band Amplitude and Phase Scintillation Measurements in the Polar Cap Ionosphere, Proc. NATO AGARD Electromagnetic Wave Panel Symp: Propagation Effects on Military Systems in High Latitude Regions, paper 2-2, 3-7 Jun, Fairbanks, AK.
9. Bishop, G.J., Klobuchar, J.A., and Doherty, P.H., (1985) Multipath effects on the determination of absolute ionospheric time delay from GPS signals, *Radio Sci.* **20**:388-396.
10. Lanyi, G. E. (1986) Ionospheric Electron Content Prediction from SERIES/GPS Data, Proc. International Beacon Satellite Symposium, 9-14 June, Oulu, Finland.
11. Lanyi, G.E. (1986) *Total Ionospheric Electron Content Calibration Using SERIES Global Positioning Satellite Data*, TDA Progress Report 42-85, pp. 1-12, Jet Propulsion Laboratory (JPL/NASA), Pasadena, CA.



**Appendix**  
**ARL:UT IONOSPHERIC**  
**MONITORING SYSTEM**  
**PERFORMANCE ANALYSIS**

Prepared by  
David S. Coco  
Clayton E. Coker

Applied Research Laboratories  
The University of Texas at Austin

June 1, 1988

## TABLE OF CONTENTS

### Page

LIST OF FIGURES

LIST OF TABLES

I. INTRODUCTION

II. AIMS DESIGN CONSIDERATIONS

A. Receiver Selection

B. Multiplexing Considerations

C. Data Rate Limitations

D. Bandwidth Selection

E. Satellite Position Information Requirements

III. DESCRIPTION OF HARDWARE COMPONENTS

A. GPS Receiver

B. External Processor

C. Peripherals

D. Racks and Power Conditioner

E. Information Flow in AIMS

IV. SYSTEM OPERATION

A. Receiver Software

B. Batch File Execution

C. Action Generation Programs

D. Ionospheric Data Collection and Processing Program

E. Start-Up Procedures

V. CALCULATION OF DERIVED IONOSPHERIC PARAMETERS

A. GPS Signal Measurements

B. Derived Ionospheric Parameters

C. Data Blocking and Storage

VI. MAINFRAME POSTPROCESSING SOFTWARE

VII. AIMS PERFORMANCE EVALUATION

- A. Laboratory Calibration Results
- B. Examples of Field Measurements
- C. System Limitations

VIII. EVALUATION OF POTENTIAL AIRCRAFT APPLICATIONS FOR AIMS

- A. Modifications to AIMS Required for Aircraft Applications
- B. Feasibility of Using AIMS to Provide GPS Navigation Information

IX. SUMMARY

APPENDIX

REFERENCES

## LIST OF FIGURES

<u>Figure</u>	<u>Page</u>
1	Information Flow in the TI 4100
2	Simplified Overview of TI 4100 Multiplexing
3	AIMS Physical Layout
4	Physical Connections between AIMS Hardware Components
5	Information Flow in AIMS
6	Simplified Diagram of Batch File Process for AIMS
7	Information Flow for IONPC
8	Nonsimultaneously Sampled GPS Data
9	Post Processing Software for AIMS
10	B-file Analysis Software
11	Time Delay and Signal Amplitude Calibration Configuration
12	Time Delay Variation with Delay Setting and Signal Attenuation
13	Time Delay Calibration
14	Signal Amplitude Calibration
15	Phase Scintillation Calibration Configuration
16	Phase Scintillation Calibration
17	Absolute TEC
18	TEC Noise Smoothed Over 30s Intervals
19	TEC Noise Sigmas Over 180s Intervals
20	Ionospheric Patch
Figures for Appendix A	
A1	Tracker 1 L2 C/No vs Time
A2	Tracker 1 Vertical TEC vs Time
A3	Tracker 1 Vertical TEC vs Time Smoothed Data
A4	Tracker 1 Relative TEC - Cumulative vs Time
A5	Tracker 1 Phase Reference Reset Times
A6	Tracker 2 L2 C/No vs Time
A7	Tracker 2 Vertical TEC vs Time

Figure

Page

A8	Tracker 2 Vertical TEC vs Time Smoothed Data
A9	Tracker 2 Relative TEC - Cumulative vs Time
A10	Tracker 2 Phase Reference Reset Times
A11	Tracker 3 L2 C/No vs Time
A12	Tracker 3 Vertical TEC vs Time
A13	Tracker 3 Vertical TEC vs Time Smoothed Data
A14	Tracker 3 Relative TEC - Cumulative vs Time
A15	Tracker 3 Phase Reference Reset Times
A16	Tracker 4 L2 C/No vs Time
A17	Tracker 4 Vertical vs Time
A18	Tracker 4 Vertical TEC vs Time Smoothed Data
A19	Tracker 4 Relative TEC - Cumulative vs Time
A20	Tracker 4 Phase Reference Reset Times

## LIST OF TABLES

<u>Table</u>		<u>Page</u>
I	High Speed Ionospheric Header Block	
II	High Speed Ionospheric Data Block	
III	AIMS Tape Storage Capacity	
IV	Data Block Types Used in AIMS	
V	Time Delay Calibration	
VI	Phase Reference Reset Summary	
VII	TI 4100 Final Tracking Bandwidths	
Tables for Appendix A		
A-1	Scenarios Used for 7-8 March 1987	

## ABSTRACT

The AIMS (Applied Research Laboratories, The University of Texas at Austin, ARL:UT, Ionospheric Monitoring System) is a transionospheric monitoring system which uses the Global Positioning System to measure ionospheric parameters in multiple directions simultaneously. The design, operation, and performance characteristics of AIMS are discussed in this report. In AIMS, a TI 4100 multiplexing receiver is controlled by an external processor which outputs ionospheric information to a variety of peripherals. System operation is controlled by the external processor with a minimum of operator interaction. Three ionospheric parameters are measured by AIMS: absolute total electron content (TEC), derived from pseudorange; relative TEC, derived from carrier phase; and amplitude scintillation index S4, derived from signal-to-noise.

Laboratory calibration experiments were performed to provide an estimate of the noise of measured parameters. Examples of AIMS measurements taken at Sondrestrom, Greenland in the Polar ARCS campaign are presented. Also, measurements from two different antenna environments are presented to demonstrate the effects of multipath on absolute TEC measurements. Limitations of the current system are discussed along with potential modifications for overcoming these limitations. The feasibility of using AIMS on board an aircraft as an ionospheric and navigation tool is also discussed.

## I. INTRODUCTION

Applied Research Laboratories, The University of Texas at Austin (ARL:UT), Ionospheric Monitoring System (AIMS) is a Global Positioning System (GPS) receiver based system that extracts the two frequency ionospheric correction from the GPS signals to provide an estimate of the ionospheric content along the line-of-sight from the satellite to the ground station. This system uses a TI 4100 receiver to track up to four GPS satellites simultaneously in a multiplexing mode. This allows the user to monitor four separate regions of the ionosphere simultaneously. Other GPS ionospheric monitoring systems have been developed in the past few years but they have been limited to tracking a single GPS satellite and thus only one region of the ionosphere could be monitored. The multiplexing feature of AIMS significantly increases the utility of GPS as a ionospheric monitoring tool.

AIMS provides three different types of ionospheric measurements to the user in a variety of formats. The first is the absolute total electron content (TEC) derived from the GPS pseudorange measurements. This absolute TEC is a measure of the number of electrons contained in a column extending from the ground station to the satellite. Although the GPS satellites are in orbit at approximately 22,000 km the majority of the electrons are concentrated in the region from 100-2000 km.

The second type of measurement is the relative TEC which is derived from the carrier phase measurements. The relative TEC simply gives a measure of the change in the absolute TEC as the line-of-sight sweeps through the ionosphere. This parameter is measured with a much higher data rate than the absolute TEC which allows characterization of the small scale ionospheric irregularities encountered in the ionosphere. The high data rate of the relative TEC allows measurement of the spectral characteristics of the irregularities and the resultant phase scintillations. The relative TEC has a maximum AIMS data rate of



8.33 Hz while the absolute TEC has a maximum data rate of 4.167 Hz. Also, because the relative TEC is derived from the more accurate carrier phase measurement, it provides a much more accurate estimate of the TEC variations than the absolute TEC measurement. The measurement noise of the absolute TEC is about 1.7 TECU ( $1 \text{ TECU} = 1 \times 10^{16} \text{ e/m}^2$ ), excluding multipath effects, while the relative TEC noise is about 0.04 TECU.

The third type of measurement is the signal strength of both GPS frequencies (L1 at 1575.42 MHz and L2 at 1227.6 MHz). These signal strength measurements provide a measurement of the amplitude scintillations produced by the ionospheric irregularities at the two GPS frequencies. The maximum AIMS data rate for the signal strength measurements is the same as that for the absolute TEC, 4.167 Hz. The widely used amplitude scintillation statistical parameter, S4 (Briggs and Parkin, 1963; Fremouw et al., 1978), is derived from the signal strength measurements.

These three ionospheric measurements are reported in a variety of formats. The ionospheric parameters can be displayed on a strip chart recorder in realtime and also recorded on 9-track tape for postprocessing. In addition, a statistical summary is output to a printer for realtime monitoring purposes.

This report gives an overview of the AIMS design, operation, and system performance. Section II discusses the major AIMS design considerations. Section III presents a general overview of the AIMS hardware components and Section IV provides a brief description of the system operation. The derivation of the AIMS ionospheric parameters from the GPS measurements is described in Section V. Mainframe postprocessing software for AIMS data is outlined in Section VI. In Section VII, the results of the laboratory calibrations for AIMS as well as some early

field measurements are presented. Section VIII discusses the feasibility of using AIMS in potential aircraft applications, and Section IX gives an overall summary.

## II. AIMS DESIGN CONSIDERATIONS

A major goal in developing AIMS was to expand the capability of ionospheric monitoring using GPS by tracking multiple satellites simultaneously. This allows simultaneous monitoring of different areas of the ionosphere so that a more complete picture of various ionospheric phenomena can be obtained. Some of the major design goals for AIMS were to

- (1) track at least 4 satellites simultaneously;
- (2) sample phase and signal strength at the highest data rate possible, with adequate bandwidths;
- (3) sample pseudorange at a data rate of about 10-60 s;
- (4) minimize the noise contributions to all three parameters;
- (5) choose tracking parameters and other parameters to maximize the robustness of the system; and
- (6) minimize programming requirements by making use of pre-existing software whenever possible.

This section discusses some of the design considerations that were important in meeting these design goals. These considerations include receiver selection, multiplexing considerations, data rate limitations, bandwidth selection, and satellite position information requirements.

### A. Receiver Selection

The TI 4100 was chosen as the GPS receiver for several reasons. The multiplexing design of the receiver allows simultaneous tracking of up to 4 satellites without introducing interchannel biases. The measurement noise levels of this receiver have been well documented (Coco and Clynch, 1986) and the receiver has undergone extensive laboratory and field testing. Another important consideration was the availability of the TI 4100 receiver when AIMS was being designed. Many other potentially suitable receivers were not yet in the production stage.

The flexibility of the software available for the TI 4100 was another major factor in its selection. There are three major software packages available for the TI 4100: the TI Navigator software, supplied by TI; GESAR geodetic surveying software, developed as the primary field surveying package for government applications; and CORE software, developed by ARL:UT to serve as an interface between the TI 4100 and a controlling external computer for a variety of applications. The CORE software package was chosen for the AIMS system because it provided the flexibility required for the various AIMS design features. Several modifications to CORE, however, were required to implement these design features. These modifications are discussed in the following sections.

#### B. Multiplexing Considerations

To understand some of the design considerations that arise from the multiplexing features of the TI 4100, it is necessary to briefly discuss how the actual pseudorange and phase measurements are made inside the receiver. In Fig. 1 the information flow for the TI 4100 is shown with the horizontal dotted line in the center separating the hardware section from the software. The signals are passed from the antenna through separate L1 and L2 filters and are then down converted. A random noise source, called the T-Code, is added and then later removed to overcome possible jamming effects. The signals are mixed with the carrier to separate the carrier from the code and then are processed through two separate channels, one for the carrier and the other for the code. After filtering and sampling, the in-phase and quadrature components are passed to the tracking loops. The output of the tracking loops are the Doppler and pseudorange values. These values are used in the propagators to provide values to complete the loop.

A simplified overview of the multiplex timing concept is illustrated in Fig. 1. The standard navigation tracking data is obtained by the method shown in Fig. 2a, while the AIMS ionospheric data is obtained by

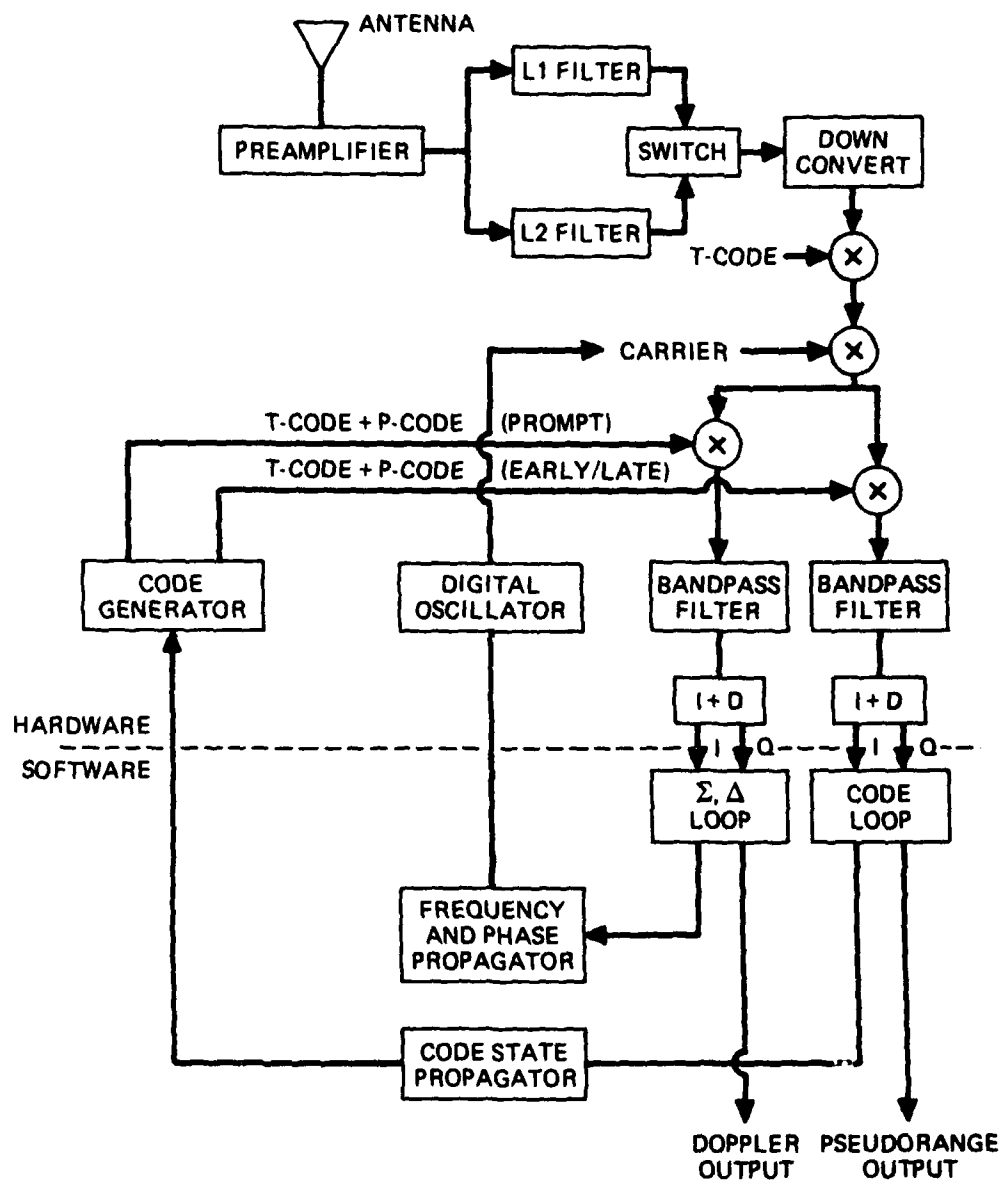


**FIGURE 1**  
**INFORMATION FLOW IN THE TI4100**

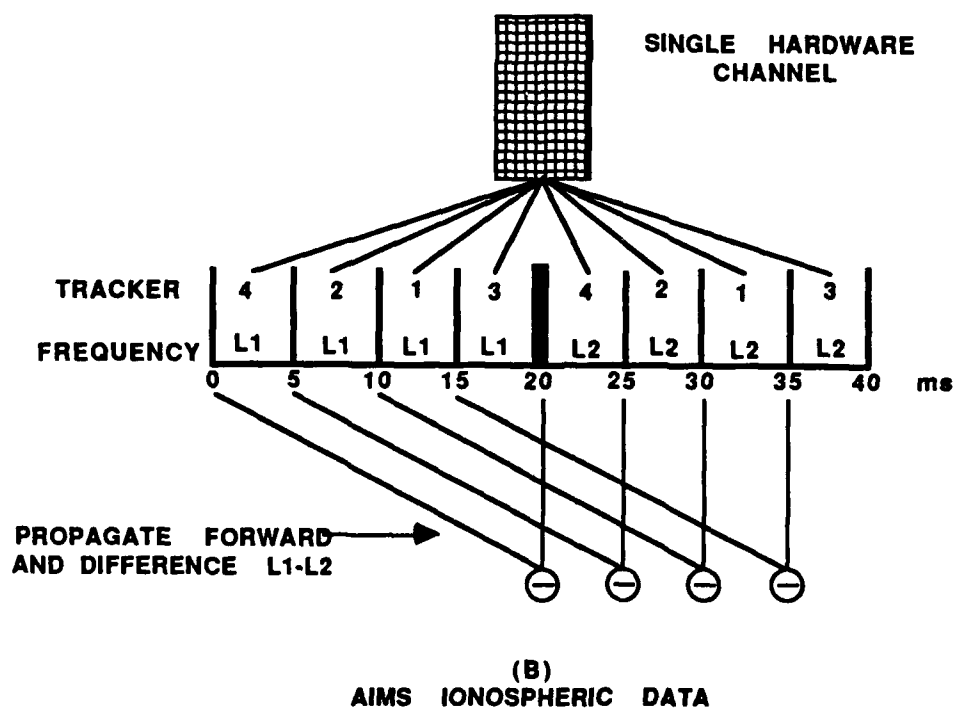
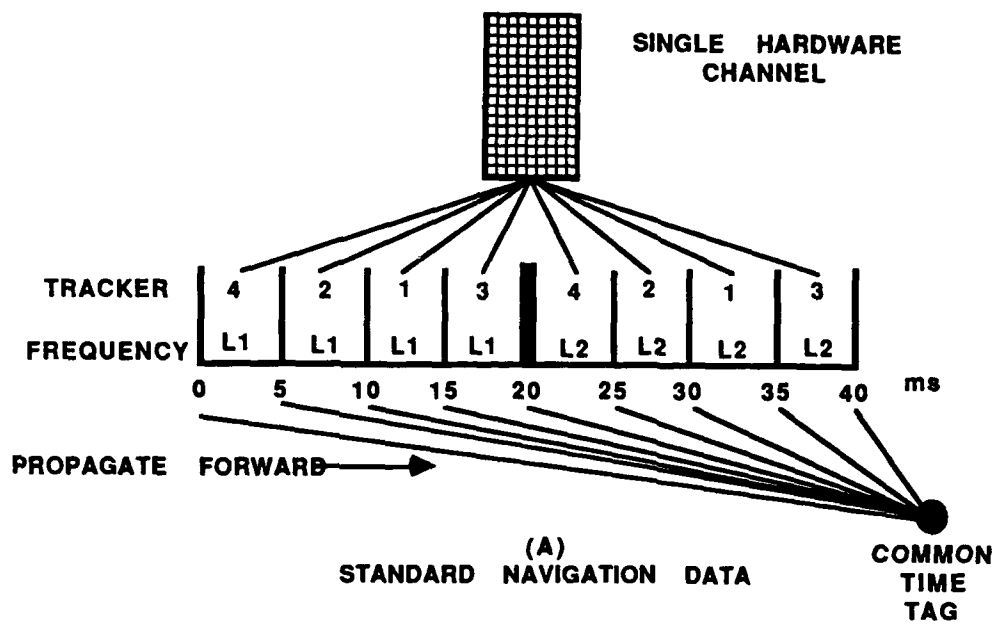


**FIGURE 2**  
**SIMPLIFIED OVERVIEW OF TI 4100 MULTIPLEXING**

the method shown in Fig. 2b. In both methods data from all four data trackers from one frequency are sampled once in 20 ms. For each tracker the data is sampled for 5 ms dwell period. The other frequency is sampled in the next 20 ms interval so the two frequency measurements for a single tracker are nominally separated by 20 ms. The order in which the trackers are sampled is changed periodically to avoid dwelling on a 50 Hz data bit edge. This reordering, called a MUX (multiplexing increment) bias change, occurs randomly but on the average about once every 20 min under normal tracking conditions. In the satellite acquisition stage, however, the MUX bias can change more rapidly.

The standard navigation data are propagated forward to a common time tag before they are passed to the user. These standard navigation data at common time tags are only available at a maximum data rate of 1 Hz due to the structure of the software. In order to access the data at a higher rate, the standard propagator was bypassed and a modified propagator was implemented as shown in Fig. 2b. This modified propagator propagates the measurement forward 20 ms to the time of the next measurement and differences the two to obtain the ionospheric measurement. The four ionospheric measurements are not exactly simultaneous but the offsets are not important to ionospheric applications.

Both the standard and modified propagators use the carrier frequency measurement to propagate the measurements. TI claims that the error produced by their propagation is negligible compared to other error sources. ARL:UT tests of the modified propagator scheme also show the errors are negligible.

One important tradeoff of multiplexing is that a receiver operated in a four satellite multiplex mode will lose phase lock approximately 6 dB sooner than if it were tracking one satellite continuously. This effect could be alleviated somewhat in the AIMS system by choosing

alternate tracking bandwidths for improved tracking performance. The TI 4100 could also be operated in a non-multiplexing mode to track a single satellite continuously. The tracking performance of AIMS has proved adequate in a variety of environments so neither of these alternatives have been implemented.

### C. Data Rate Limitations

One of the major design goals of AIMS was to achieve the highest data rate possible for carrier phase in order to characterize small scale ionospheric irregularities. This requires that the corresponding bandwidth be adequate to prevent aliasing. In general, it is necessary to achieve a data rate at least twice as large as the relevant bandwidth to satisfy Nyquist sampling criteria. The limiting factor for phase measurements in AIMS is the data rate.

The CORE software version available prior to development of AIMS output the pseudorange and phase measurement at a maximum rate of one complete sample (4 satellites/2 frequencies) per second (1 Hz). The TI 4100, however, is capable of acquiring data internally at a data rate of one complete sample per 40 ms (25 Hz). The data throughput at the TI 4100 external interface, however, is not sufficient to output all of the standard phase and pseudorange measurements at 25 Hz. It was possible to increase the carrier phase data rate beyond 1 Hz by changing both the quantity and format of the data that flowed through the interface. A maximum data rate of one complete sample of ionospheric phase data (4 satellites) per 120 ms (8.33 Hz) was proven feasible.

To achieve this data rate for phase measurements, CORE had to be modified in several ways. First, the L1/L2 phase differences were output rather than the individual parameters for each frequency. This required that the L1 and L2 measurements be propagated to a common epoch and



differenced inside the TI 4100. Second, a different data blocking format was developed to accommodate the high data rate.

One important consequence of the decision to output only the L1/L2 differences from the TI 4100 is that future security restrictions will be reduced. More stringent security restrictions may be required for systems capable of determining platform positions at a high data rate than for systems without this capability. Because position information is not available at the high data rate in AIMS the security restrictions may be less severe. The modified version of CORE remains capable of outputting the undifferenced pseudorange and phase data, when the differenced data is not being output, but is limited to a 1 Hz rate.

The data rate requirements for the pseudorange (absolute TEC) and signal strength measurements were easier to satisfy than for phase. The pseudorange measurements are only needed often enough to characterize the slow trends in the TEC. A bandwidth of 0.05 Hz was chosen which would require a 10 s data rate to satisfy the Nyquist sampling criteria. It would be desirable to sample the signal strength at a rate comparable to the phase but the sampling is limited by the effective bandwidth available, which is about 1 Hz. The structure of the data blocking fixes the pseudorange and signal strength measurement data rates to one half the phase data rate so that a maximum rate of 4.167 Hz is possible for both measurements. This data rate oversamples both pseudorange and signal strength but appropriate averaging in postprocessing can remove the aliasing effects.

#### D. Bandwidth Selections

The TI 4100 provides the user with the capability of modifying the tracking bandwidths and loop orders. The user can select bandwidths and loop orders for the delay (pseudorange) and carrier phase loops from a table of preset values. Instead of two separate tracking loops for the

two frequencies, there are separate tracking loops for the sum ( $L1 + L2$ ) and difference ( $L1 - L2$ ) frequencies to reduce the noise. The bandwidths of primary interest to this application are the difference loop bandwidths for the delay (pseudorange) and carrier tracking loops. The bandwidths allowed for delay range from 0.05-3 Hz, while those for the carrier range from 0.4-6 Hz. The bandwidth for signal strength is fixed at 1 Hz and cannot be modified by the user.

It was decided to maximize the carrier difference loop bandwidth and select the other parameters to optimize tracking performance. This was feasible because even the lowest delay bandwidth of 0.05 Hz was suitable for absolute TEC measurements. A series of experiments using different sets of parameters were conducted to select the set which provided optimum tracking performance.

#### E. Satellite Position Information Requirements

There are two separate requirements for satellite position information in the AIMS system. The first requirement is to provide an estimate of Doppler frequency shift to aid in satellite acquisition. This requirement is embedded in the program control software in the external processor. This is satisfied by collecting an almanac from the GPS message data and storing it for future use.

The second requirement is to have a rough satellite position available at each measurement time epoch to convert the slant TEC to vertical and to generate an ionospheric intercept position. This satellite position is needed in both realtime, within the external processor, and in postprocessing. This requirement is satisfied in realtime by using the current almanac. In postprocessing either the ephemeris or almanac information could be used since both are written to tape. The ephemeris was chosen to simplify the necessary programming, but the program could be easily modified to use the almanac.

There is no need for a precise knowledge of the satellite position but if the satellite almanac or ephemeris is missing or corrupted AIMS operation will be affected.

### III. DESCRIPTION OF HARDWARE COMPONENTS

The various hardware components of AIMS are discussed in this section. In brief, a TI 4100 GPS receiver tracks the satellites and provides the ionospheric measurements to an external processor. This external processor controls the TI 4100 functions and also outputs the ionospheric measurement information to three peripheral devices: a 9-track tape drive, a strip chart recorder, and a printer. The system status is displayed on a monochrome monitor. The AIMS system also includes a power conditioner, a power supply for the TI 4100, and two racks to hold the components. The physical layout of the AIMS is shown in Fig. 3.

Figure 4 illustrates the fundamental power and data connections between the major AIMS hardware components. The components that require ac power are connected to the power conditioner via a power strip. A brief description of each major component is given below followed by a discussion of the overall information flow in the system.

#### A. GPS Receiver

The GPS receiver/antenna system is a TI 4100 GPS receiver (RAM version) with the standard TI 4100 omnidirectional antenna. It receives signals from up to four satellites via the antenna, decodes and processes the signals, and sends the resulting data to the external processor. The receiver is connected to the antenna by either 200 ft of standard rf cable or up to 400 ft of low-loss rf cable. The GPS signals travel along the rf line along with 12 Vdc power for the preamplifier located in the base of the antenna. An optional built-in-test (BIT) line can be used by the receiver to test the entire receiver system except for the antenna element power to preamp. This link is not required under normal AIMS operations. The receiver is also connected to the external processor from the recorder port (GPS data line) and the other J2 port

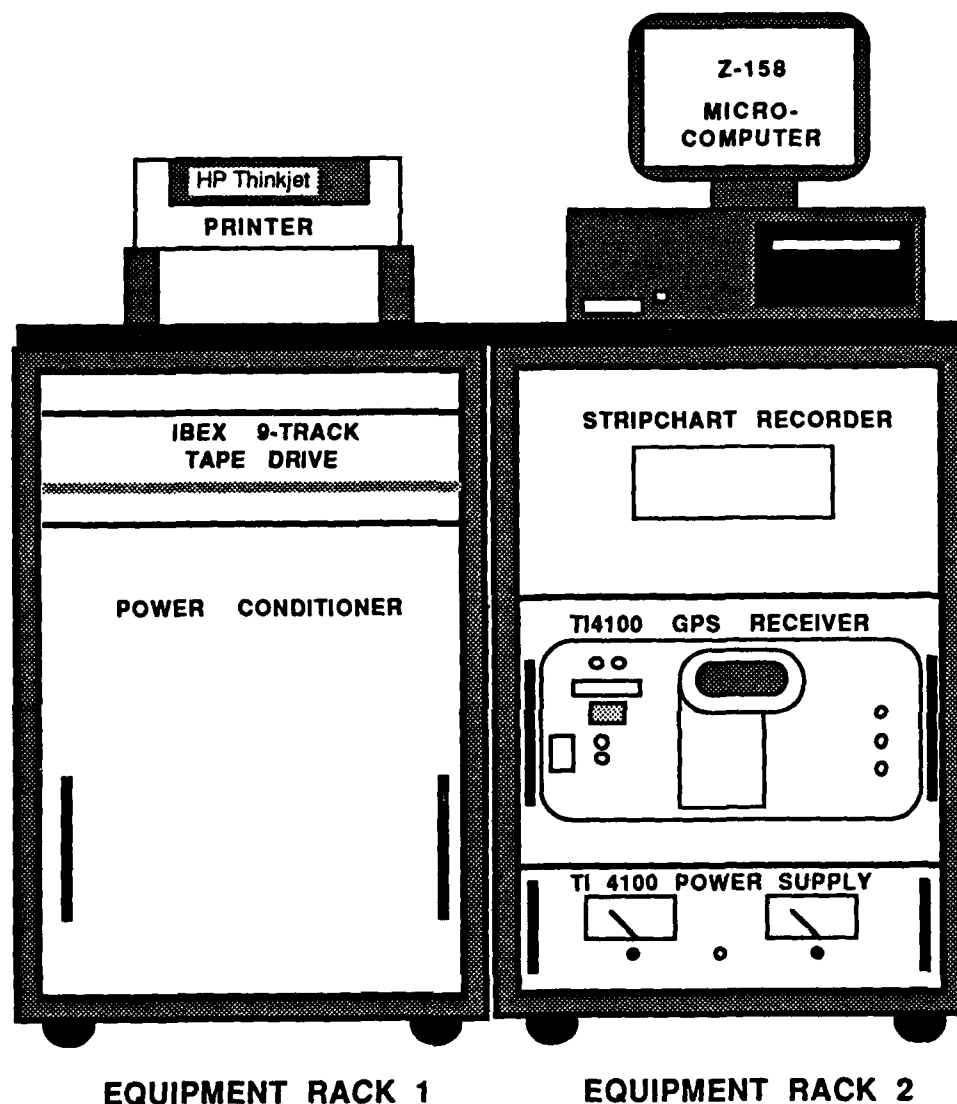


**FIGURE 3**  
**AIMS PHYSICAL LAYOUT**

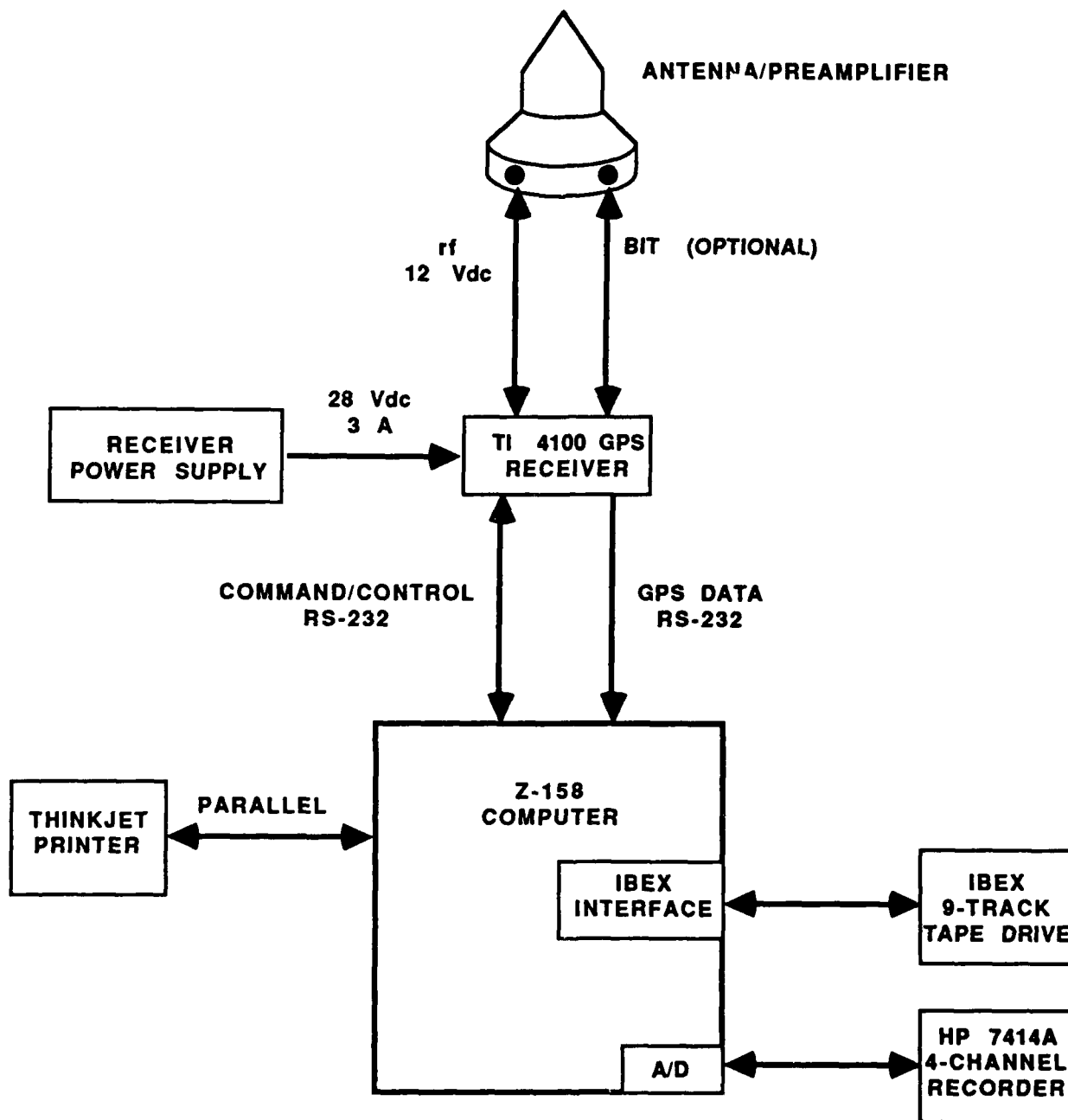


**FIGURE 4**  
**PHYSICAL CONNECTIONS**  
**BETWEEN AIMS HARDWARE COMPONENTS**

(command/control line) via RS-232 lines. The receiver is powered by 28 Vdc from a Lambda power supply. The receiver can also be connected to an external oscillator; however, this is not needed for ionospheric measurements.

#### B. External Processor

The external processor has four major functions: to issue satellite tracking commands to the receiver, to receive and process the GPS ionospheric measurements from the receiver, to output ionospheric information to the various peripherals, and to output status information to the monitor. Each of these functions is discussed in more detail later. To execute these functions the basic microcomputer requires a variety of accessories. A list of the major accessories is given below along with some of their more important functions.

- 1) Two serial ports - to connect with the receiver
- 2) Parallel port - to connect with printer
- 3) Clock/calendar card - used for rough timing purposes
- 4) 20 MByte hard drive (hardcard) - expanded memory simplifies main program execution and can be used for auxiliary data storage
- 5) Two floppy drives - used to load software, only one required
- 6) 512 kBytes additional memory (768 kBytes total) - required memory for main program execution
- 7) 8087-2 math co-processor - increased processing speed required for realtime computations
- 8) IBEX interface - required to interface with IBEX 9-track drive
- 9) Digital-to-analog card - required to interface with strip chart recorder

### C. Peripherals

The tape drive is an IBEX TS-100 9-track tape subsystem and is used to record the data received by the external processor and certain messages about the system generated by the external processor. Several tape utility commands, which are issued from the external processor, are available for the IBEX tape drive. These commands control archival/retrieval of data and programs, tape positioning, and a tape scan utility function. The ionospheric data on the tape cannot be read back to the external processor with the present system, but this feature could be easily implemented. These utility functions are provided in the IBEX software utility package which is stored on the external processor.

The strip chart recorder is an HP 7414A 4-channel analog recorder and is used to record realtime ionospheric measurements selected by the operator. It is connected to the D/A card in the external processor via an ARL:UT designed direct current cable. There is a one-to-one correlation between the four trackers of the receiver and the four strip chart channels; information recorded on the *i*th channel corresponds to the satellite being tracked on the *i*th tracker. On/off control over the strip chart motion and time marks are provided through the external processor. This is accomplished by the remote on/off box built by ARL:UT which connects the strip chart recorder to the external processor.

The printer is an HP Thinkjet Personal Printer and is used to record ionospheric parameter statistics, information about the tracking session, and error messages.

### D. Racks and Power Conditioner

Power is supplied to all the components through a 2 kVA Topaz Line 2 power conditioner. It is connected to standard 120V/60 Hz external power



source through a connection in the rack. The two racks are joined together and covered by a tabletop. As part of the rack system, a blower is located behind the GPS receiver to prevent overheating.

#### E. Information Flow in AIMS

The basic flow of information in AIMS is presented in Fig. 5. The rf signals are sent from the antenna to the GPS receiver where they are sampled in the multiplexing scheme described earlier and passed on to the external processor in what is called the raw data format. This raw data format contains the L1/L2 differences for pseudorange and phase and the C/No values for L1 and L2. The data are written directly to 9-track tape in this format.

This raw data format must be processed to generate the derived ionospheric parameters, which are the absolute TEC, relative TEC, and signal-to-noise (C/No) values in proper units and format for display. This processing takes place both in the mainframe postprocessing software and in the external processor in realtime. The derived ionospheric parameters generated in realtime are output to the strip chart recorder; a statistical summary of the parameters is also output to the printer. The external processor receives user commands from the keyboard and, in turn, controls the GPS receiver via a command and control line. The external processor monitor is used to display realtime status information about the satellites being tracked.

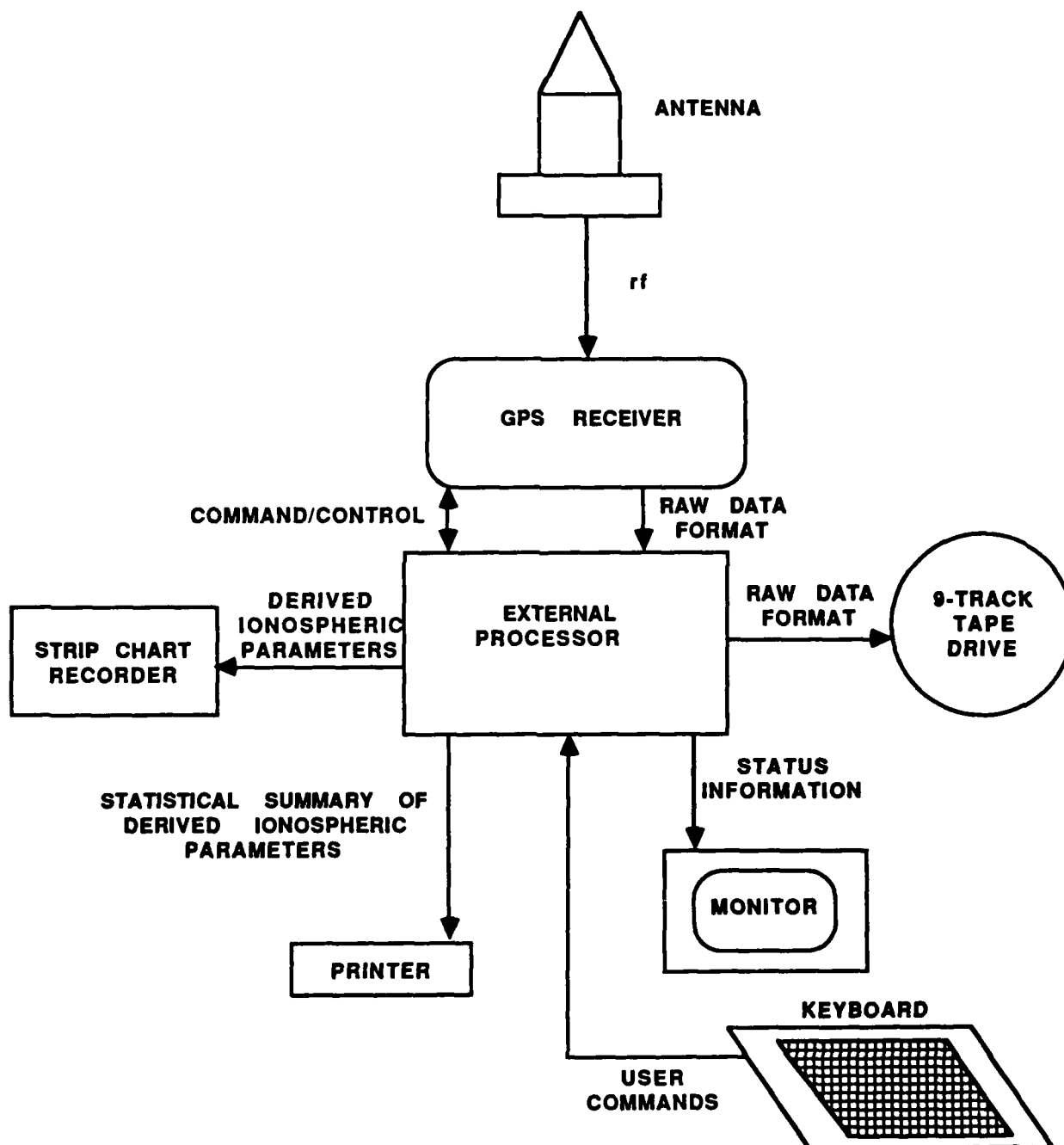


**FIGURE 5**  
**INFORMATION FLOW IN AIMS**

#### IV. SYSTEM OPERATION

The external processing software system is built around components from two similar systems developed by ARL:UT: the Large Ship System (LSS) and the Basic External Processor Program (BEPP). The major difference between these three software systems (LSS, BEPP and AIMS) is the type of processing of the GPS information performed inside the external processor and the type and format of data output. The three systems share the same basic structure and many of the same subroutines. In particular, the LSS, BEPP, and AIMS software systems all use the technique of pseudo multi-tasking by using a background task scheduler within the program execution loop. This allows low frequency tasks, such as status checking of the receiver and keyboard handling, to be executed concurrently with high frequency, time consuming data processing tasks.

Most of the system operation functions are controlled by the external processor. A few of the important operation functions controlled by the external processor are

- (1) downloading CORE software into the GPS receiver,
- (2) generating and updating the tracking scenario,
- (3) issuing commands to the receiver to control satellite tracking and signal processing,
- (4) generating derived ionospheric parameters from the raw data format,
- (5) outputting data to peripherals, and
- (6) monitoring system for problems and outputting status.

Downloading the CORE software is performed once before the main program IONPC begins execution. The other functions are executed by IONPC on a recurring basis.

#### A. Receiver Software

The receiver software (CORE 20.9) is a special version of the CORE software developed for AIMS. This software interprets and responds to commands issued from the external processor. The primary functions of CORE are to acquire and track satellites, process the GPS signals to generate the raw data format, output this raw data format to the external processor, and issue status and error messages. The timing constraints of the receiver do not allow the data processing to be conducted concurrently with satellite acquisition. Therefore, when the receiver is in the acquisition stage, standard GPS navigation data are output at a 6 s data rate. When acquisition is complete, the high speed ionospheric data is output. This constraint means that if one or more satellites fall out of track the high speed ionospheric data stream must be interrupted in order to reacquire.

#### B. Batch File Execution

Once the receiver software is loaded and all input parameter files contain the correct information, system operation is begun by executing a batch file. Execution of the batch file invokes a recurring sequence of programs which operates the system. Figure 6 illustrates this process. The sequence of programs entitled Action Generation Process are responsible for generating and updating the scenario of satellites to be tracked. The program IONPC is responsible for issuing commands to the receiver to control satellite tracking and signal processing, generating derived ionospheric parameters from the raw data format, outputting data to peripherals, monitoring the system for problems, and outputting status information.

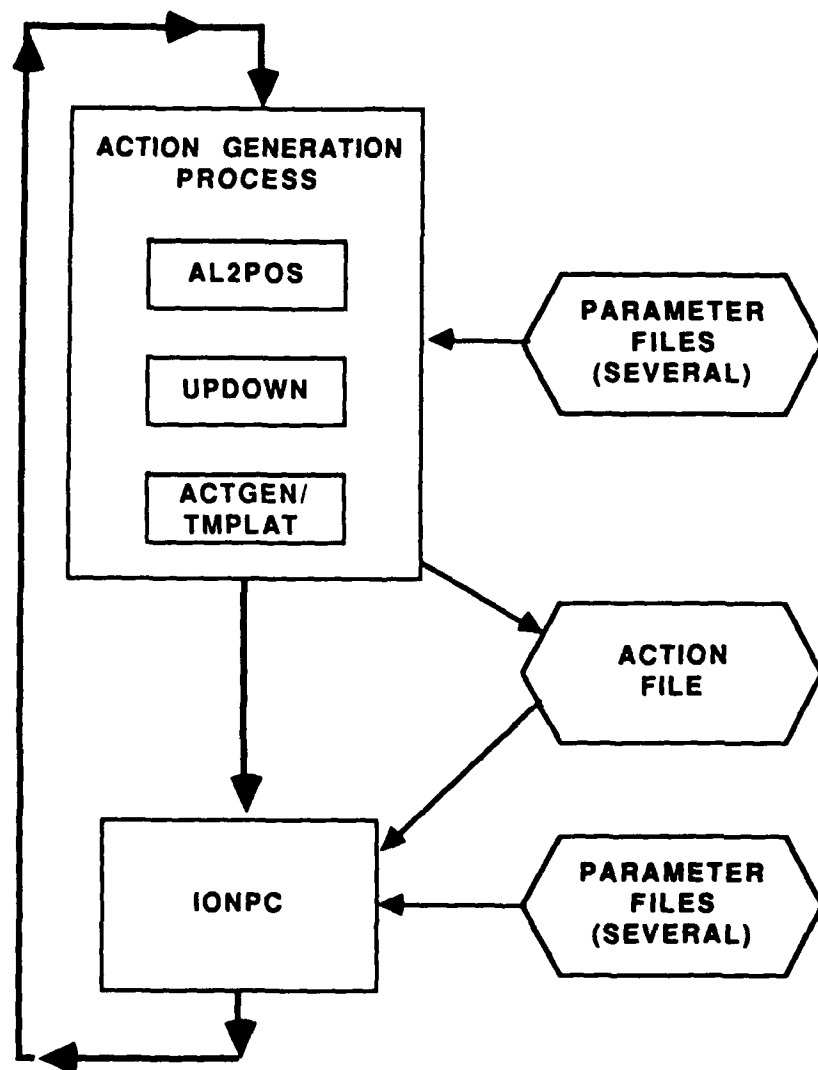


**FIGURE 6**  
**SIMPLIFIED DIAGRAM OF BATCH FILE PROCESS FOR AIMS**

### C. Action Generation Programs

The action generation process is accomplished by executing the programs AL2POS, UPDOWN, and ACTGEN/TMPLAT. Parameter files containing the station position and other parameters are used as input to these routines and can be modified by the operator. AL2POS computes the location of all active satellites at 15 min intervals; UPDOWN computes the rise and set times of the satellites from the tables prepared by AL2POS and the station's position; and ACTGEN/TMPLAT computes the tracking scenario controls to be used by the program IONPC.

ACTGEN and TMPLAT provide two different methods of computing a tracking scenario. ACTGEN automatically selects the satellites to be tracked based on the optimum position dilution of precision (PDOP) value. This option was developed for navigation purposes and presents several limitations when used for ionospheric monitoring purposes. The main limitations are that a minimum of two satellites must be tracked and the scenario can change every 15 min if the PDOP values are changing rapidly.

To provide more control over satellite selection, a new program TMPLAT was developed to replace ACTGEN. This program simply updates an existing scenario by changing the times by the appropriate amount (4 min/day) to make the scenario apply to the current day. This allows the user to manually produce one scenario and reuse the same scenario on subsequent days. This scenario generation program is used for most applications of AIMS. The main limitation of this method is that it does not account for satellite motion outside of the 4 min/day propagation. If the user has reason to believe that a satellite is being moved from its current orbital position, then a new scenario should be generated from a current almanac as often as necessary. As a standard operational procedure, it is suggested that a new scenario be generated from a current almanac once a week to insure against changes in satellite orbit positions.

#### D. Ionospheric Data Collection and Processing Program

The main driver program for data collection, processing, and output is IONPC. The information flow for this program is given in Fig. 7. The system is initialized and begins to collect standard 6 s navigation data using the system definition parameters stored in several parameter files. These data are output to tape in the raw data format and then the system is checked to see if all the requested satellites are in track. If all the requested satellites are in track, then high speed ionospheric data collection begins; if all the satellites are not in track, then standard data collection continues until this condition is satisfied.

After the high speed ionospheric data are collected, the data are processed to generate the derived ionospheric parameters using the equations in Section V. These parameters are output to the strip chart recorder and statistics of the parameters are output to the printer. Background tasks are performed on a time available basis using a background scheduler positioned within the realtime processing loop. The data collection loop continues until the user stops the system. Both standard navigation data and the high speed ionospheric data are output to tape, but the two data types cannot be collected concurrently.

The operator can issue a variety of commands during program execution. These commands can modify the scenario, the type of information sent to the strip chart recorder, the bandwidth selections, the time interval for statistics calculations and many other parameters.

#### E. Start-up Procedures

Several steps must be taken to begin using AIMS. From a cold start (all equipment off) the procedure takes about 45 min. Most of this time is taken downloading the TI 4100 receiver. When the system is powered

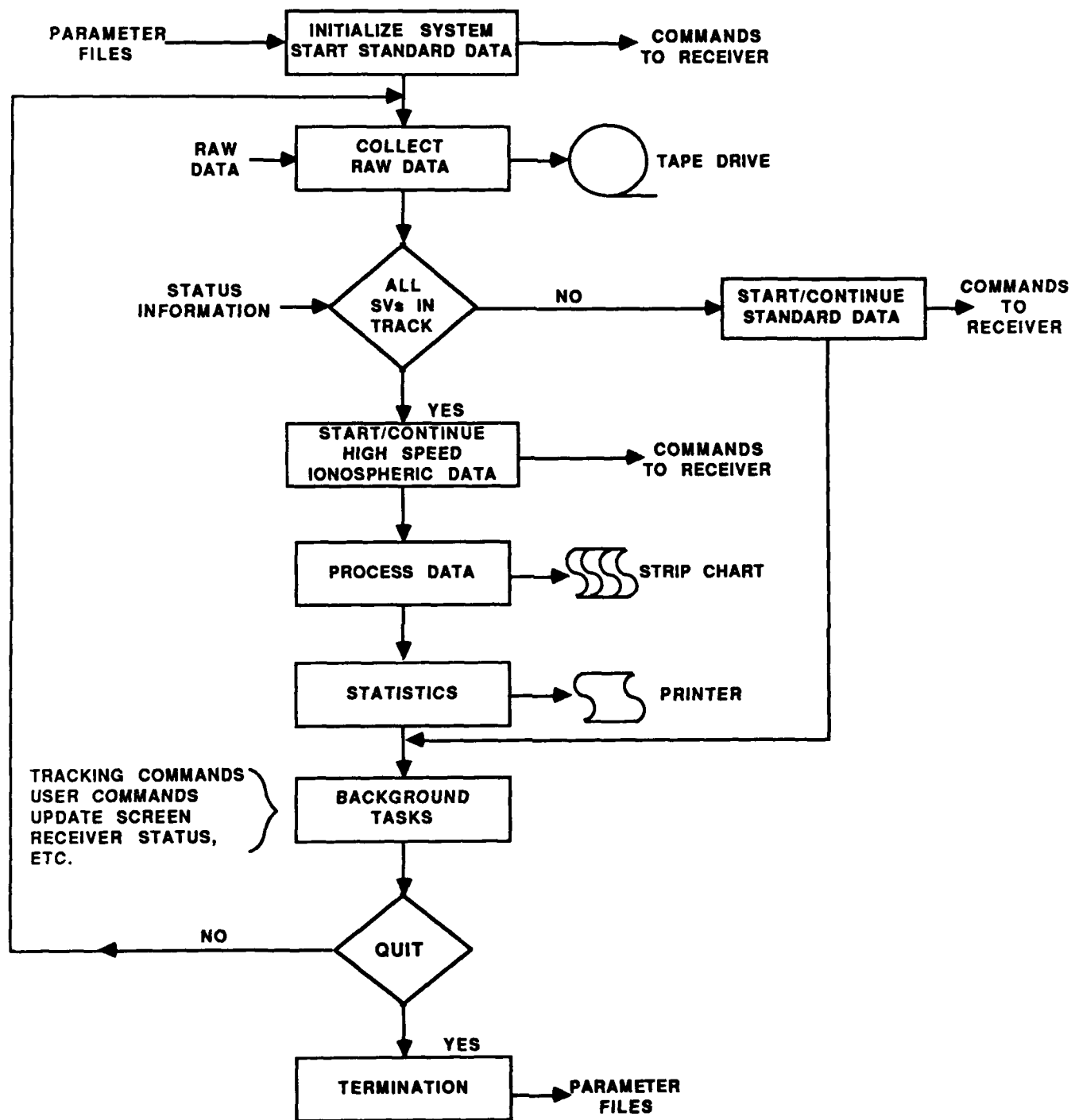


**FIGURE 7**  
**INFORMATION FLOW FOR IONPC**



on, the external processor initializes itself and places the prompt in the AIMS RUN directory where all of the basic operations may be executed. This directory is located on one of two disk drives, drives C and D, which are partitions containing 25% and 75%, respectively, of the 20 MByte Hardcard. Drive D holds the AIMS RUN directory and if necessary data can be written to this drive. Downloading the receiver software from this point is accomplished by running the program DLOADPC and responding to the subsequent prompts.

Once system operation is initiated, no interaction is required unless data recording supplies are depleted or other problems occur.

## V. CALCULATION OF DERIVED IONOSPHERIC PARAMETERS

This section discusses the calculation of the derived ionospheric parameters from the fundamental GPS signal measurements. Section A presents some background information on GPS signals that is required to develop the equations that relate the GPS signal measurements to the derived ionospheric parameters. These equations are presented in Section B. Section C discusses how these ionospheric parameters are formatted and how the tape capacity is calculated.

### A. GPS Signal Measurements

Each GPS satellite transmits a unique signal on two L-band frequencies, L1 at 1575.42 MHz and L2 at 1227.60 MHz (approximately 19 cm and 24 cm wavelengths, respectively). The signals consist of the L-band carrier waves modulated with coded information. The coded information consists of the "coarse acquisition" or C/A code (also known as "standard" or S-code), the "precise" or P-code, and a navigation message. Measurements made using the codes are called pseudoranges, and those made using the carrier signal are called integrated Doppler measurements, or referred to here as phase measurements.

Pseudorange measurements are essentially measurements of the transit time of the signal, or the time from transmission of the signal to reception of the signal, plus satellite/receiver clock offsets. Phase measurements are integrated cycle counts of the carrier wave referenced to the frequency standard inside the receiver. There is an unknown bias in the phase measurements which remains constant when lock on the signal is maintained. With knowledge of the signal frequency and receiver generated offsets, the phase measurement provides a measure of the change in satellite-to-receiver range sometimes referred to as delta range. The amplitudes of the received signals are also measured with a known offset

and this is reported in the form of a carrier-to-noise spectral density ratio, C/No, measurement.

#### B. Derived Ionospheric Parameters

The GPS range measurement  $R_m$  is simply the integral of the group delay index of refraction  $n_g$  over the satellite to receiver path,

$$R_m = \int n_g ds \quad (1)$$

The group velocity index of refraction can be approximated at L band frequencies by

$$\begin{aligned} n_g &\cong 1 + \frac{f_p^2}{f^2} \\ &= 1 + \frac{AN_e}{f^2} \end{aligned} \quad (2)$$

where  $f_p$  is the plasma frequency,  $f$  is the frequency of the radio wave,  $N_e$  is the electron density and  $A$  is a constant. Thus, the range is related to the integrated columnar total electron content TEC by

$$\begin{aligned} R_m &= R_o + \frac{A}{f^2} \int N_e ds \\ &= R_o + \frac{A \cdot \text{TEC}}{f^2} \end{aligned} \quad (3)$$

where  $R_0$  is the true geometric range. The difference in the ranges measured at the two frequencies is given by

$$R_{m1} - R_{m2} = A \cdot \text{TEC} \left[ \frac{1}{f_1^2} - \frac{1}{f_2^2} \right] \quad (4)$$

The ranges in this equation can be replaced by the GPS pseudorange measurements since the biases in the pseudoranges are the same for the two frequencies.

The equations relating the fundamental GPS measurements to the derived ionospheric parameters are presented in this section. The calculations for absolute TEC and relative TEC basically involve differencing across frequencies (L1-L2), propagating to common epochs, and scaling to the proper units. To reduce the amount of data that has to be moved across the TI 4100/external processor interface, the differencing across frequencies is performed inside the receiver in the CORE software.

At the highest data rates, there is not sufficient time for remaining calculations to be performed inside the receiver so they are performed after the data have been moved outside the receiver. These remaining calculations are performed both in the postprocessing software and in the external processor. This dual processing provides flexibility for the analyst in postprocessing by allowing access to the data in the raw data format.

The sampling scheme for AIMS data is diagrammed in Fig. 8. The solid lines represent the continuous GPS pseudorange and phase at the two frequencies. The circles represent the sampled measurements using the multiplexing scheme discussed earlier. The L1 and L2 measurements are usually separated by a multiplexing increment of 20 ms while consecutive

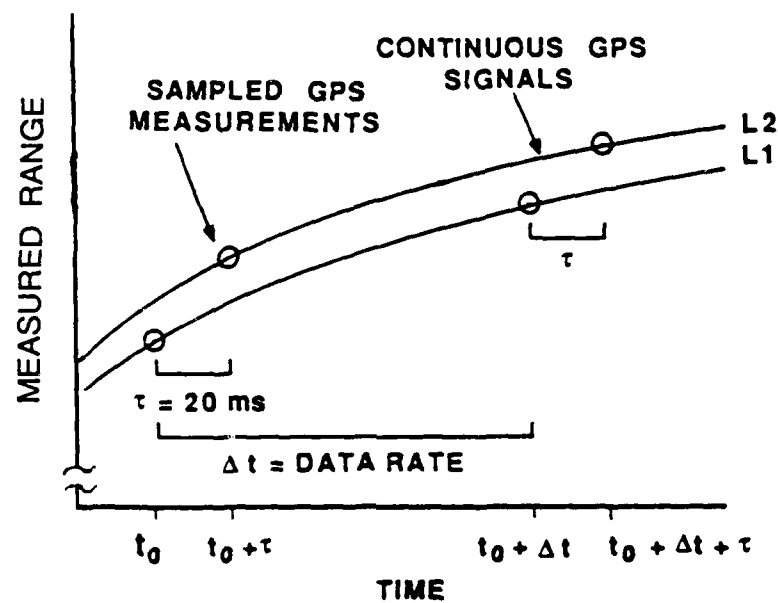


**FIGURE 8**  
**NONSIMULTANEOUSLY SAMPLED GPS DATA**

measurements at any one frequency are separated by the data rate interval.

The following symbols are used in equations presented below for the calculation of the derived ionospheric parameters.

$T_i$	=	transmit time for $L_i$ signal (ns)
$\phi_i$	=	carrier phase for $L_i$ (integrated Doppler) (cycles)
$\dot{\phi}_i$	=	carrier frequency for $L_i$ (phase rate of change) (cycles/s)
$\Delta t$	=	data rate
$\tau$	=	interval between $L_1$ and $L_2$ measurements (normally 20 ms)
$f_1$	=	$L_1$ frequency (1575.42 MHz)
$f_2$	=	$L_2$ frequency (1227.60 MHz)
$\Delta f_1$	=	$L_1$ frequency bias (-6000 Hz)
$\Delta f_2$	=	$L_2$ frequency bias (7600 Hz)
$\alpha$	=	$(f_2/f_1)^2 = (60/77)^2$
$B$	=	$\frac{\alpha}{\alpha-1} \cdot \frac{c f_1^2}{A}$ (conversion constant from ns to TECU)
$c$	=	speed of light ( $2.9979 \times 10^8$ m/s)
$A$	=	conversion to TECU ( $40.308 \times 10^{16}$ m-Hz <sup>2</sup> /TECU)
$C/N_0$	=	carrier-to-noise density ratio

The TEC is derived from the pseudorange difference at a common epoch using Equation 4 above. Since the pseudorange (divided by the speed of light) is the receipt time minus the transmit time  $T$  encoded on the signal, the TEC can be expressed in terms of the transmit time if the receipt times for the two frequencies are the same. If the common epoch is at  $t_0 + \tau$ , then

$$TEC = B \left[ T_2(t_0 + \tau) - T_1(t_0 + \tau) \right]. \quad (5)$$

There is no L1 sample at  $t_0 + \tau$ , so the nearest L1 measurement must be propagated to the common epoch using

$$T_1(t_0 + \tau) = T_1(t_0) + \left( 1 + \frac{\dot{\Phi}_1 - \Delta f_1}{f_1} \right) \tau. \quad (6)$$

The TEC now is given by

$$TEC = B \left[ T_1(t_0) + \left( 1 + \frac{\dot{\Phi}_1 - \Delta f_1}{f_1} \right) \tau - T_2(t_0 - \tau) \right]. \quad (7)$$

The actual calculation of TEC is divided between the receiver and the external processor. The calculation step performed inside the receiver is a simple difference between the measured L1 and L2 transit times adding the L1/L2 separation interval,

$$\Delta T = T_1(t_0) + \tau - T_2(t_0 + \tau), \quad (8)$$

and the calculation performed by the external processor adds the propagation term and then converts to TECU,

$$TEC = B \left[ \Delta T + \left( \frac{\dot{\Phi}_1 - \Delta f_1}{f_1} \right) \tau \right]. \quad (9)$$

The cumulative relative TEC derived from phase measurements is the sum of all the point-to-point differences in relative TEC given by

$$RTEC = \sum(\Delta TEC). \quad (10)$$

The point-to-point difference in TEC is derived from the difference in consecutive phase measurements differenced across frequencies, taking into account the frequency bias generated by the receiver itself;

$$\Delta TEC = B \left[ \begin{aligned} & \left( \phi_1(t_0 + \Delta t + \tau) - \phi_1(t_0 + \tau) - \Delta f_1 \Delta t \right) \frac{1}{f_1} \\ & - \left( \phi_2(t_0 + \Delta t + \tau) - \phi_2(t_0 + \tau) - \Delta f_2 \Delta t \right) \frac{1}{f_2} \end{aligned} \right] \quad (11)$$

The L1 measurements again must be propagated to the common epochs using

$$\begin{aligned} \phi_1(t_0 + \Delta t + \tau) &= \phi_1(t_0 + \Delta t) + \dot{\phi}_1(t_0 + \Delta t) \tau \\ \phi_1(t_0 + \tau) &= \phi_1(t_0) + \dot{\phi}_1(t_0) \tau. \end{aligned} \quad (12)$$

Combining these equations and using the subscript p to represent the measurements at  $t_0$  and  $t_0 + \tau$  (previous measurements) and the subscript c for those at  $t_0 + \Delta t$  and  $t_0 + \Delta t + \tau$  (current measurements) gives

$$\Delta TEC = B \left[ \begin{aligned} & \left( \left( \phi_{1c} + \dot{\phi}_{1c} \tau \right) - \left( \phi_{1p} + \dot{\phi}_{1p} \tau \right) - \Delta f_1 \Delta t \right) \frac{1}{f_1} \\ & - \left( \phi_{2c} - \phi_{2p} - \Delta f_2 \Delta t \right) \frac{1}{f_2} \end{aligned} \right] \quad (13)$$



The calculation step performed inside the receiver differences the phase measurements across time and then differences across frequencies after the values are scaled to a common unit,

$$\Delta\phi = 60(\phi_{1c} - \phi_{1p}) - 77(\phi_{2c} - \phi_{2p}), \quad (14)$$

and the calculation performed by the external processor is

$$\Delta\text{TEC} = \frac{B}{60f_1} \left[ \Delta\phi + 60(\dot{\phi}_{1c} - \dot{\phi}_{1p})\tau + \Delta t(77\Delta f_2 - 60\Delta f_1) \right], \quad (15)$$

and

$$\text{RTEC} = \sum(\Delta\text{TEC}).$$

The amplitude scintillation index S4 is derived by taking the ratio of the standard deviation of the received power to the mean of the received power over a specified interval.

$$S4 = \frac{\sigma_1}{\mu_1}. \quad (16)$$

The TI 4100 carrier-to-noise spectral density ratio measurement C/No, also referred to as the signal-to-noise measurement in this report, is used to calculate the signal amplitude scintillation parameter. The C/No parameter (dB-Hz) should be multiplied by the noise bandwidth to get the true signal-to-noise ratio, but since this bandwidth is constant, the ratio of the two quantities is fixed. The signal amplitude is thus linearly related to C/No, within the normal operational range, so C/No can be used to calculate the normalized received power.

$$I = 10^{-\left[ \frac{C/No - \langle C/No \rangle}{10} \right]} \quad (17)$$

The only calculation step performed inside the receiver for this parameter is an encoding step to reduce the number of bytes passed. The external processor uses the two equations above (16) and (17) to derive the S4 value over the interval.

### C. Data Blocking and Storage

The receiver outputs the ionospheric data in the raw data format in the form of blocks. Each block contains a header, data, and delimiters indicating the beginning and end of the block. The header indicates the type and length of the data contained in the block. These blocks include the standard data - standard navigation GPS measurements, almanac information, etc.; and the ionospheric data - high speed ionospheric measurements and ionospheric header information. A more complete listing of the block types used in AIMS is presented in Section VI. A brief description of the high speed ionospheric header block (block 52) and the high speed ionospheric data block (block 63) is presented here.

Table I describes the contents of block 52, the high speed ionospheric header block and Table II describes the contents of block 63, the high speed ionospheric data block. Block 52 only contains information which requires periodic updating. This block contains a number of items essential to data processing including

- 1) timing information - data rate, GPS time references, and time offsets due to multiplexing; and
- 2) tracking information - satellite PRN number and tracking status for each tracker.

A block 52 is output once every minute or whenever the value of any one of the parameters in this block changes.

Block 63 contains 10 phase-derived samples taken at the data rate defined in the block 52, and 5 pseudorange-derived and signal-to-noise (L1 and L2) samples taken at one half of this data rate. Also contained in block 63 are the phase rate-of-change values which are used in the propagation scheme described in Section II. There are actually 4 samples for each parameter and data point, one for each of the 4 trackers. Phase and pseudorange measurements have been differenced across the two frequencies as a result of a data reduction step performed inside the receiver.

TABLE I  
HIGH SPEED HEADER BLOCK

Block Number: 52

Output Frequency: Normally 1 block per 60 s or whenever any parameter value in the block changes

Essential Items: Time tag information  
SV PRN numbers  
Multiplex biases  
Tracking modes

TABLE II  
HIGH SPEED DATA BLOCK

Block Number: 63

Output Frequency: Data rate/10  
Usually 1 block per 1.2 s (for 8.33 Hz data rate)

Essential Items: Time tag information for all measurements  
10 consecutive L1/L2 phase difference measurements  
5 consecutive L1/L2 pseudorange difference measurements  
5 consecutive L1 C/No measurements  
5 consecutive L2 C/No measurements

As the data blocks are received by the external processor, they are placed into a buffer and then written to tape in the form of fixed length physical records. As the data are buffered, copies of the blocks are also processed through the system in realtime. Once the data in the buffer exceed the record length of 2560 bytes, a record is output to the tape drive. The data in excess of 2560 bytes remain in the buffer to output with the next record. The total length of a block 63 including its header and delimiters is 546 bytes, and so, slightly more than four Block 63s fit in a physical record.

Records are written to the tape operating at 1600 bpi with an inter-record gap of approximately 0.9 in. This implies an effective storage rate of 1024 bpi, since the record alone requires 1.6 in. (2560 bytes/1600 bpi). Therefore, a standard 2400 ft tape with records of length 2560 bytes holds approximately 29.5 MBytes.

The storage capacity for an AIMS data tape, that is, the number of operational hours a standard 2400 ft tape can continue to accept data, depends upon the data rate and the satellite coverage. Table III presents the tape capacity for AIMS assuming a 24 hour satellite coverage. For example, 120 ms data produces a block 63 every 1.2 s, since a block 63 contains 10 data points. This implies a byte rate of 455 bytes/s (546 bytes/1.2 s). The contribution from Block 52s is small since these are output only once every 60 s (1.7 bytes/s = 102 bytes/60 s) giving a total byte rate of 456.7 bytes/s. The tape duration is calculated by dividing the effective tape capacity of 29.49 MBytes by the total byte rate 456.7 bytes/s and converting from seconds to hours. This yields a tape duration of 17.9 h for 120 ms data. Similar calculations have been performed for various data rates and the results are presented in Table III. Also included are the maximum number of Block 63 and 52s that can be stored on the tape.

TABLE III  
AIMS TAPE STORAGE CAPACITY

<u>Data Rate</u>	<u>Byte Rate (bytes/s)</u>	<u>Tape Duration (h)</u>	<u>Number of Block 63s</u>	<u>Number of Block 52s</u>
80 ms	684.2	12.0	53877	718
120 ms	456.7	17.9	53810	1076
160 ms	343.0	23.9	53743	1433
200 ms	274.7	29.8	53677	1789
240 ms	229.2	35.7	53610	2144
480 ms	115.5	70.9	52216	4257
1 s	56.3	145.5	52380	8730
6 s	10.8	758.5	45509	45509

## VI. MAINFRAME POSTPROCESSING SOFTWARE

A series of programs have been developed on the CDC Cyber 180 at ARL:UT to process the AIMS data that are recorded on 9-track tape. This software package called AIMLIB was delivered to AFGL and implemented on their Cyber so that both facilities are now capable of postprocessing AIMS data. This software package was built around pre-existing software in use at ARL:UT and was developed as an analysis tool for viewing the data during the testing and development of AIMS. The data flow structure is not the optimum one for processing large amounts of campaign data nor was it intended to be.

The main goals of this software development effort were to allow maximum visibility of the data during different stages of processing and to utilize pre-existing software as far as possible. The data flow for this package is shown in Fig. 9.

The 9-track tape written on the AIMS tape drive contains the data in what is called the "D-file" format, which is a series of records with physical record lengths of 2560 bytes. The logical records have variable record lengths depending on the type of data contained in the record and the logical records may span the physical record boundaries.

The first conversion entails converting the data to the "C-file" format using a program called AIMCVT. The C-file format contains the data in engineering units, such as meters, in a more structured format that is easier to manipulate than the D-file. The data are broken up into blocks, with two binary FORTRAN records per block: one is a header record that has the block ID and length and the other record contains the data assigned to that block type. There are separate blocks for the almanac, the ephemeris, ionospheric data, and other data types. Table IV gives a short description for all of the blocks types used in AIMS.

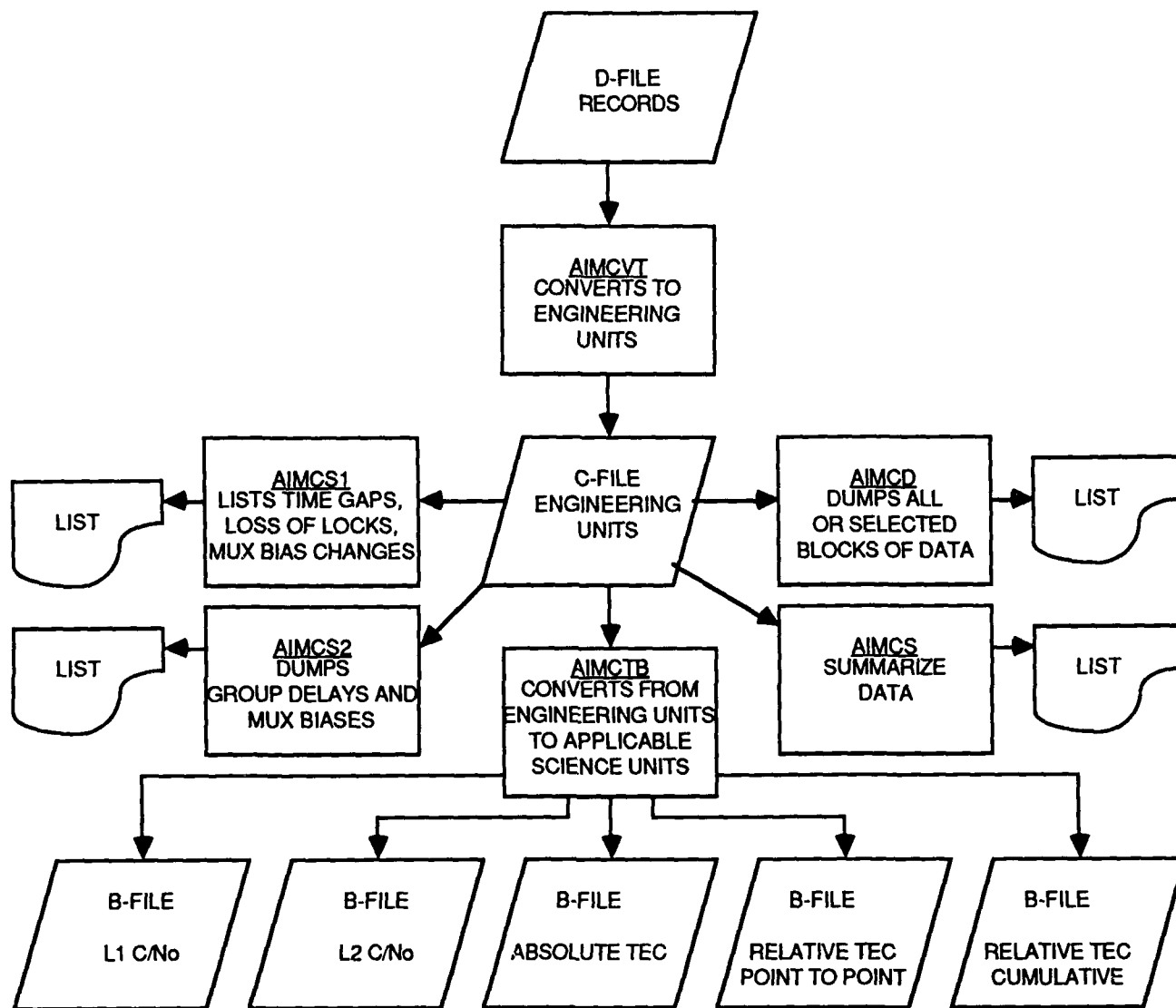


**FIGURE 9**  
**POST PROCESSING SOFTWARE**  
**FOR AIMS**

TABLE IV  
DATA BLOCK TYPES USED IN AIMS

<u>Block ID</u>	<u>Block Description</u>
2 or 62	GPS almanac message data
102 or 162	GPS almanac message data, packed format
6	Standard navigation GPS measurements
7	Standard navigation GPS auxiliary parameters
8	Standard navigation tracking configuration parameters
9	GPS ephemeris message data
109	GPS ephemeris message data, packed format
11	CORE error block
13	File delimiter block
52	High speed ionospheric header block
55	Standard navigation GPS measurements
63	High speed ionospheric data block
1004	AIMS system configuration block
1006	Parameter definition block
1008	AIMS error block



There are a series of programs that operate on the C-file format as shown in Fig. 9. These programs allow viewing of specific aspects of the data without actually dumping all of the data points. Two of the programs, AIMCS and AIMCD, allow the user to view individual data points. AIMCD prints all of the values in each selected block whereas AIMCS prints only selected key parameters, such as the time, the satellite PRNs in track, and the quality vectors of the data. The other two programs, AIMCS1 and AIMCS2, are specialized dump programs that allow the user to print selected data over specified intervals. These four programs are useful for getting a close-up look at the data but not for gaining an overall view.

To get an overall view of the data and to display data trends over a long interval, the B-file format was created along with a variety of analysis programs (see Fig. 10). This format is a binary file that contains a header and a series of data records. The header contains two titles and a data type flag which indicates what type of data follows in the data records. There are five different data types used in the present system (L1 C/No, L2 C/No, absolute TEC, relative TEC point-to-point, and relative TEC cumulative). Each C-file is broken up into five B-files, one for each data type, all with the same format. The B-files contain the data in science units applicable to the particular parameter (dB-Hz for C/No and TECU for TEC parameters).

Individual data points from the B-files can be printed using AIMBD or plotted using AIMBP. This plot program allows the user to select specified intervals and/or to limit the data so that every data point does not have to be plotted. There is a statistics program for B-files, AIMBS, that calculates the statistics over specified intervals for the different parameters. In this program, the C/No parameters are used to generate S4 values. There is also a quick scan program for B-files, AIMBQ, that prints out the beginning and end times for specified intervals.

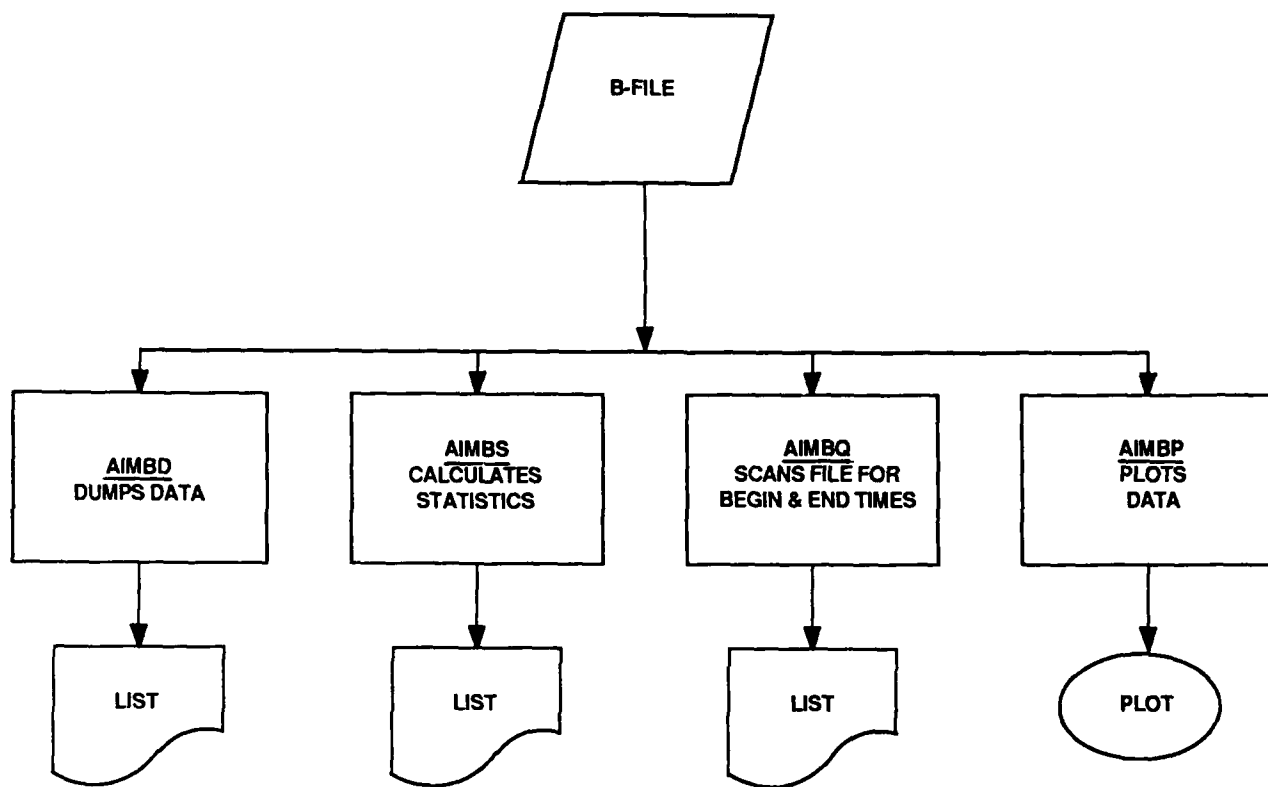


**FIGURE 10**  
**B-FILE ANALYSIS SOFTWARE**

This software package has been very useful in analyzing the data in the test and development stage due to the flexibility provided by its multi-stage conversion structure. This structure presents some serious drawbacks, however, when used for processing large amounts of data that are typically collected in a field campaign, such as the Sondrestrom campaign described elsewhere in this report. A typical day of data with the current GPS constellation produces a D-file that requires one full 2400 ft 9-track tape recorded at 1600 bpi. This will in turn require a C-file that is approximately 2 tapes long and 5 B-files with a total length of 2 tapes. This represents a total of 5 tapes for storing all three formats for one day of data. In addition, the costs of reading and writing the data twice becomes large when multi-day campaigns are considered.

The questions of an alternative system for processing AIMS field campaign data will not be addressed in this report; however, mention should be made of some of the features that should be considered in developing the design for this system. First, the streamlining of the data flow should be one of the primary considerations. Second, a spectral analysis package should be developed in tandem with the new data processing package. Third, the C-file format should be dropped and an alternate format adopted. A more thorough discussion of the various types of analysis that might be appropriate for the AIMS field campaign data will probably yield further design features that should be considered.

## VII. AIMS PERFORMANCE EVALUATION

### A. Laboratory Calibration Results

The purpose of the laboratory calibration tests was to verify the performance of both the hardware and software components of AIMS. These tests do not provide an absolute calibration of the accuracy of the AIMS measurements because the signal sources used for the calibration were not calibrated absolutely. These tests were very useful, however, in determining the precision of the measurements and verifying the overall performance of the system.

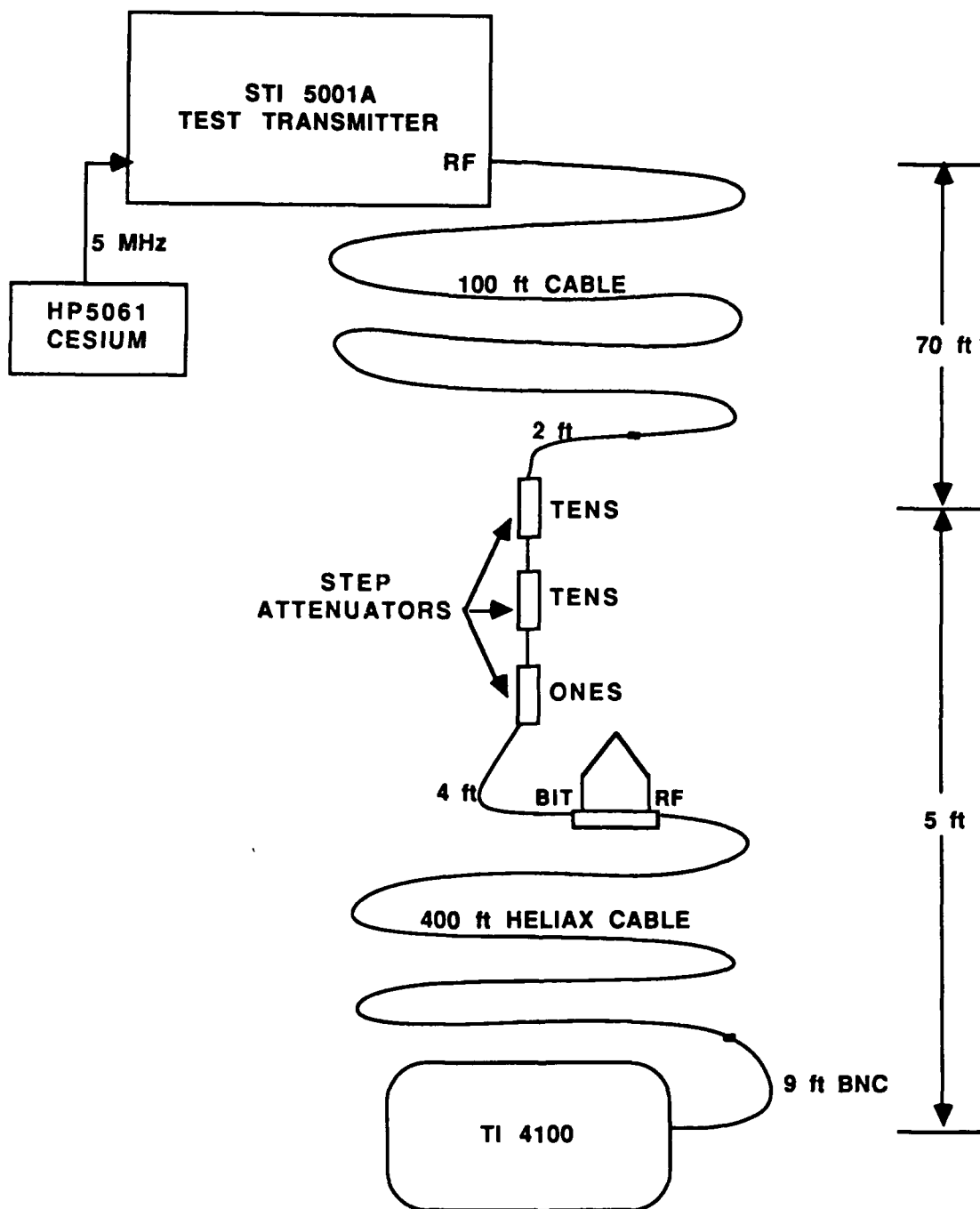
An STI 5001A NAVSTAR test transmitter was used to provide the test signals for the calibration tests. This transmitter provides GPS signals at both frequencies for a single satellite with the P-code and Doppler. Using the test transmitter, it is possible to introduce a time delay between the L1 and L2 P-code signals to simulate the ionosphere's effect on AIMS. This is the method used for the calibration of the absolute TEC. A variation of this method using variable attenuators was implemented to calibrate the signal amplitude measurements.

The relative TEC measurement, derived from the carrier phase measurements, was not able to be calibrated using the test transmitter alone. Although the test transmitter manual indicated that the Doppler could be modulated using the test transmitter, this function could not be made operational during our tests. To generate a modulated Doppler, an additional signal generator was used in conjunction with the test transmitter. This method was successful in generating a modulated Doppler which simulated phase scintillations.

## 1. Time Delay

The experiment configuration used for both the time delay and amplitude calibrations is shown in Fig. 11. An HP 5001 cesium oscillator provided a stable 5 MHz signal to the test transmitter. Test transmitter signals at L1 and L2 were run through a set of calibrated step attenuators and then into the BIT port of the TI 4100 antenna. After passing through the TI 4100 preamplifier inside the antenna the signals were sent to the TI 4100 receiver via a 400 ft low loss heliax cable. It was necessary to locate the test transmitter in a separate room from the TI 4100 to prevent cross talk from signal leakage. The time delay between the L1 and L2 signals was varied by a dial on the test transmitter. This time delay is linearly related to the absolute TEC parameter discussed in Section V. The signal amplitude was varied using the step attenuators.

Early results of the L1/L2 time delay calibration showed the need for data to be taken at various signal amplitudes in order to determine the role signal amplitude played in the measurements. The results from such a test are presented Figs. 12 and 13 for a wider range of values than would be expected from the ionosphere. Figure 12 plots the TEC data resulting from stepping through a series of time delay settings, changing the signal amplitude, and stepping through the series in the opposite direction. This procedure was repeated for attenuation settings of 40, 50, and 55 dB corresponding to C/No values of 48, 38, and 33 dB-Hz, respectively. Negative delay values (L1 leading L2) are allowed by the test transmitter. After eliminating the transition points between time delay changes, the statistics shown in Table V were obtained. For each delay setting, Table V gives the mean and standard deviation of the observed delays in TECU at the three attenuation levels. In Fig. 13, the same means of the observed delays are plotted as a function of the test transmitter time delay settings.



\* rf LEAKAGE FROM 5001A REQUIRED ISOLATION OF THE TRANSMITTER FROM THE RECEIVER TO ENSURE PROPER ATTENUATION

**FIGURE 11**  
**TIME DELAY AND SIGNAL AMPLITUDE**  
**CALIBRATION CONFIGURATION**

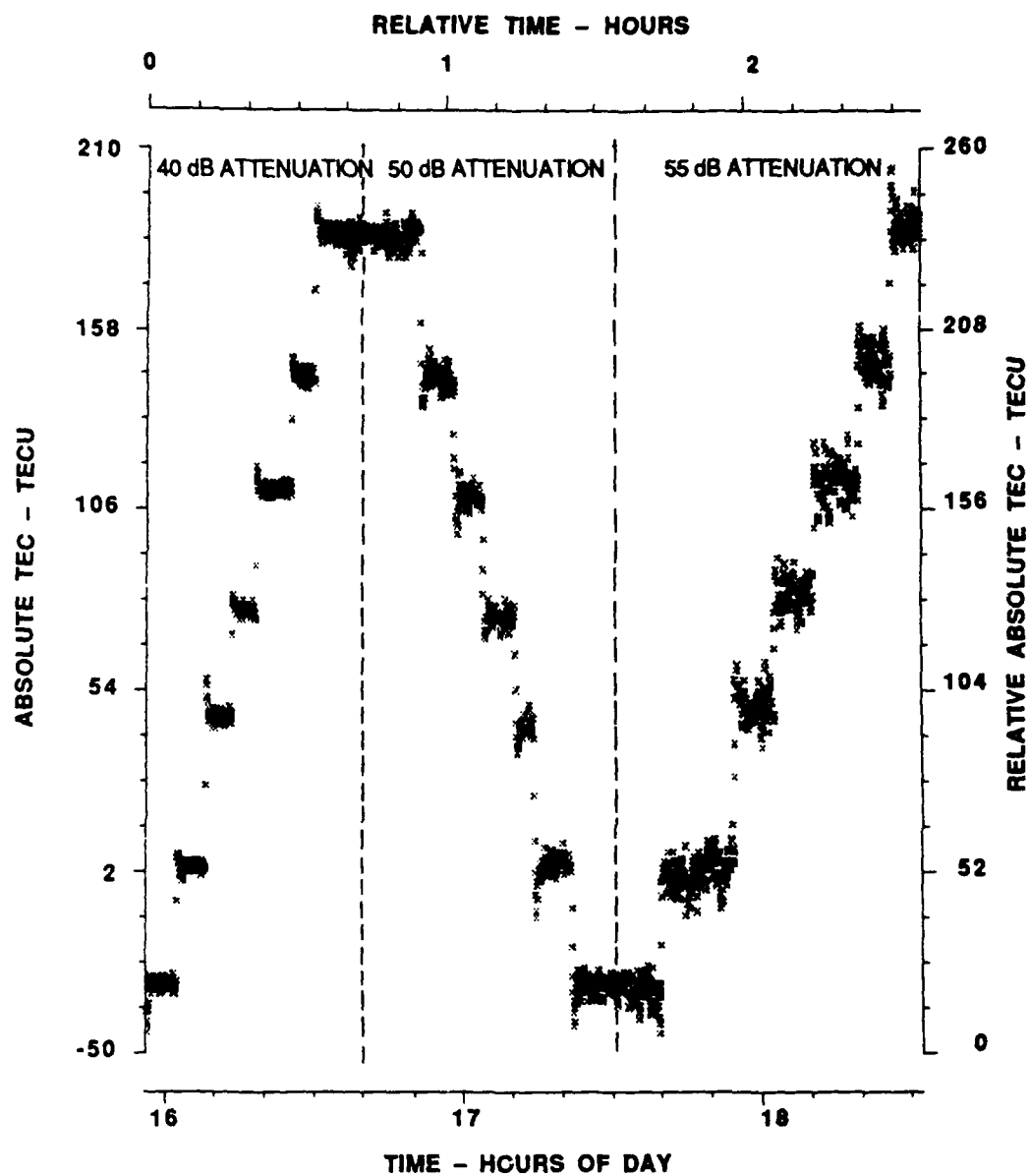


**FIGURE 12**  
**TIME DELAY VARIATION WITH DELAY SETTING**  
**AND SIGNAL ATTENUATION**

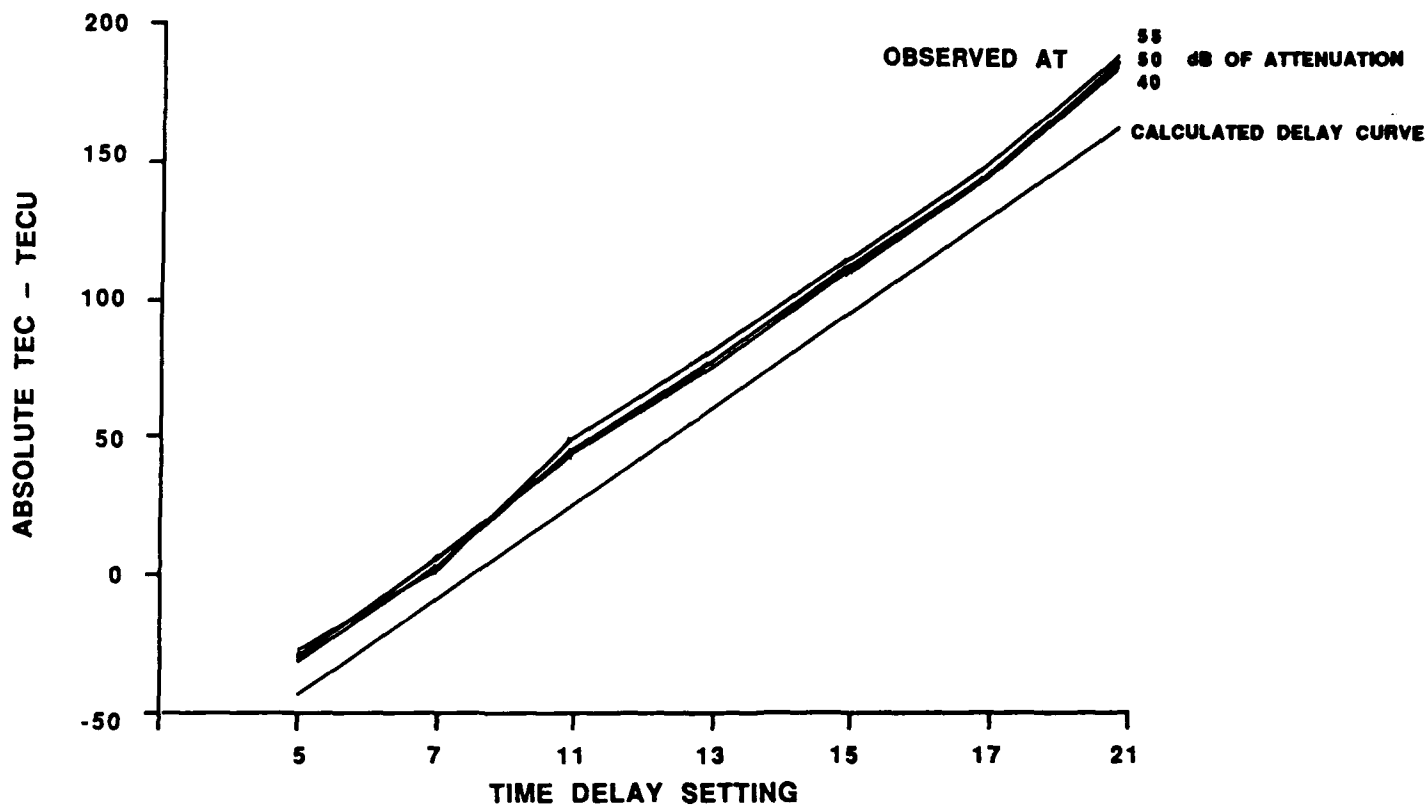


**FIGURE 13**  
**TIME DELAY CALIBRATION**  
**ABSOLUTE versus DELAY SETTING FROM**  
**STI 5001A POWER 36**



DELAY SETTING	L1-L2 CALCULATED DELAY (TECU)	MEAN OF OBSERVED DELAY WITH ATTENUATION			STANDARD DEVIATION OF OBSERVED DELAY AT		
		40 dB	50 dB	55 dB	40 dB	50 dB	55 dB
5	-42.8	-30.1	-30.5	-32.0	1.23	1.95	3.29
7	-8.6	3.0	4.9	2.0	1.37	2.33	3.86
11	25.7	46.3	44.9	49.5	1.23	2.06	4.56
13	59.9	77.1	75.1	81.1	1.26	2.42	3.44
15	94.2	111.7	109.4	114.3	1.25	2.07	4.15
17	128.4	143.9	143.7	146.5	1.28	2.38	3.58
21	162.6	185.0	186.3	188.3	1.30	2.16	3.98

TABLE V  
TIME DELAY CALIBRATION  
(IN TECU)

Using the specifications of the test transmitter, it is possible to calculate the nominal time delay expected from each time delay setting. These values are also shown in Table V and in Fig. 13. The slopes of the observed time delays are consistent with the slope of the calculated values, but a bias of roughly 10-25 TECU is evident. The source of this bias could be either from the test transmitter and/or the receiver. Neither the test transmitter nor the TI 4100 have been calibrated absolutely. The absolute calibration of either unit is considered possible, but is not a trivial task.

Figure 13 shows that there are small differences between the measurements for the same time delay settings, but different attenuation levels. These differences are not all consistent in magnitude or sign and are smaller than the standard deviations shown in Table V. The bias between the true delay and the measured delay may depend somewhat on the attenuation level, but it is within the noise levels of the measurements.

The variation of the time delay measurements within a given group is given by the standard deviation values in Table V. These values increase as the signal attenuation increases, as expected, due to the increased noise in the pseudorange measurements. The TI 4100 pseudorange receiver noise (due exclusively to noise generated by the receiver itself) has been measured in a separate set of experiments, (Coco and Clynch, 1986), to be about 20 cm at L1 for the bandwidths used by AIMS. The typical C/No level for the actual GPS satellites used in these experiments was about 42 dB-Hz. The pseudorange noise measurement can be converted to a time delay (L1-L2) noise estimate of 1.74 TECU (assuming the L1 and L2 noise is uncorrelated, which is a valid assumption for this level of estimation). This value is approximately midway between the standard deviation values for 40 and 50 dB, which is expected because these attenuation values correspond to C/No values of 38 and 48 dB-Hz which bracket the typical value of 42 dB-Hz. These two measurements taken together indicate that 1.74 TECU is a fair estimate of the absolute

TEC noise (pseudorange derived) generated by the receiver itself. This does not include noise generated by sources outside the receiver, such as multipath.

## 2. Signal Amplitude

The purpose of the signal amplitude calibration was to verify the range in which the TI 4100 signal-to-noise values are linearly related to signal amplitudes. In addition, the signal amplitude at which tracking loss occurred was measured.

TI reports that the TI 4100 C/No measurement represents the signal amplitude referenced to an average noise value (169 dBm) within a specified range of 29-43 dB-Hz. Outside this range, the C/No measurement is dampened by the receiver. Thus, the C/No measurement should be linearly related to the signal amplitude within this range but not necessarily outside of the range.

Signal amplitude calibration measurements were made using the same hardware configuration as for the time delay calibration with the time delay setting fixed. The results of a typical calibration test, shown in Fig. 14, indicate that the C/No values are linearly related to the signal amplitude within the specified range.

Results from the same calibration test showed loss of lock occurring roughly at 59 dB of attenuation which corresponds to a signal amplitude of -137 dBm, or 32 dB-Hz as recorded by the L2 C/No measurement. This represents a 3 dB loss in fade margin over the TI 4100 operational characteristics of 29 dB-Hz for loss of lock. This 3 dB loss is attributed to the different bandwidths used in AIMS as compared to those normally used by the TI 4100.

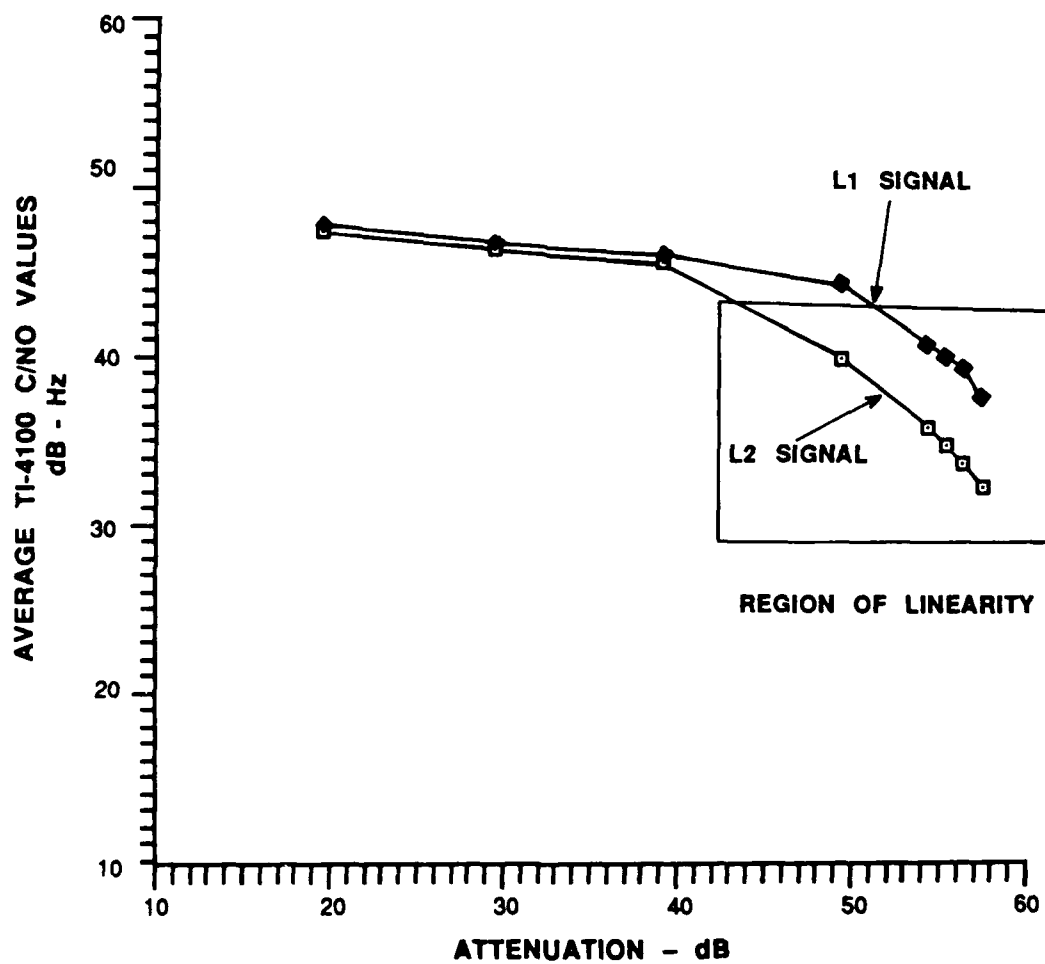


**FIGURE 14**  
**SIGNAL AMPLITUDE CALIBRATION**

### 3. Phase Scintillation

The phase scintillation calibration test was designed to verify and measure the precision of the relative TEC measurement which is derived from the carrier phase measurements. The L1 and L2 carriers experience phase advances as the signals pass through the ionosphere. These phase advances change due to the change in the number of electrons in the path between the satellite and the receiver. By artificially modulating one of the carrier frequencies while the other remains constant, ionospheric scintillations (rapid changes in the number of electrons encountered by the signals) are simulated.

Figure 15 shows the configuration for the phase scintillation calibration. A synthesized signal generator (20.46 MHz source) is used to produce constant phase for the L2 channel and a synthesizer/function generator (20.46 MHz plus modulation) is used to produce a modulated phase for the L1 channel. The modulation has a saw-tooth shape with a period of 2 s and an amplitude of 0.05 Hz. This pattern should result in a relative TEC measurement that oscillates with the same period with an amplitude of 1.74 TECU.

The observed relative TEC measurements (120 ms data rate) taken from an actual strip chart recording from this phase scintillation calibration test are shown in Fig. 16. The relative TEC-cumulative values are shown for trackers 1 and 3 while the relative TEC-point-to-point values, derived by differencing consecutive phase measurements, are shown for trackers 2 and 4. The relative TEC-point-to-point measurements reflect the expected sawtooth pattern and the relative TEC-cumulative exhibit a time integrated sawtooth pattern.

In order to examine the data more carefully, the observed relative TEC-cumulative measurements were differenced from a computer generated, time integrated, sawtooth pattern and statistics were

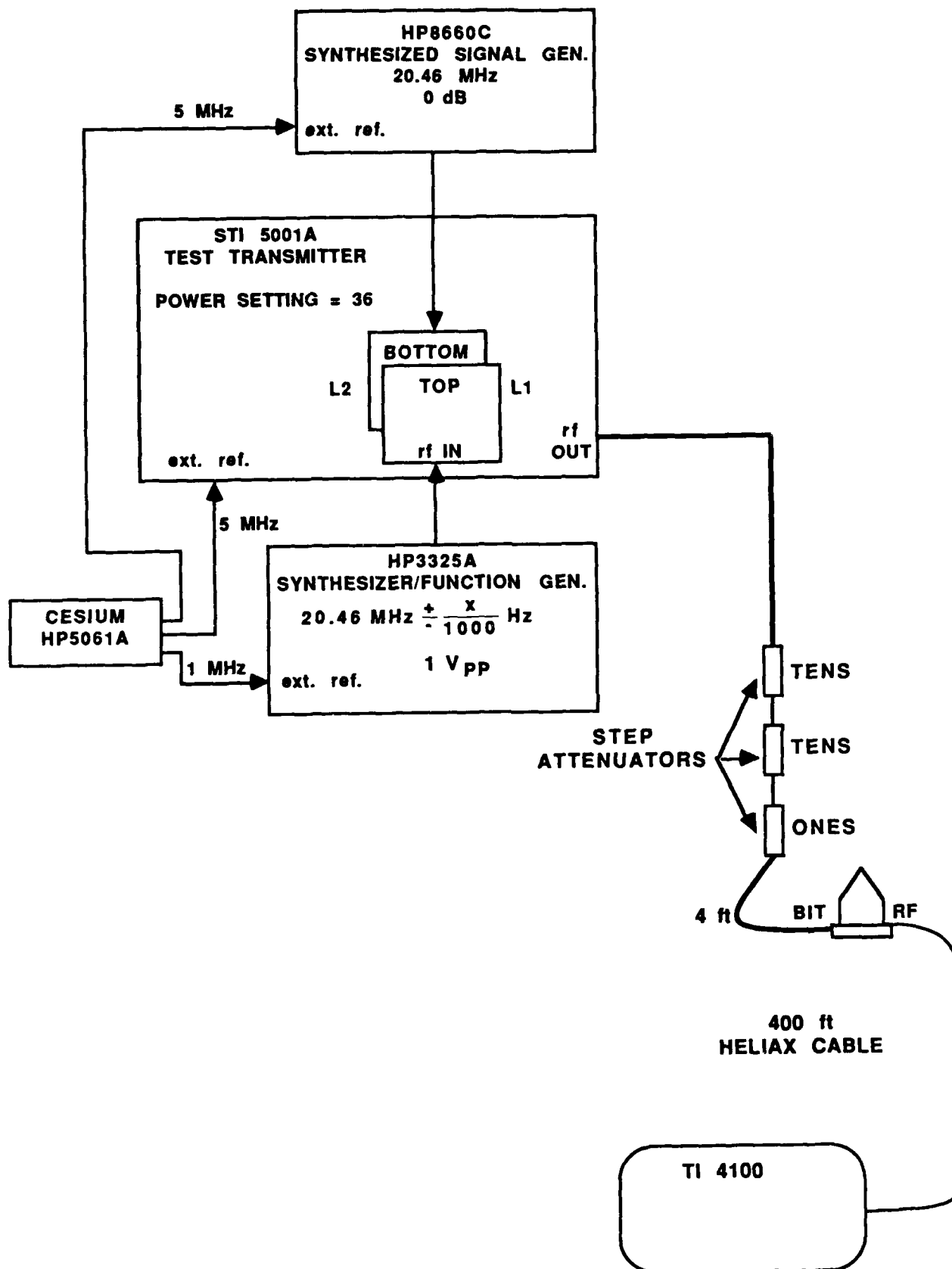


**FIGURE 15**  
**PHASE SCINTILLATION CALIBRATION CONFIGURATION**

ARL:UT  
 AS-88-9  
 CC - GA  
 1-19-88

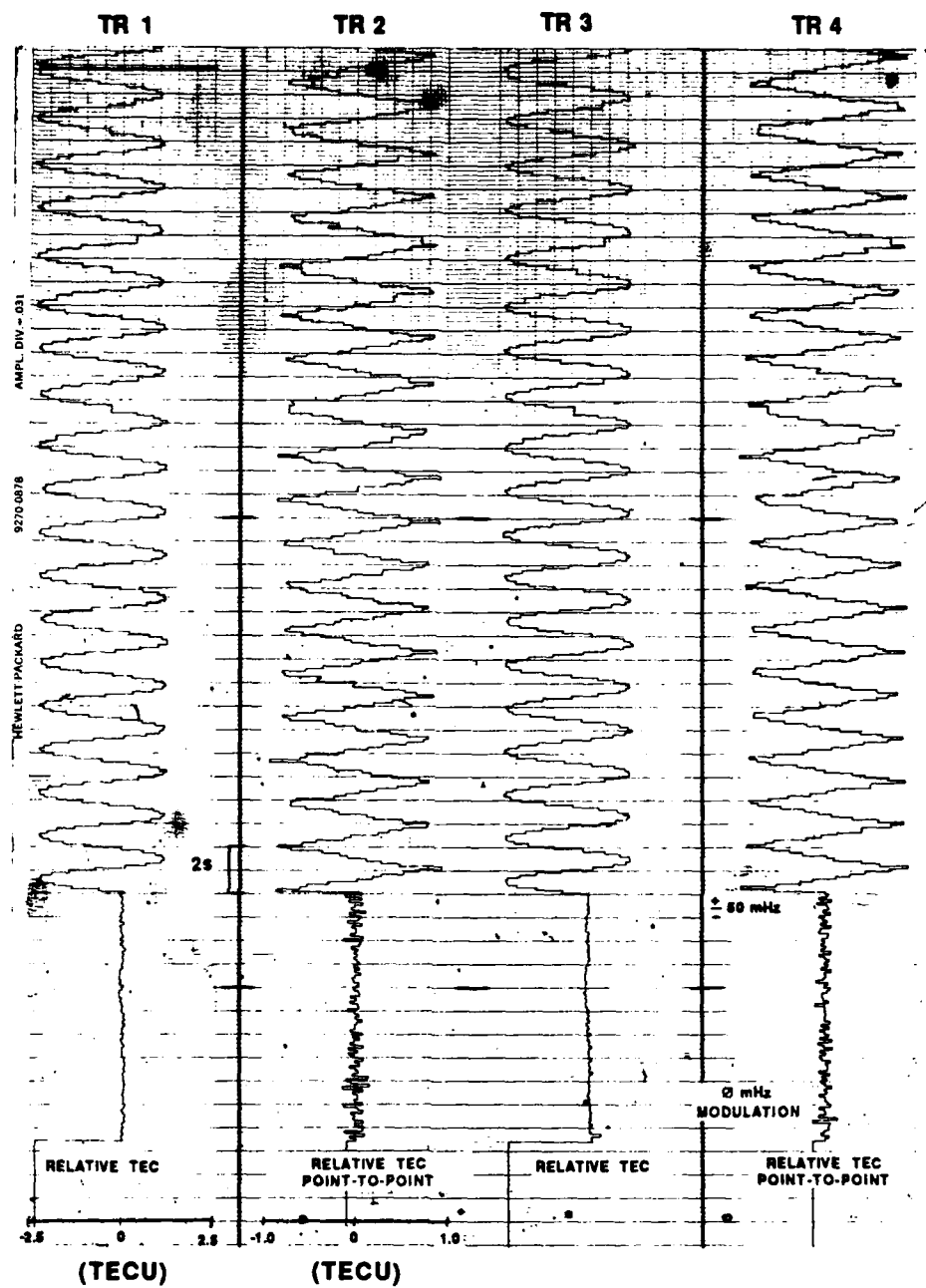


**FIGURE 16**  
**PHASE SCINTILLATION CALIBRATION**

calculated. Multiple samples of 128 measurements were examined for all four trackers, showing the average noise on the observed measurements to be approximately 0.045 TECU (16 ps of differential delay). This value is very close to the differential phase noise calculated for the receiver while undergoing no phase modulation, 0.043 TECU (15 ps).

This noise value applies to the time interval over which the statistics were computed, which is about 15 s. There is evidence that there may be an additional long term drift in the difference between the observed TEC and the generated pattern on the order of 13.5 TECU/h over a one hour time scale, but a sufficient quantity of data were not recorded to fully investigate this effect.

#### B. Examples of Field Measurements

AIMS has been used in several different field tests in which actual GPS signals were tracked. The first tests were conducted on the ARL:UT rooftop which is a medium to high multipath environment due to the clutter of nearby metallic structures. The system was later operated on the ARL:UT antenna test range which is an open field approximately 60 m by 100 m that provides a low multipath environment. These tests probed a mid-latitude ionosphere during a low sunspot number period and therefore one would not expect to detect a large number of complex TEC structures or a significant amount of L-band scintillation. The first test of AIMS in a polar ionosphere environment was conducted in February-March 1987 in Sondrestrom, Greenland during the Polar ARCS campaign.

##### 1. Mid Latitude Low Multipath Environment

Data were taken at the ARL:UT antenna test range prior to deployment of the system to Sondrestrom in order to identify the effects of multipath on the system. The antenna test range is a large field with no obstructions (60 m x 100 m) used for its low multipath environment.



Multipath effects result from interference between signals which have traveled from the satellite to the receiver along different path lengths. These effects are generally caused by objects nearby the receiving antenna which reflect signals back to the antenna. GPS pseudorange measurements are more severely affected by multipath than are carrier phase measurements because of the longer wavelengths of the coded information (30 m for pseudorange versus 20 cm for phase). Since the geometry or position of the GPS satellites relative to a station is repeated every 24 h less 4 min, the multipath is repeated at the same rate. Comparison of two days of data with multipath taken at the same station will show evidence of correlation when the data are aligned for similar satellite geometries.

The antenna test range data were taken at a 1 s rate for 5 days, 18-22 December 1986, with the antenna mounted four ft above the ground on a tripod. This allowed reflections from the ground to be the major source of multipath since there were no other objects within 30 m of the antenna. Segments of the data from the five days were aligned for geometry and then examined for multipath effects.

Figure 17 shows two one hour segments of slant TEC data taken on two consecutive days after they have been aligned for similar satellite geometries. The noisy pseudorange-derived, absolute slant TEC measurements are overlaid with the smooth, phase-derived, relative TEC measurements. The relative TEC measurements have had an arbitrary bias added so that they appear to pass through the center of the absolute TEC measurements. This bias is merely an aid in visualizing the noise contributed by multipath and other sources and is not crucial to the analysis.

The scatter of the absolute TEC about the relative TEC is due to two principal noise sources. The noise contributed by the receiver itself and the noise due to multipath. The receiver noise should appear

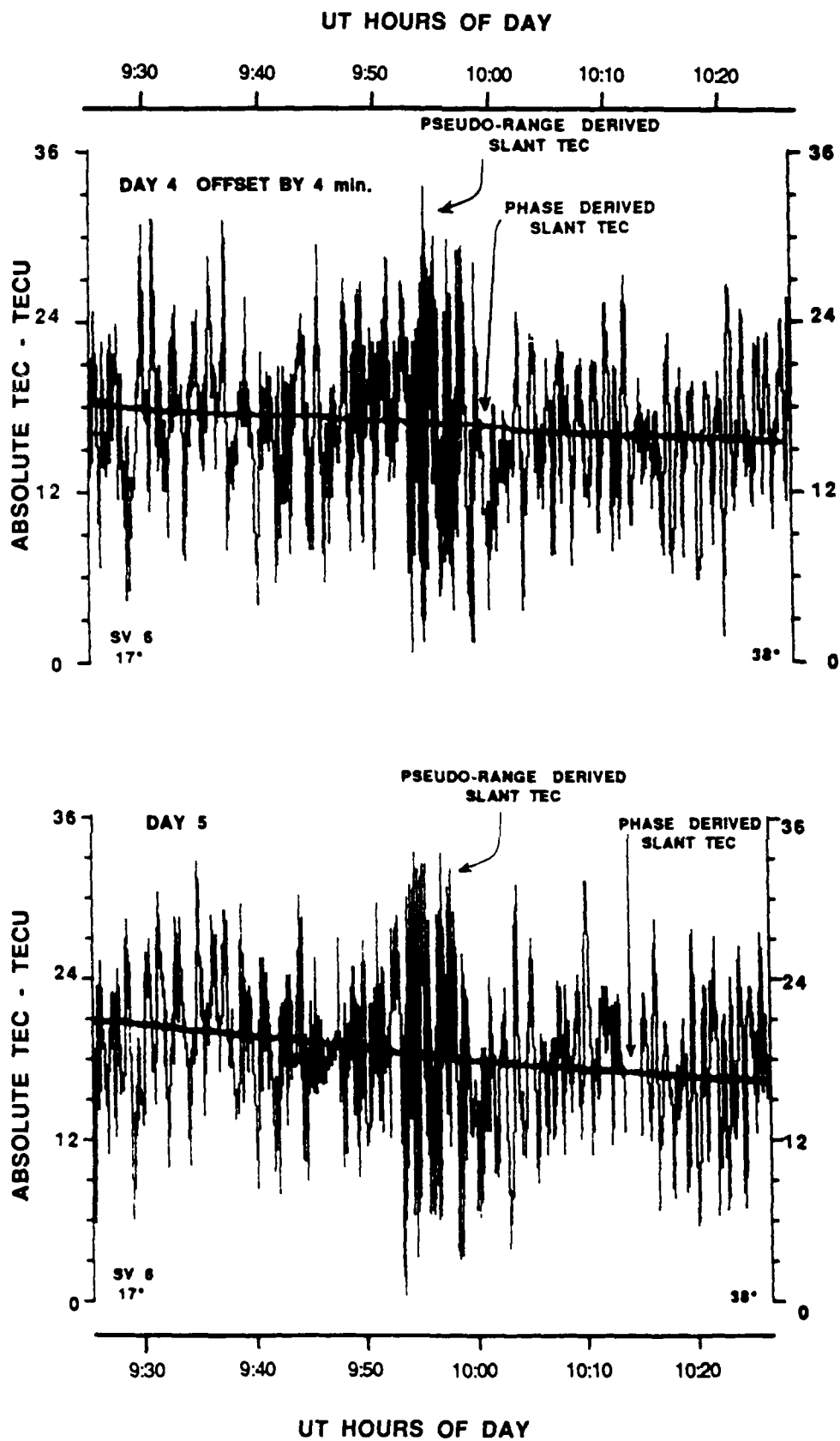


FIGURE 17  
ABSOLUTE TEC

as random noise with a constant magnitude throughout the pass. The multipath noise, however, will exhibit a non-random signature depending on the environment, the satellite geometry and the data rate of the measurements. If the environment and data rate are kept constant, the multipath noise signature should repeat itself on a day-to-day basis for similar satellite geometries. It is difficult, but possible, to see a correlation between absolute TEC noise for the two days in Fig. 17. It is clear, however, that the noise signature in the middle of the data set is repeated from day to day.

To examine the absolute TEC noise more carefully, the slowly varying trend exhibited by the relative TEC is removed by differencing the absolute TEC and relative TEC measurements and the resulting values are centered about zero. This, in essence, removes the TEC from the measurement and leaves the noise of the absolute TEC measurements. These TEC noise values are averaged over 30 s to suppress the random receiver noise as shown in Fig. 18. These plots show a much clearer evidence of a day-to-day correlation of the noise signature. There are a large number of oscillations with a period of about 3 min. that are very highly correlated between the two data sets. There are also correlations between oscillations with a period of 20 min.

Another method of viewing the correlation of the multipath noise signature is to look at the standard deviation of the TEC noise over specified intervals. In Fig. 19, the standard deviation ( $\sigma$ ) of the original TEC noise (Fig. 17) calculated over 180 s intervals is shown. This provides a measure of the variation of the TEC noise over the interval. This value is also highly correlated from day-to-day with very high values during the center of the data set where multipath noise is apparently the greatest.

The TEC noise  $\sigma$  values shown in Fig. 19 have contributions from both receiver noise and multipath noise. If TEC receiver noise

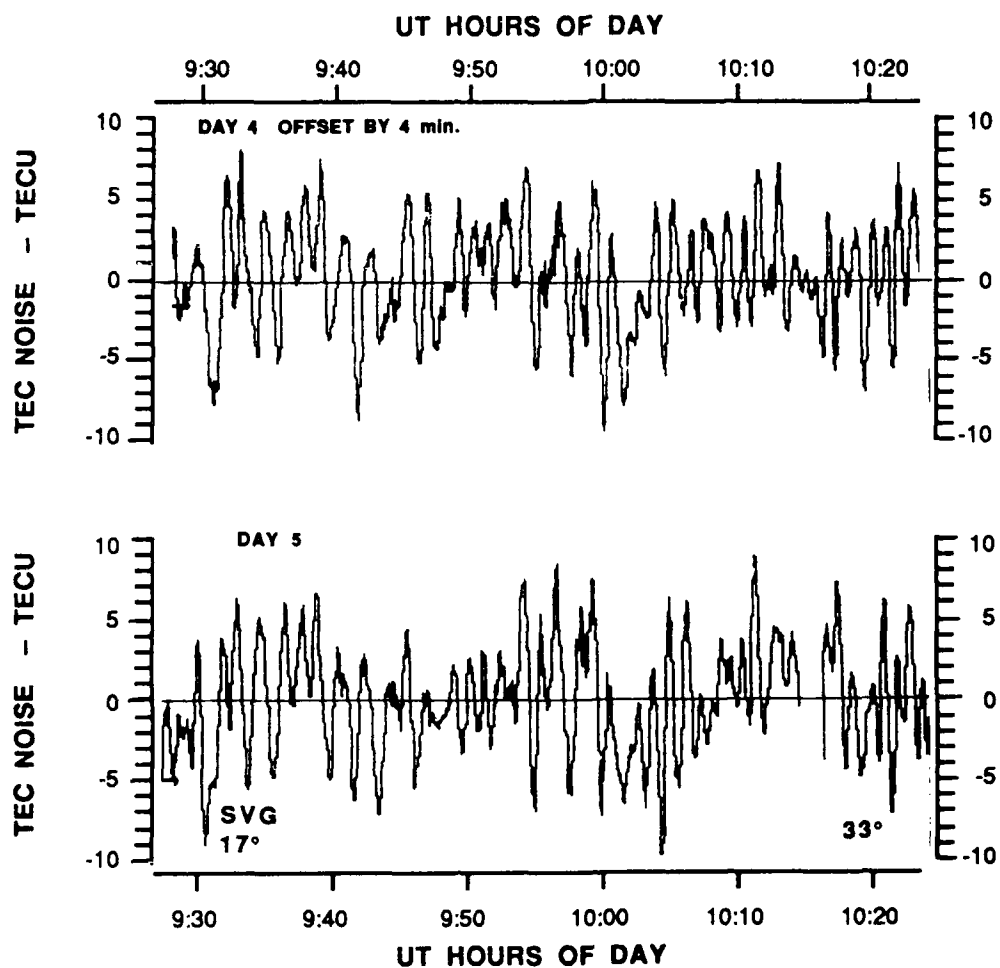


**FIGURE 18**  
**TEC NOISE SMOOTHED OVER 30 s INTERVALS**  
**IONOSPHERIC CONTENT REMOVED**

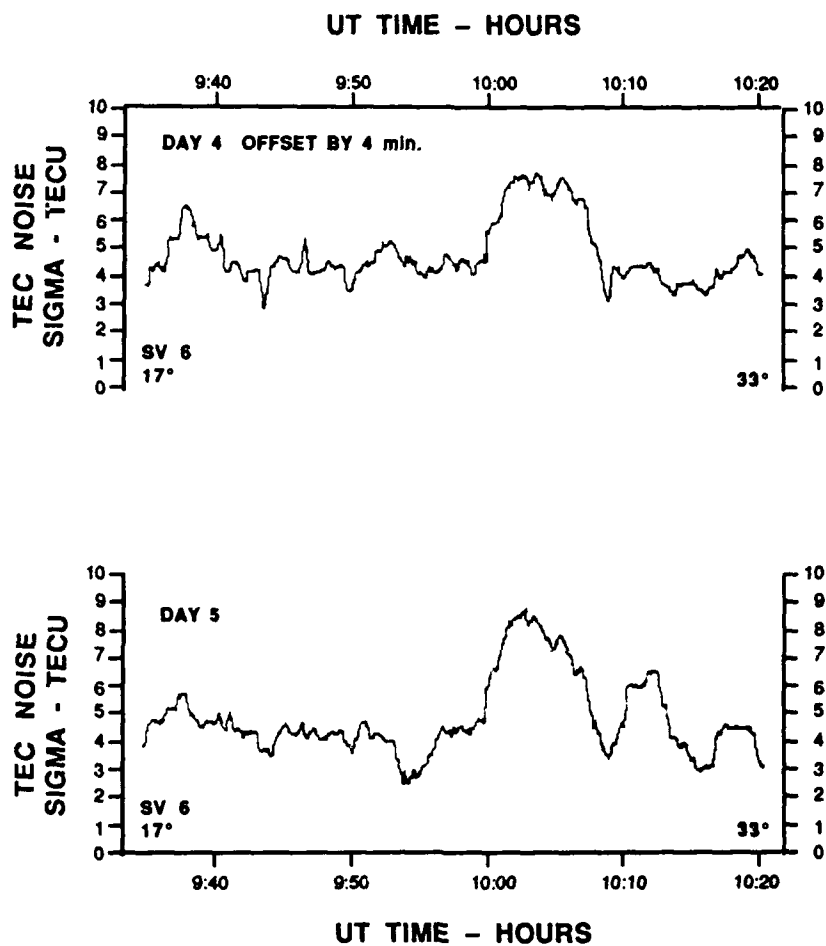


**FIGURE 19**  
**TEC NOISE SIGMAS OVER 180 s INTERVALS**  
**IONOSPHERE CONTENT REMOVED**

value of 1.74 TECU measured in laboratory calibration tests is removed from the total TEC noise (difference of the squares) then an estimate of the TEC multipath noise remains. This TEC multipath noise estimate ranges from 2.5 to 7.3 TECU with an approximate mean value of 4.2 TECU. The source of this multipath is almost certainly the forward scattering of radio waves from the ground to the antenna since there were no obstructions nearby.

## 2. AIMS Measurements from Sondrestrom

Appendix A contains a series of plots derived from data taken at Sondrestrom, Greenland on 7-8 March 1987 during the Polar ARCS campaign. The plots are divided into four groups with one group for each tracker. The scenario for this data set is also given in the Appendix as Table A-1. Each group contains five plots in the order, L2 C/No, Vertical TEC, Vertical TEC Smoothed Over One Minute, Relative TEC - Cumulative, and Phase Reference Reset. On each plot, vertical lines are drawn to indicate the time when a different SV is acquired. The SV PRN number being tracked is shown to the right of the line; if the tracker is idle, a zero is shown in this space. In addition, the TEC and C/No plots have the SVs' elevation angles shown.

The C/No plots show very little fluctuation in signal amplitude above the measurement noise of 1-2 dB-Hz except in the regions where the SVs are being acquired and dropped near the horizon. This indicates that very little L-band amplitude scintillation is occurring.

The vertical absolute TEC plots show the slowly changing trend in the ionospheric content over the day. The increases in the noise are primarily due to the obliquity effect explained in the previous section. There are a number of points that have values off the graph as indicated by the points at the upper and lower edges of the plots. These points

are not valid measurements of the TEC and most of them are edited out before the 60 s averages are computed. However, some of these invalid points are not detected by the editing process and appear in the smoothed data as shown in Fig. A3, top plot, right after UT 22 hours of day where a large spike occurs. The editing process used for these plots is a simple one and should be improved to remove all of the invalid data points. These points are discussed in more detail later.

In the Sondrestrom campaign, the antenna was placed in a small depression in the ground and the edges of the antenna were packed with snow. This configuration would be expected to reduce multipath produced by forward scattering. An example of the multipath noise from the Sondrestrom data can be seen in Fig. A7 in the top plot. The total TEC noise is about 2.4 TECU in first segment after UT 20 hours of day corresponding to a TEC multipath noise of 1.7 TECU. This indicates that antenna positioning directly on the ground provides lower multipath noise than tripod mounting. Note that the TEC noise is decreasing as the satellite elevation decreases in Fig. A7; this is due to the fact that vertical TEC is displayed rather than the slant TEC.

These examples indicate that multipath can be a significant problem even in an environment without obstructions. The effects of multipath noise can be reduced somewhat by averaging in postprocessing, but residual effects will probably remain. The ground siting configuration used in the Sondrestrom campaign appears to be effective, but studies should be performed to see if further reductions can be obtained.

The relative TEC - Cumulative plots show the change in the TEC derived from the phase measurements. The values represent the change in the TEC from the last reference point, where the relative TEC value is set to zero. The times at which the relative TEC references are reset are marked in the last plot of each group, the Phase Reference Reset

plot. In this plot, a value of one indicates valid relative TEC data are available in this time period, referenced to the previous vertical line. A value of zero indicates that only invalid data (bad quality vector or mode) are available and a missing line indicates that no data are available. This plot should be viewed in conjunction with the relative TEC plot.

There are three reasons for a phase reference reset to occur. First, a scenario change at that time which would require returning to standard navigation data collection to acquire the new SVs. This means that all four trackers would show a reference reset since high speed ionospheric data cannot be collected simultaneously with standard navigation data. This produces 10 reference resets for this particular data set since there are 10 scenarios as shown in Table A-1. Second, one of the SVs could fall out of track and require a return to standard navigation data collection. This happens rather infrequently, about once every 40 min. on the average, but again produces a reference reset on all four trackers. Third, if one or more data points are lost in data transfer from the receiver to the main frame used for postprocessing, then the current software will reset the reference. This is the reason for most of the reference resets in this data set and in all of the Sondrestrom data. Since all four trackers are reset simultaneously under the current processing scheme, the four Phase Reference Reset plots are identical except for times when a tracker is idle.

The reasons behind these reference resets are discussed later in the system limitations section, but the major point to be made here is that the number of reference resets are far larger than the number of tracking losses. Most of the reference resets could be avoided if the full cumulative phase value were recorded rather than the point-to-point change, as is currently done. Also, the reference resets produced by data transfer errors only affect the postprocessed data; they do not affect the realtime data observed on the strip chart recorder. Many of



the data transfer reference resets could be avoided by improved postprocessing techniques.

Many examples of complex TEC structures were observed during the Polar ARCS campaign. A typical observation of an ionospheric patch is shown in Fig. 20. This plot shows the observed relative TEC - cumulative (with one phase reference reset marked by a vertical line) along with calculated curves for two different absolute TEC levels. The calculated curves indicate the change in the slant relative TEC due to geometry only assuming typical absolute TEC values. The calculated curves have been offset slightly from zero to facilitate the comparison. A comparison of the observed and calculated values indicates that the observed values are not due solely to changes in the line-of-sight geometry, but reflect actual localized patches of enhanced electron density.

### C. System Limitations

There are several system limitations that need to be addressed in order for the system to achieve its full utility. These limitations are discussed briefly below along with suggestions for the type of modifications that are needed to overcome these limitations. A complete discussion of the details involved in the modifications is not presented since this is outside the scope of this report.

#### 1. Data Rate

It would be helpful to be able to increase the phase measurement data rate to allow smaller scale ionospheric irregularities to be detected. The maximum data rate currently achieved by AIMS is 120 ms data for carrier phase measurements when four satellites are in track. The absolute maximum rate allowed by the TI 4100 multiplexing scheme for tracking a single satellite is 20 ms (50 Hz). The data

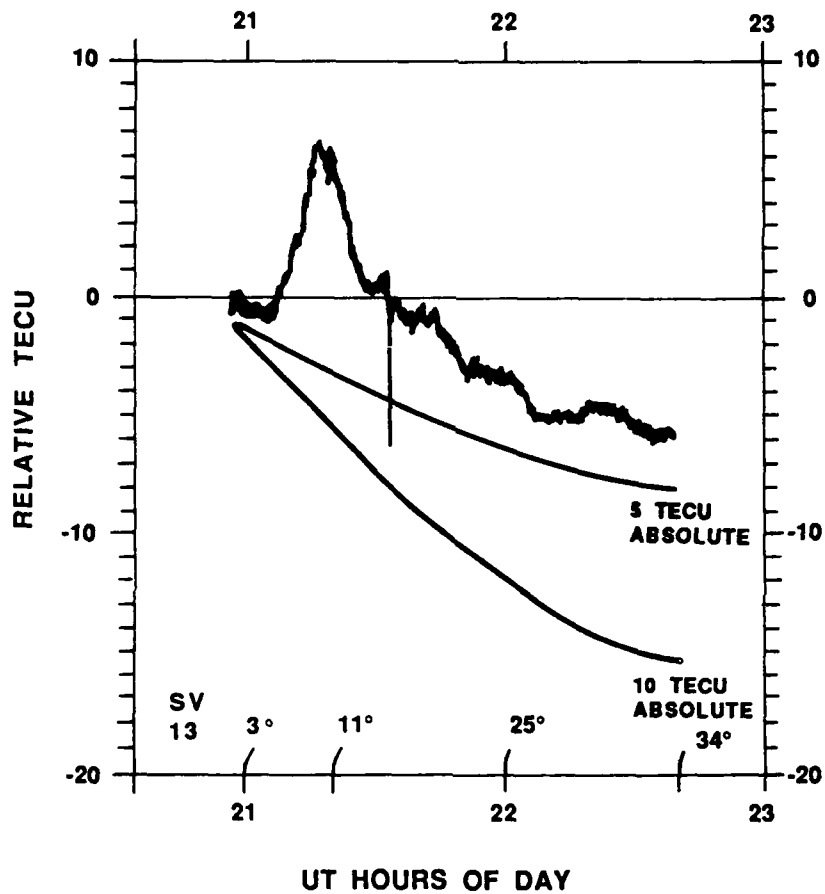


**FIGURE 20**  
**IONOSPHERIC PATCH**  
**RELATIVE TEC DATA FROM**  
**SONDRESTROM 13 FEB 1987**

throughput limitations, the data processing demands and the tracking of multiple satellites are the factors that prevent the absolute maximum from being achieved.

A large amount of effort has been expended to minimize the data throughput and data processing demands in order to achieve a higher data rate. The option of tracking fewer than four satellites to achieve a higher data rate, however, has not yet been seriously investigated. Brief test runs, however, have shown that 80 ms data (4 FTF) is feasible when only three satellites are in track. Longer test runs and more analysis will be required to investigate the long term effects of this higher data rate on system performance. Also, other test runs may show that even higher data rates are possible when a single satellite is being tracked.

## 2. System Crashes

A system crash is defined as any event which does not allow continued data collection without operator interaction. Typically, to restart the system, the operator must reload the receiver software, an operation that takes from 30-45 min. System crashes can occur when the receiver accepts control data (e.g., almanacs from the satellites or commands from the external processor) that are corrupted. There is a series of error detectors in the system, but if the corrupted control data gets past these built-in safeguards then a system crash may occur.

The system crashed approximately once every three days in the Sondrestrom campaign over approximately a one month timeframe. This behavior has not been duplicated in tests conducted at ARL:UT. The system has operated continuously for two weeks or more at ARL:UT without crashing. It was suggested that the more frequent system crashes at Sondrestrom may be related to tracking PRN 7. This SV was classified as unhealthy because of the degraded condition of its oscillator, but this

did not affect its usefulness for ionospheric measurements. It does mean that its performance was not as closely monitored because relatively few users were tracking this SV.

This SV was included in almost all of the scenarios at Sondrestrom. Short term tests at ARL:UT have tracked PRN 7 without system crashes, but it has not been included in any of the long term tests. It is possible that its message information, which was collected periodically, was somehow corrupted causing the abnormal behavior in AIMS. This problem will require further investigations before firm conclusions can be drawn.

### 3. Phase Reference Resets

The relative TEC - cumulative parameter is derived from the point-to-point phase change measurements output from the receiver. The point-to-point changes are summed up in both the external processor and in postprocessing to provide the change in TEC from the beginning of this summation. This summation is reinitialized whenever a valid point-to-point measurement is not available. This reinitialization is referred to as a phase reference reset.

As discussed in Section VII. B, there are three reasons for a phase reference reset. First, a scenario change which requires a return to standard navigation data collection. Second, a loss of lock on one or more satellites which also requires a return to standard data collection. Third, a loss of one or more data points in the data transfer from the receiver to the external processor or to the mainframe used for postprocessing.

The phase reference resets found in postprocessing are summarized for several data sets in Table VI. The first three of these data sets (I2124, I2122, I2052) are high speed (120 ms) data sets

TABLE VI  
PHASE REFERENCE RESET SUMMARY

DATA SET NUMBER	DATA PARTITION (BLOCKS/1000)	TOTAL RESETS	TRACKING LOSSES			DATA TRANSFER LOSSES (BLOCKS)
			SCENARIO CHANGE	OTHER <100s	>100s	
I2124	0-10	9	4	2	3	0
	10-20	12	4	1	0	24
	20-30	108	3	2	1	32
	30-40	218	3	4	3	390
	40-50	11	4	5	0	6
	50-56	7	2	5	0	0
	<hr/> 0-56	<hr/> 365	<hr/> 20	<hr/> 19	<hr/> 7	<hr/> 746
I2122	0-22	65	7	9	8	224
I2052	7-24	19	3	8	4	20
I2043	0-2	15	1	3	3	8
I2045	0-2	14	1	2	2	9

recorded at Sondrestrom and the last two (I2043, I2045) are lower speed (1 s) data sets recorded at ARL:UT. The second column of this table gives the data partitioning which represents the location of the data on the 9-track tap, as well as the total quantity of data in the data set. The first data set, I2124, contains 56,000 block 63s which corresponds to one complete 9-track tape covering 18 h of tracking. The third column gives the total number of phase reference resets found in the corresponding data partition. The first data set has the resets calculated for individual sections of 10,000 blocks as well as the total data set. I2124 has a much larger number of data resets than the other sets simply because it contains a larger amount of data.

The fourth column in Table VI gives the number of phase reference resets due to scenario changes. The fifth and sixth columns give the number of resets due to tracking losses other than a scenario change (random loss-of-lock), which is further divided into loss-of-lock periods lasting less than or more than 100 s. The seventh column gives the number of Block 63s that were lost in the data transfer to postprocessing. If two or more of the Block 63s lost in data transfer are contiguous they will only be counted as one phase reference reset. Therefore, the numbers of blocks lost may be larger than the number of resets so the columns do not always add up exactly.

The phase reference resets due to tracking losses are about what one would expect from the system. The scenario related losses are determined by the planned scenarios. The data sets shown in Table VI and others show an average of 1-2 phase reference resets per hour due to loss-of-lock occurrences other than planned scenario changes. This is in line with the one loss-of-lock per hour average that has been measured for the TI 4100 in typical field campaigns when standard (low speed) geodetic data are recorded. Both the high speed data sets and the low speed show similar loss-of-lock averages.

The only improvement envisioned for reducing the number of phase reference resets due to tracking losses would be to avoid the resets on the trackers that do not actually lose lock. When the system returns to standard navigation data collection due to the loss-of-lock of one SV, the other three SVs maintain their phase lock during the transition from standard data to high speed data and back. This feature is not used in the current system since only point-to-point data are output from the receiver. If the cumulative phase were output instead of the point-to-point then the phase reference would only have to be reset for those SVs that actually lost lock. This same method would work for scenario changes.

To implement a method of outputting the cumulative phase is a possibility but probably would require some compromises. The cumulative value would require a larger word size which would further tax the data throughput. It may not be feasible to output the full cumulative value for each point but it may be possible to output the cumulative value every tenth point or so. This could be used in postprocessing to reconstruct the missing data. Further investigations are needed to determine the feasibility of this approach.

The phase reference resets due to data transfer losses pose a more perplexing puzzle that has not yet been fully resolved. All of the data recorded at Sondrestrom show a very high incidence of data transfer losses with the majority of losses occurring near the center of the 9-track tape. This pattern can be seen in Table VI for data set I2024. All of the other Sondrestrom tapes shown a similar pattern except for data set I2052. These data were recorded on a tape from a different source and was the first tape used. It was returned to ARL:UT soon after it was recorded whereas the other tapes were stored in Sondrestrom for the duration of the campaign. This data set shows far fewer data transfer losses than the others. In addition, the data recorded at

ARL:UT does not show either the quantity of data transfer losses or the particular pattern of losses concentrated near the center of the tape.

These clues do not provide enough evidence to identify the source, or sources, of the data transfer losses but they do suggest that the environment may play an important role. It is suspected that the low-humidity environment of Sondrestrom may be the culprit. Further tests will be required to clearly identify the reasons for these data transfer problems. The phase reference resets due to data transfer losses could be avoided by the above method of outputting the cumulative phase rather than the point-to-point.

The phase reference reset problem can also be overcome to some extent by more sophisticated postprocessing techniques. This would entail estimating the missing TEC data from the surrounding points by an appropriate interpolation technique. If the missing data only spanned a short time interval and the TEC was not changing rapidly this method would not generate a significant amount of error. A brief look at the Sondrestrom data indicates that many of the reference resets could be avoided by this technique.

#### 4. Spikes in Absolute TEC Data

The absolute TEC data derived from the pseudorange measurements occasionally show spurious values which are clearly invalid values. These spurious values are produced inside the TI 4100 and their source is currently unknown. They usually have a constant value which can be easily distinguished from valid TEC values, but sometimes the invalid value will differ from the constant. A simple filter is currently implemented to detect and edit these constant values. A more sophisticated filter should be implemented to detect those spurious values that differ from the constant.



The system limitations discussed in this section do not prevent AIMS from acquiring useful ionospheric data but they should be investigated to gain the full utility of the system.

## VIII. EVALUATION OF POTENTIAL AIRCRAFT APPLICATIONS FOR AIMS

The AIMS system was designed with a possible future aircraft installation in mind. The goal was to design a ground based ionospheric monitoring system that could be used on board a research type aircraft with a minimum of modifications. Whenever feasible, hardware components were chosen with potential aircraft applications in mind. Section A discusses the modifications that would be required to operate the TI 4100 based AIMS system on board an aircraft to obtain the same type of ionospheric measurements that the ground based AIMS system records. In Section B the feasibility of using the AIMS GPS receiver to provide aircraft navigation information, in addition to the ionospheric information, will be discussed.

### A. Modifications to AIMS Required for Aircraft Applications

This section focuses on four areas of the AIMS system which might require modifications for aircraft operations: TI 4100 tracking bandwidths, GPS antenna suitability, receiver position updating procedures, and data recording media. The general issue of the aircraft specific installation requirements (weight/size/power limitations) is not addressed here since the specifics of the aircraft are not available at this time but they are an important issue which needs to be studied.

#### 1. TI 4100 Tracking Bandwidths

The TI 4100 receiver was designed for potential aircraft applications and has been used successfully in this mode by several agencies, e.g., Texas State Department of Highways and Public Transportation (TSDHPT) and the National Geodetic Survey (NGS). To accommodate the dynamic environment of the receiver the TI 4100 allows the user to change tracking loop bandwidths with external commands. In general, the greater the range of the expected dynamics (usually

specified by the maximum acceleration value) the larger the bandwidths required to maintain track. There are four separate tracking loops with bandwidths and loop orders that can be adjusted independently of each other.

The primary objective for the bandwidth selection for the ground based AIMS system was to select the bandwidth set which maximized the resolution of the ionospheric phase advance measurements while maintaining acceptable tracking performance for the system as a whole and minimizing the measurement noise levels. Through a series of tracking performance tests a bandwidth set was selected that provided the maximum allowable effective bandwidth for ionospheric phase advance measurements for the TI 4100 (PLL DIFF = 6 Hz, see Table VII). The bandwidths which do not directly affect the resolution of ionospheric phase measurements were then chosen to optimize the tracking performance of the system as a whole and minimize the measurement noise levels. Table VII gives the bandwidths selected for the AIMS system along with a more detailed explanation of their functions. This bandwidth set is referred to as User Dynamics Class 50 (UDC 50).

The standard set of tracking loop bandwidths recommended for aircraft applications with medium dynamics (acceleration less than  $15 \text{ m/s}^2$ ) is also given in Table VII. This set, which is referred to as UDC 3, has a narrower bandwidth for the phase lock difference loop (PLL DIFF) than UDC 50, but wider bandwidths for the other categories. This means that the effective bandwidth for ionospheric phase measurements would be decreased roughly by a factor of two if the recommended bandwidths for medium dynamics were used. It is possible, however, that using modified UDC 3 with a 6 Hz PLL DIFF bandwidth would provide acceptable tracking performance for the AFGL aircraft application.

The current AIMS system allows for adjusting the bandwidths using external commands so that no software modifications will be

TABLE VII  
TI 4100 FINAL TRACKING BANDWIDTH COMPARISON

USER DYNAMICS CLASS	TRACKING BANDWIDTH (Hz)			
	<u>DLLSUM</u>	<u>DLLDIFF</u>	<u>PLLSUM</u>	<u>PLLDIF</u>
50	0.05	0.05	5.0	6.0
3	1.0	1.0	8.0	2.5

User Dynamics Class 50 is currently used for AIMS ground based applications.

User Dynamics Class 3 is recommended by TI for aircraft applications with medium dynamics (maximum acceleration =  $15 \text{ m/s}^2$  -  $1.5g$ ).

DLLSUM/DIFF represents the delay lock loop sum ( $L1 + L2$ ) or difference ( $L1 - L2$ ) tracking loops which are used to provide pseudorange measurements.

PLLSUM/DIFF represents the phase lock loop sum ( $L1 + L2$ ) or difference ( $L1 - L2$ ) tracking loops which are used to provide phase measurements.

required for these tests. One option that might be explored is to develop a menu of bandwidth sets for different dynamics which the user could control depending on the aircraft planned maneuvers. This could be easily implemented in the current software. Another option which could be investigated is the effects of modifying the loop orders.

In summary, the recommended bandwidth set for aircraft dynamics provides an effective bandwidth of 2.5 Hz for the ionospheric phase measurements. If the maximum 6.0 Hz bandwidth is required then a series of tracking performance tests would be required to search for a bandwidth set that provides acceptable tracking performance. Even if the recommended bandwidth set were used, this set would have to be tested to insure that tracking performance was satisfactory for the typical aircraft dynamics likely to be encountered in an actual campaign. A limited amount of testing could be performed in a laboratory environment but the majority of testing would have to be done in flight.

## 2. GPS Antenna Suitability

The TI 4100 antenna is not the optimum choice for aircraft applications because of its high profile. The TSDHPT and NGS have both chosen to replace the TI 4100 antenna with a low profile Dorne and Margolin antenna for their aircraft applications. The antenna has a dome shape, approximately 3 in. in diameter and 1.5 in. in height, and costs approximately \$1000.

In order to use the Dorne and Margolin antenna with the TI 4100 a preamplifier must be installed in the antenna. The hardware is commercially available and ARL:UT is capable of making the necessary modifications. (ARL:UT performed this same modification for the TSDHPT antenna in 1986.) The hardware costs would be around \$1500 and the technician time required would be approximately one man-month. It is

possible that other commercially available antennas could also be feasible for this application.

The issue of the multipath level for this particular antenna and for the aircraft installation in general would have to be addressed. No exceptional problems of multipath have been noted in the TSDHPT aircraft data but it has not been investigated in detail. It might be feasible to obtain a sample data set from TSDHPT to investigate this problem before an antenna was chosen. The optimum placement of the antenna on the AFGL aircraft would also require some testing.

### 3. Receiver Position Updating Procedure

The current AIMS system requires that the user input a receiver position to be used in the satellite search portion of the TI 4100 initialization procedure. The input receiver position along with the satellite almanac information is used to calculate an estimated Doppler frequency for each of the satellites. This receiver position does not have to be precise because the receiver searches through a frequency window to find the satellite Doppler frequency. The window width determines the acceptable position error but this width also determines the average satellite acquisition time.

The ground based AIMS system has a fixed frequency search window of 200 Hz which allows for roughly 100 km in station position error. This window provides an average satellite acquisition of 60 s which is acceptable for most applications. There is currently no provision in the AIMS software for changing the search window width but this could be easily implemented, if needed.

If the AIMS system is operating on board a moving aircraft, the Doppler must be estimated to an accuracy within the constraints of the search window. To estimate the Doppler, the satellite-to-receiver line

of sight velocity is needed. This will require knowledge of the receiver position and velocity.

If the receiver position is known precisely and the line of sight velocity is estimated to be zero, the nominal 200 Hz window would allow acquisition for a line of sight velocity up to 40 mph. The horizontal velocity is related to the line of sight velocity by

$$v \text{ (line of sight)} = v \text{ (horizontal)} * \cos \text{ (elevation angle of sv)}$$

so the 40 mph would also represent a maximum for the horizontal velocity error that could be tolerated.

The 200 Hz window will allow for either a 100 km position error or a 40 mph velocity error before acquisition will be affected. These rough estimates indicate that some sort of receiver position/velocity update procedure will be required to maintain the nominal 200 Hz search window. Widening the search window is an option but the question of acceptable acquisition times would have to be addressed. There are two different types of procedures that could be used for updating the receiver's position and velocity: externally provided updates and internally generated updates.

An externally provided update procedure could take many forms but basically the receiver would have to be provided with the estimated position and velocity on an ongoing basis. The accuracy and update rate would depend on the flight dynamics. An internally generated position/velocity could be generated by the GPS navigation information but would require extracting this information from the AIMS system. This option is discussed in more detail below. The position accuracy requirements could be easily satisfied with either of these two options. They should be investigated in more detail, however, to see which option is easier to implement.

It is obvious that a more rigorous analysis will be required in order to recommend a specific procedure. This analysis will require estimates of the flight dynamics, typical campaign flight patterns, and information regarding other navigation systems available on board.

#### 4. Recording Media

The ground based AIMS system records the ionospheric data on a 9-track IBEX tape system that may not be suitable for aircraft operations. Although IBEX claims that the system can be used for helicopter operations, personal experience has indicated that this may not be feasible. Operator intervention is often required for system adjustments, which may not be possible in an aircraft environment. Two other alternative systems that may be more reliable are discussed below.

It is possible to use the TI cassette drive for recording the data but if the maximum AIMS data rate (approximately 275 Bytes/s for 4 FTF rate sampling) is to be achieved then the cassettes, with a 256 kbyte capacity, would have to be changed about every 15 min. A playback system would have to be developed for reading the data off the cassette tapes after the mission. This is a viable option but one major disadvantage would be the time involved in reading the cassettes: it takes approximately 15 min to read each cassette.

Another possible option would be to purchase a removable hard disk system such as one made by Syquest Corporation. This system provides 10 MByte of memory and is designed for use in dynamic environments. This type of system would cost approximately \$1000 - 1500 for the hard disk and a controller card needed to interface with a PC compatible.



## 5. Summary

In summary, it appears it is feasible to adapt the AIMS system to aircraft applications. The antenna and recording media would probably require modification but there are reasonable alternatives available for these components. The tracking bandwidths issue will have to be explored but in the worst case the effective bandwidth would probably only have to be reduced by about a factor of 2. The internal software for providing position updates to the TI 4100 receiver is already in place but a source for the position/velocity data needs to be selected.

### B. Feasibility of Using AIMS to Provide GPS Navigation Information

The AIMS system has all the necessary input GPS information available to perform navigation functions with an accuracy of 15-20 m for a medium dynamics application. The problem lies with accessing this information while maintaining the fast ionospheric data rate. The TI 4100 external processor interface has a limited throughput rate that is used to its capacity when the maximum data rate (4 FTF) is used. In reality, the 4 FTF data rate has not been achieved except in limited laboratory tests and a 6 FTF rate is used for most applications. The exact reasons for this inability to achieve the maximum rate are not completely understood but they are most certainly connected with the limited throughput.

The AIMS software inside the TI 4100, called CORE, performs the frequency difference prior to output of the data in order to reduce throughput. In order to perform positioning or navigation operations the undifferenced data must be output. This is possible only if the data rate for the ionospheric data is reduced. Prior experience indicates that an 8 FTF rate will probably be achievable with the added navigation data if a 15 s data rate for the navigation data is acceptable.

The next step is to use this information in the external processor to generate position/velocity updates. This involves incorporating a Kalman filter into the system and developing the appropriate displays. Much of the work for this task has been performed for large ship navigation systems but the Kalman would have to be modified for aircraft dynamics. The question of whether the current Z-158 microcomputer would be adequate to perform the added functions would also have to be addressed.

This task appears technically feasible but a careful study should be made of the alternatives. The primary advantage of using the TI 4100 to provide navigation information is its capability to operate independently of other systems. The primary disadvantage of this approach is the manpower time and costs involved. The modifications required to the CORE software inside the TI 4100 would require several man-months of effort for development and testing, with several more man-months required for external processor software development.

An alternate approach would be to use a totally different navigation system to provide position/velocity information. There are GPS systems on the market such as the Magnavox 4400 (L1 C/A code) that are designed for aircraft applications and could provide the accuracies needed for this application.

In summary, it appears that it is technically feasible to modify the AIMS system so that it could provide position/velocity information but this approach should be carefully compared to other alternatives.

## IX. SUMMARY

The ARL:UT Ionospheric Monitoring System, enhances ionospheric monitoring capabilities by tracking multiple satellites. This is accomplished by using the multiplexing feature of the TI 4100 receiver. Design considerations led to the selection of measurement bandwidths and sampling rates which optimized the effective sampling rate of scintillation parameters while maintaining sufficient tracking bandwidths. Relative TEC (phase-derived) is measured with a bandwidth of 6 Hz and sampled at 8.33 Hz. Amplitude scintillation (C/No derived) is measured with a bandwidth of 1 Hz and sampled at 4.167 Hz. Absolute TEC (pseudorange-derived) is measured with a bandwidth of 0.05 Hz and sampled at 4.167 Hz.

The system is built around the receiver, an external processor, and a number of peripheral devices including a tape drive, a stripchart, a monitor, and a printer. The external processor software controls the receiver software (CORE) which processes the GPS signals. CORE samples the GPS signals, differences the data across the two L-band frequencies, and passes the data to the external processor. The external processor software then processes the data from the receiver into ionospheric parameters and outputs the data in realtime. Execution of these processes is automated with the use of a batch file designed to run continuously with little or no operator interaction. The operator is required to change the 9-track tape every 18 h of satellite tracking at 8.33 Hz. Data are stored on the tape without modification as they are collected from the receiver. A multi-step postprocessing software package developed on the CDC CYBER 180 is used to process the data recorded on tape to ionospheric parameters while providing maximum visibility of the data at each step of the processing.

Laboratory calibrations were performed on the system to verify the system operation and estimate the measurement noise of the ionospheric

parameters. Results from the time delay calibration for the pseudorange-derived absolute TEC show a dependence of the time delay measurement noise on the signal strength with a noise value of 1.74 TECU for a typical L2 C/No of 42 dB-Hz. Calibration of the phase-derived relative TEC shows a measurement noise value of 0.046 TECU when the signal is subjected to artificially induced scintillation with a 2 s period.

Samples of high latitude data from Sondrestrom, Greenland taken during the 1987 Polar ARCS campaign are presented. These data show evidence of complex ionospheric structures appearing as patches in the relative TEC measurements. The Sondrestrom data show reduced multipath effects when compared to mid-latitude data due to the improved antenna mounting procedures.

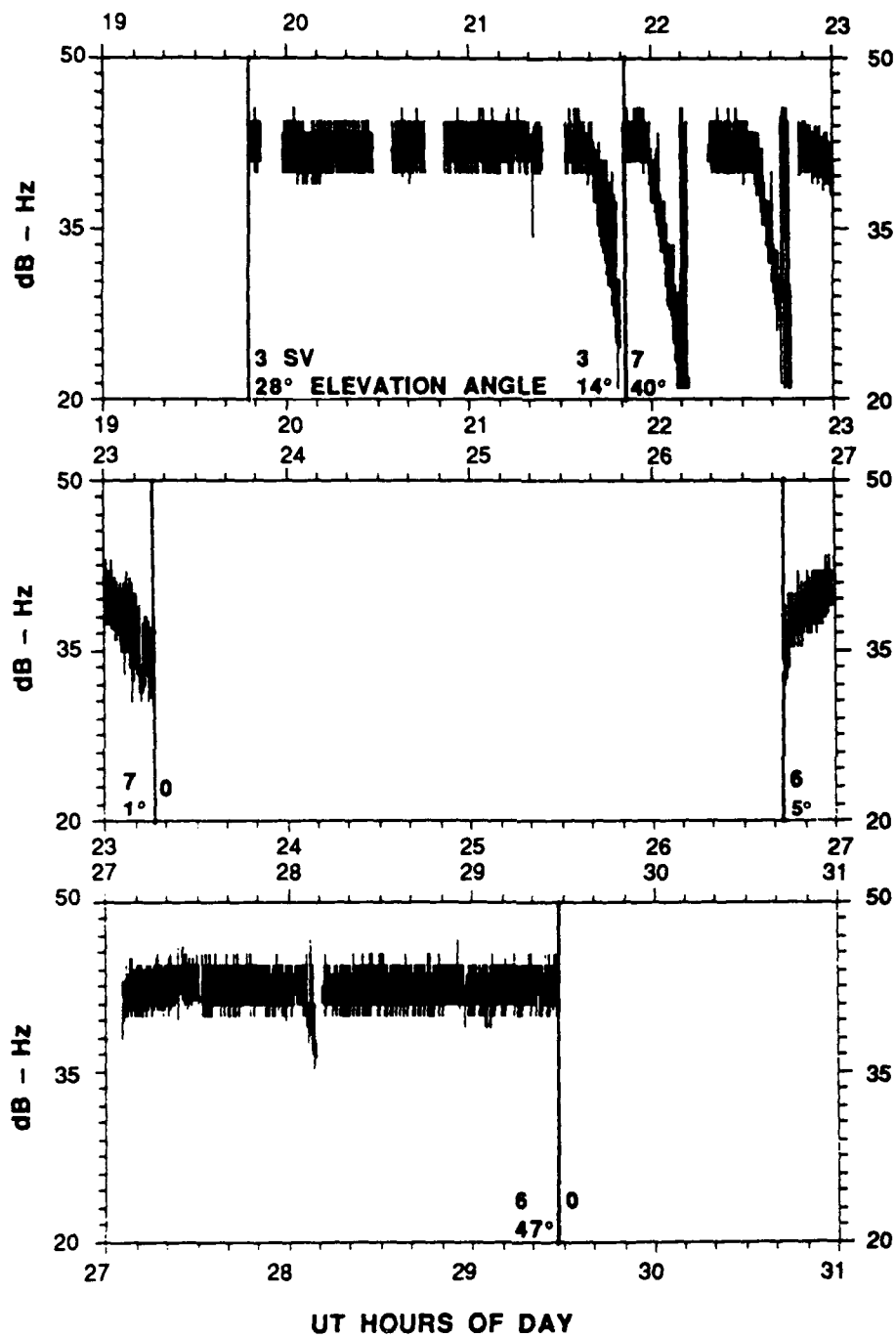
There are several system limitations that should be addressed in future work. The most severe limitations arise from the fact that AIMS currently outputs the point-to-point change in the phase-derived TEC change rather than the cumulative value. This feature arises from the desire to minimize the data throughput in order to attain the maximum possible data rate. The limitations due to this feature can be overcome to a great extent by outputting periodic cumulative values. This modification can probably be implemented without reducing the data rate. These limitations do not prevent the acquisition of useful ionospheric data, but they do limit the full utility of the system.

It appears to be feasible to adapt AIMS to aircraft applications. The antenna and tracking bandwidths would probably require modifications, and a source for the position/velocity update needs to be selected. It is probably feasible to modify the system to provide position/velocity information in addition to ionospheric information, but this approach should be carefully compared to other alternatives.

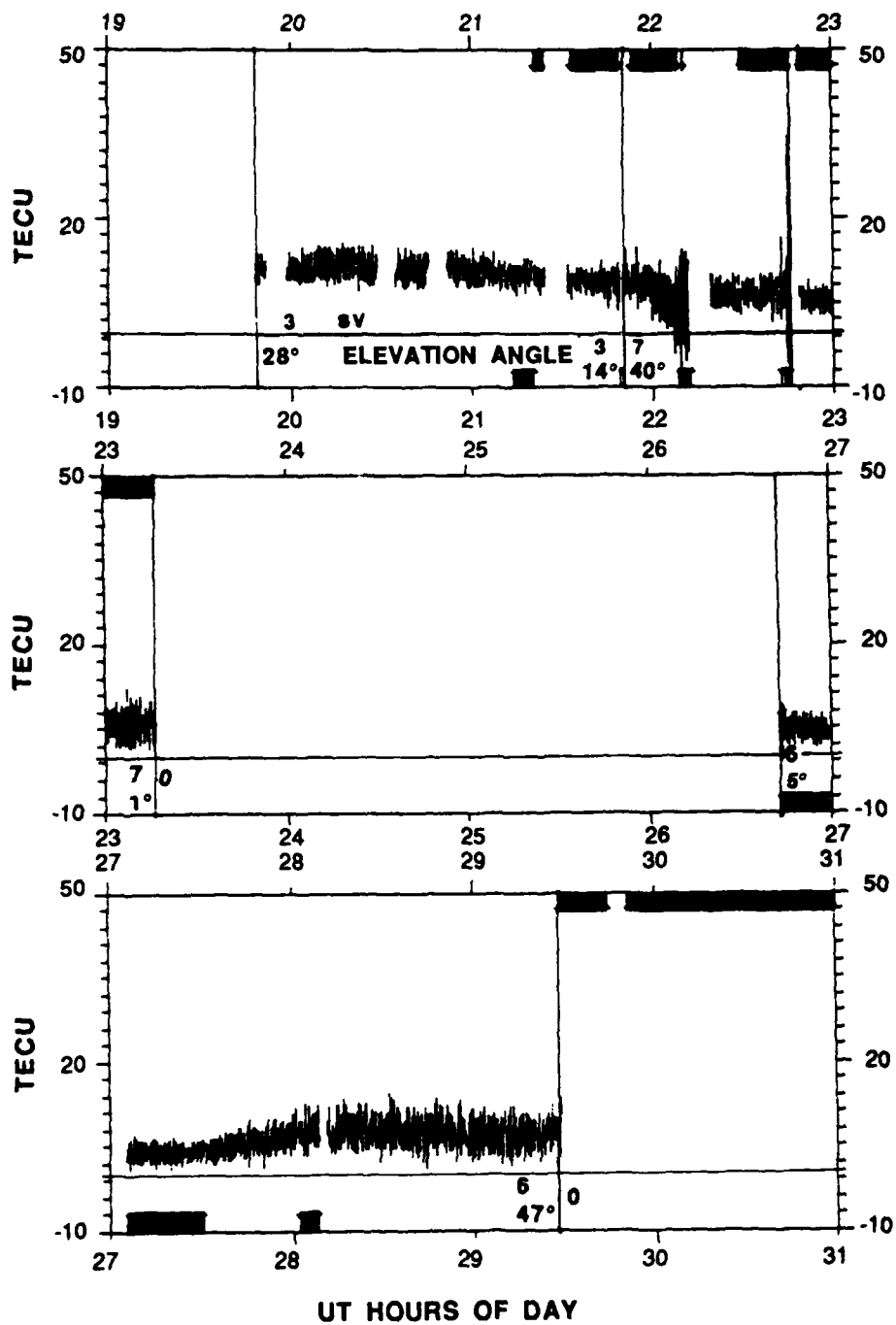
APPENDIX A  
SONDRESTROM DATA  
7-8 MARCH 87

TABLE A-1  
SCENARIOS USED FOR 7-8 MARCH 1987

<u>DATE</u>	<u>UT (HR)</u>	<u>SVs (PRN)</u>			
7 March 1987	1948	3	7	13	12
	2120	3	7	13	13
	2151	7	7	13	13
	2249	7	7	7	0
	2316	0	0	0	0
8 March 1987	0243	6	6	6	0
	0330	6	6	8	8
	0408	6	6	8	9
	0456	6	11	8	9
	0528	0	11	8	9



**FIGURE A1  
TRACKER 1  
L2 C/NO versus TIME**



**FIGURE A2**  
**TRACKER 1**  
**VERTICAL TEC versus TIME**



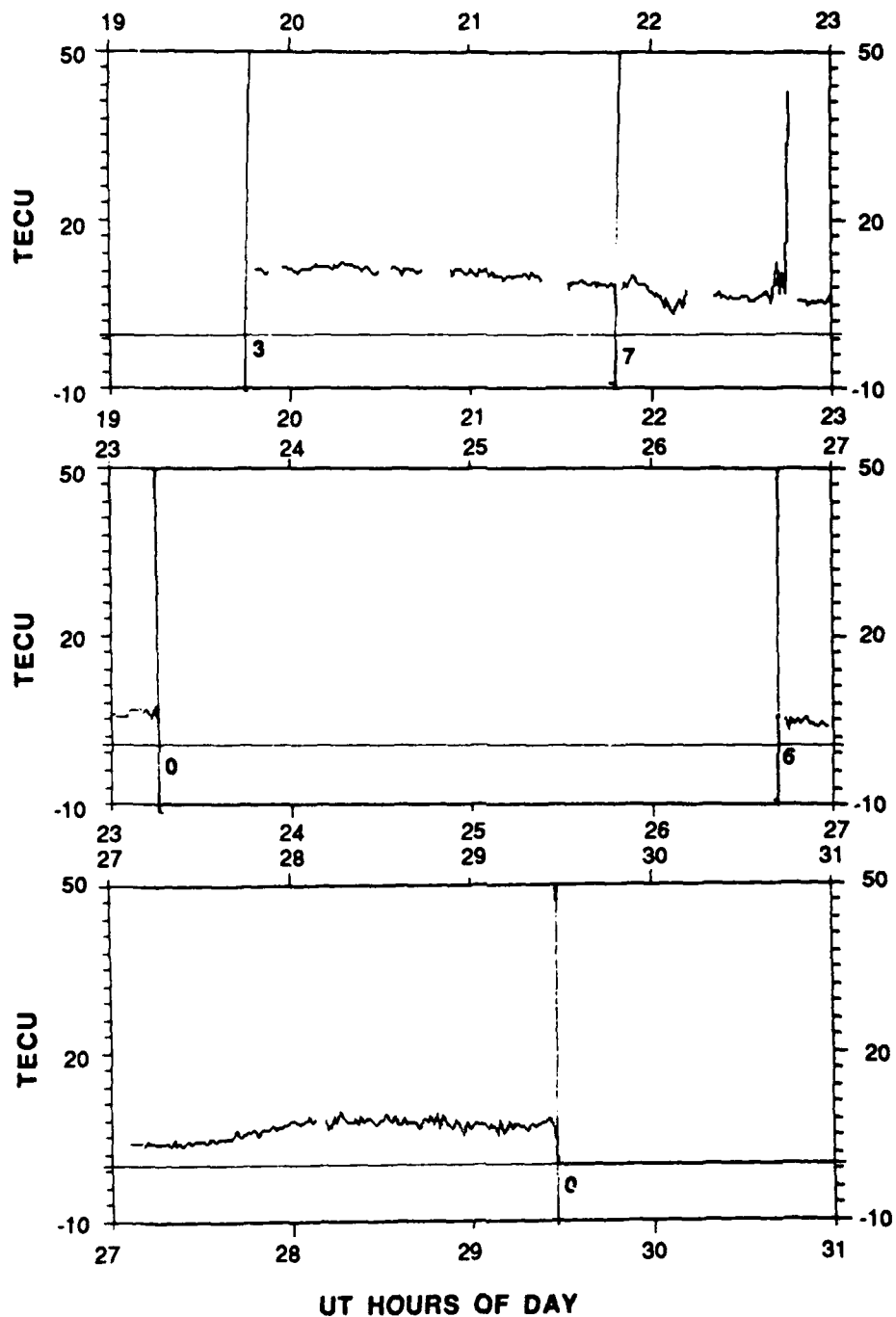


**FIGURE A3**  
**TRACKER 1**  
**VERTICAL TEC versus TIME**  
**SMOOTHED DATA**

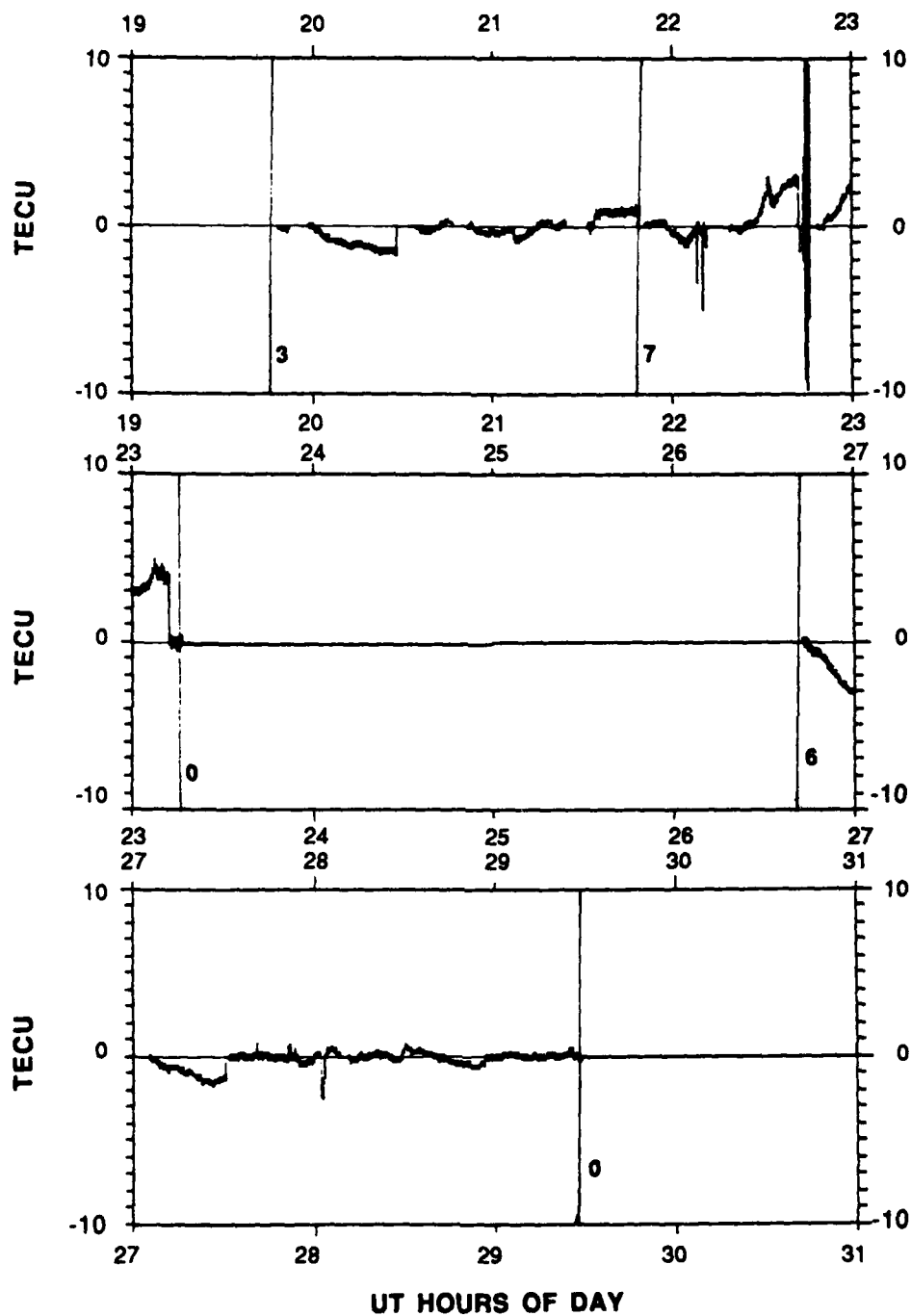


**FIGURE A4**  
**TRACKER 1**  
**RELATIVE TEC - CUMULATIVE versus TIME**

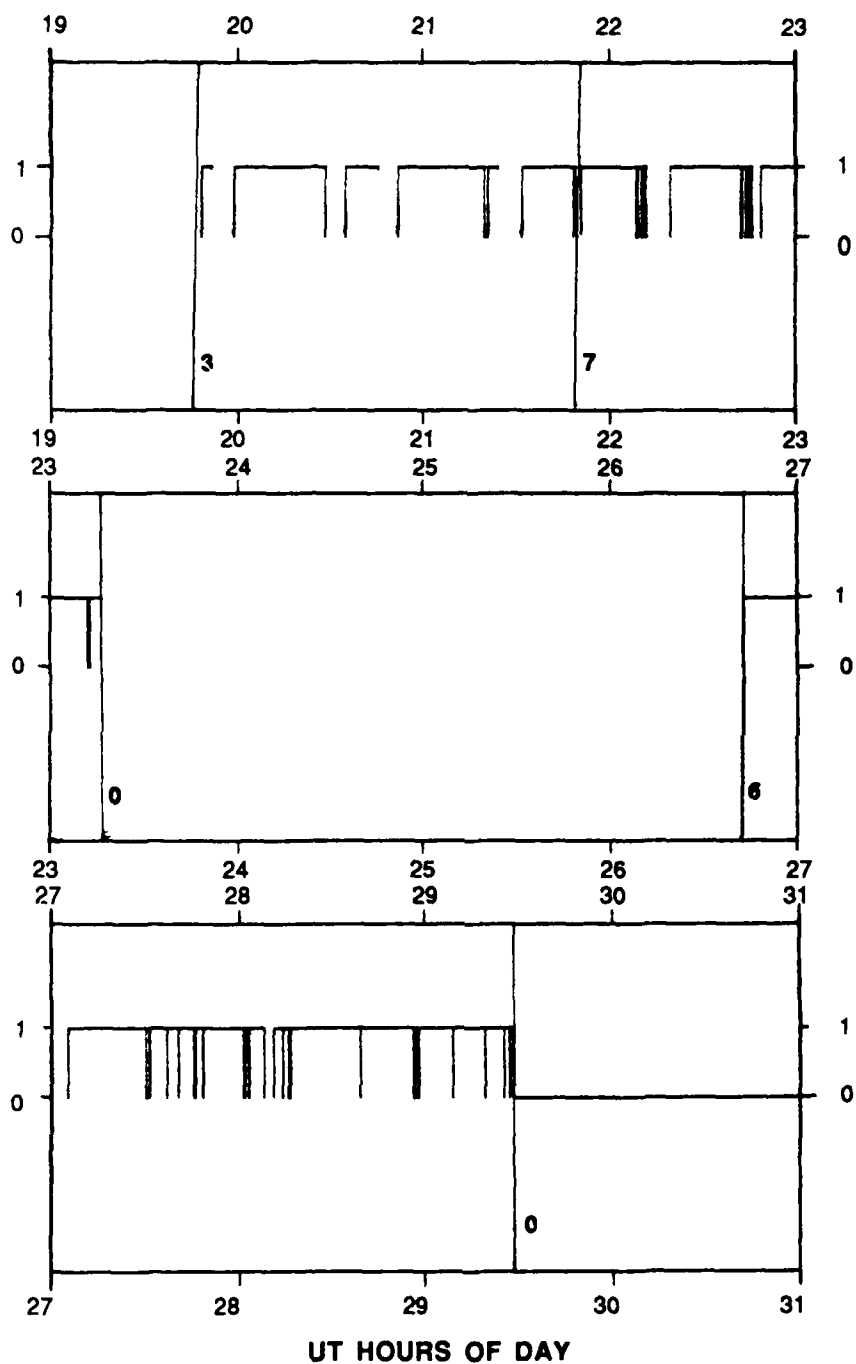


**FIGURE A5  
TRACKER 1  
PHASE REFERENCE RESET TIMES**

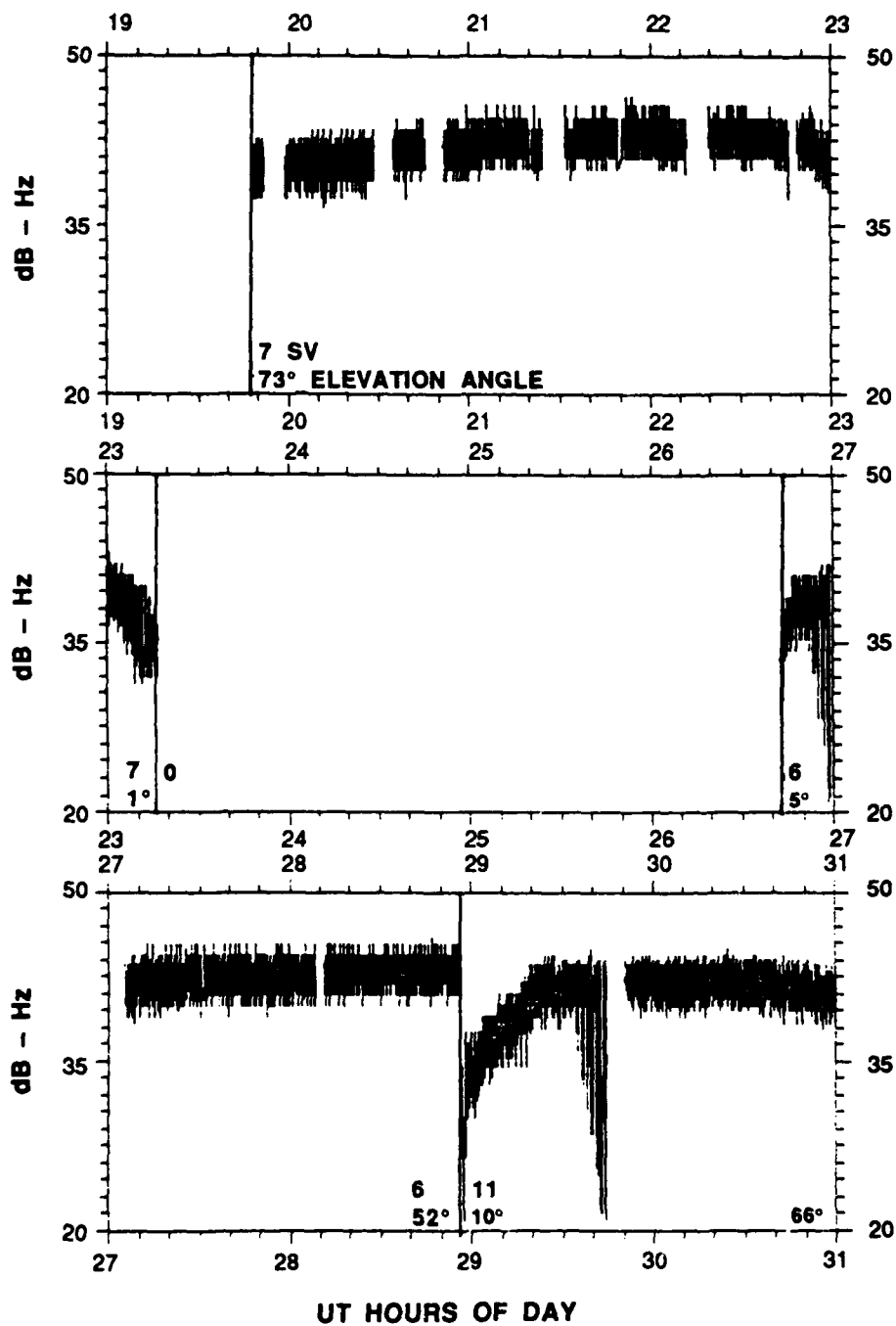


**FIGURE A6  
TRACKER 2  
L2 C/N0 versus TIME**

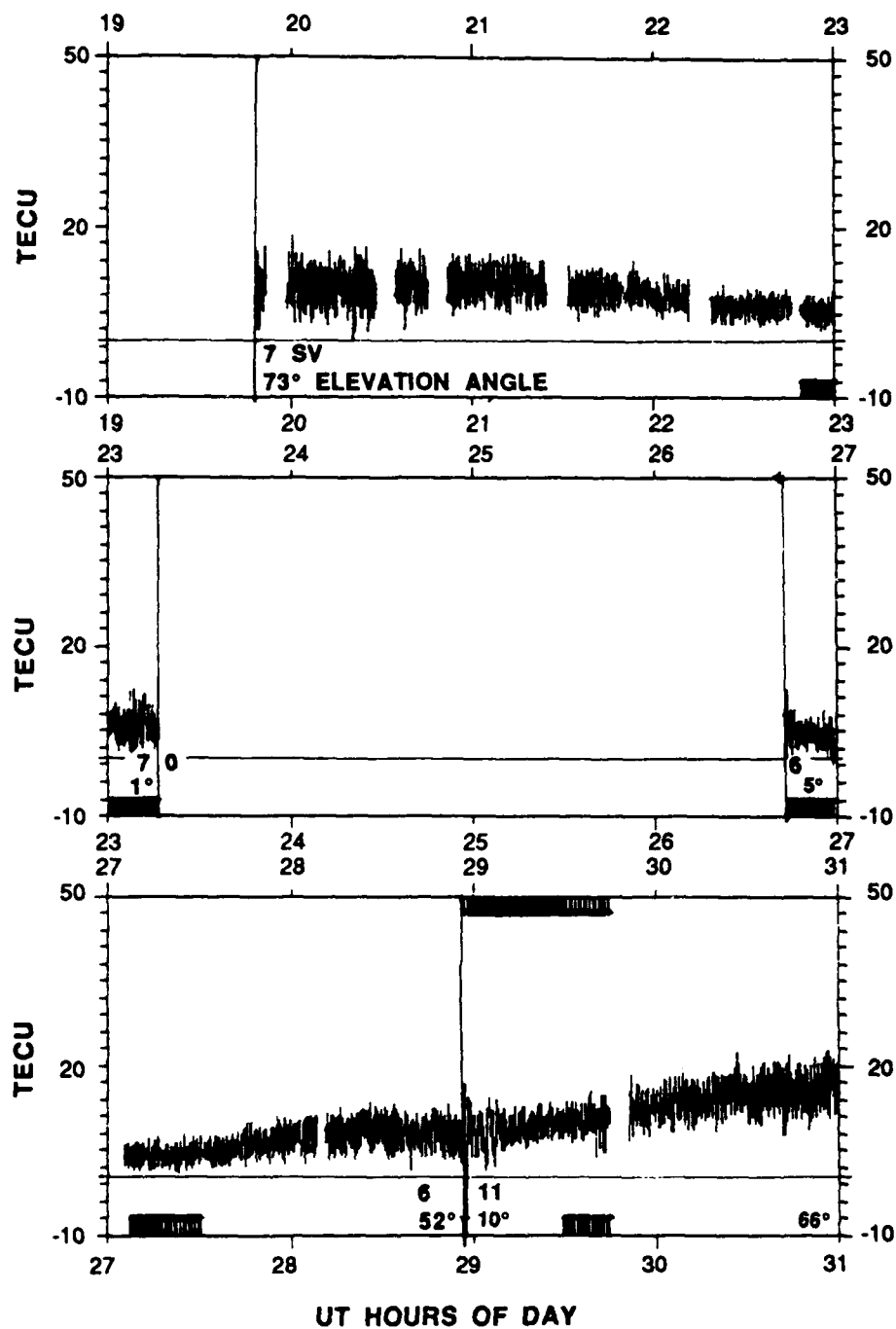


**FIGURE A7  
TRACKER 2  
VERTICAL TEC versus TIME**

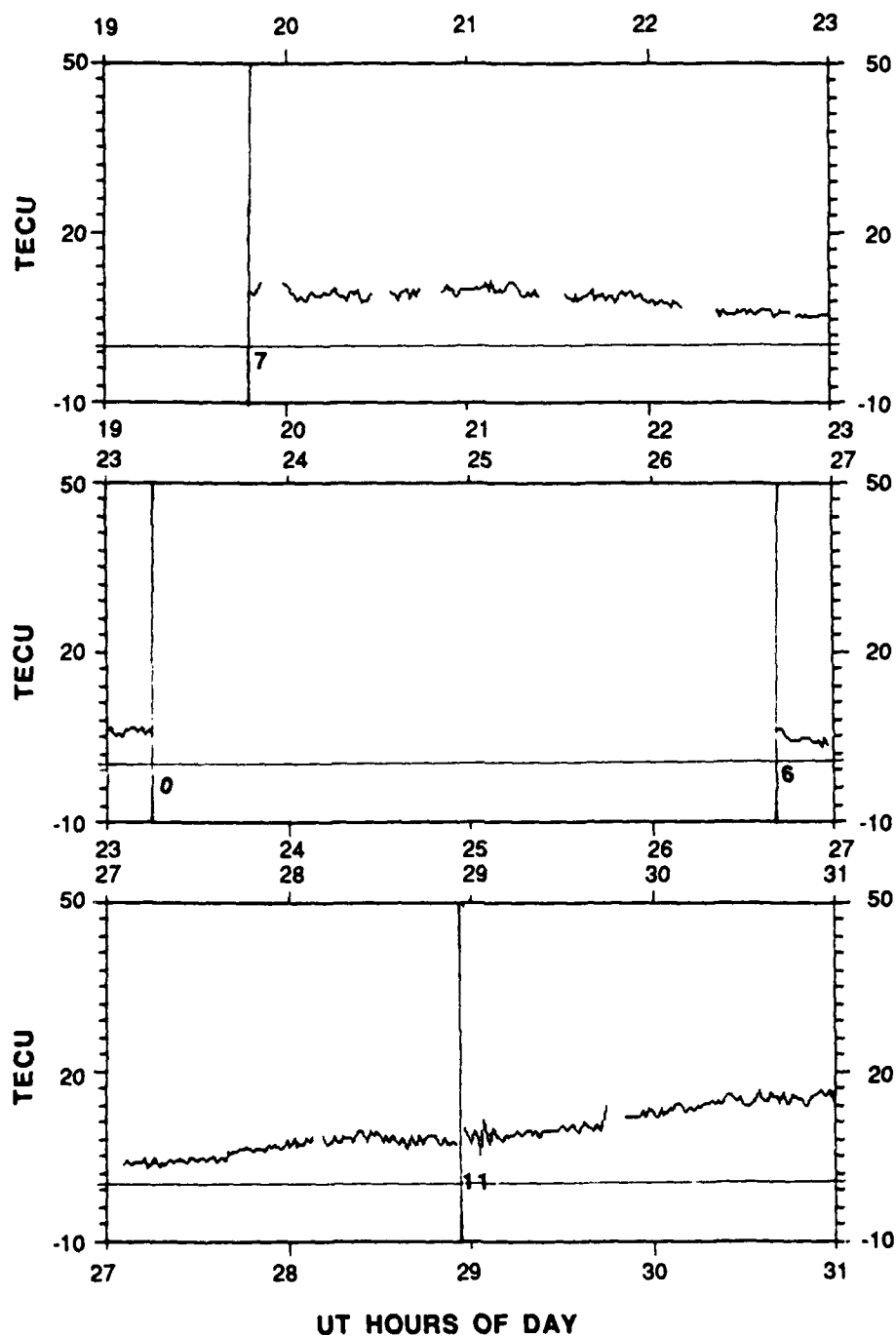


**FIGURE A8**  
**TRACKER 2**  
**VERTICAL TEC versus TIME**  
**SMOOTHED DATA**

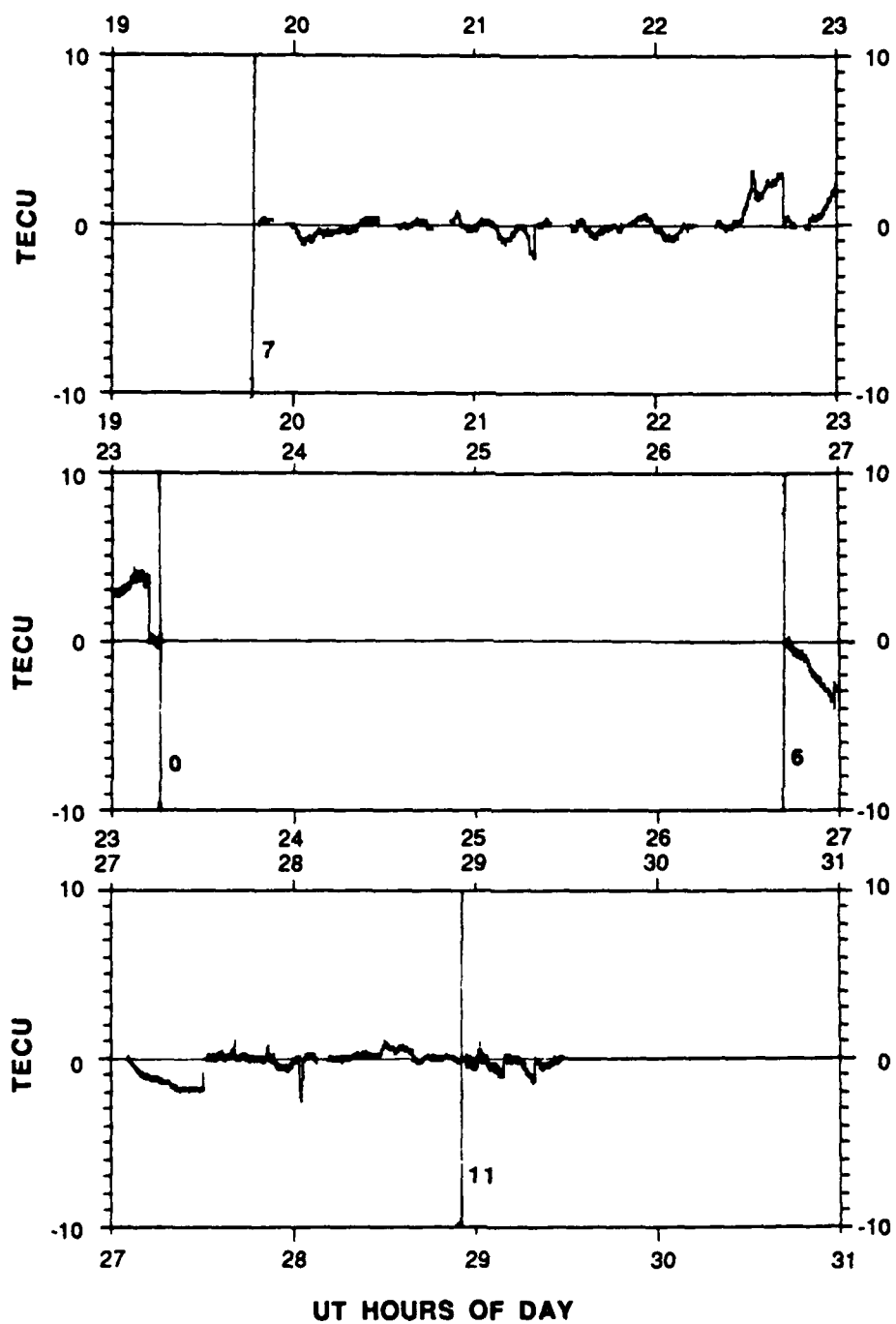


**FIGURE A9**  
**TRACKER 2**  
**RELATIVE TEC - CUMULATIVE versus TIME**

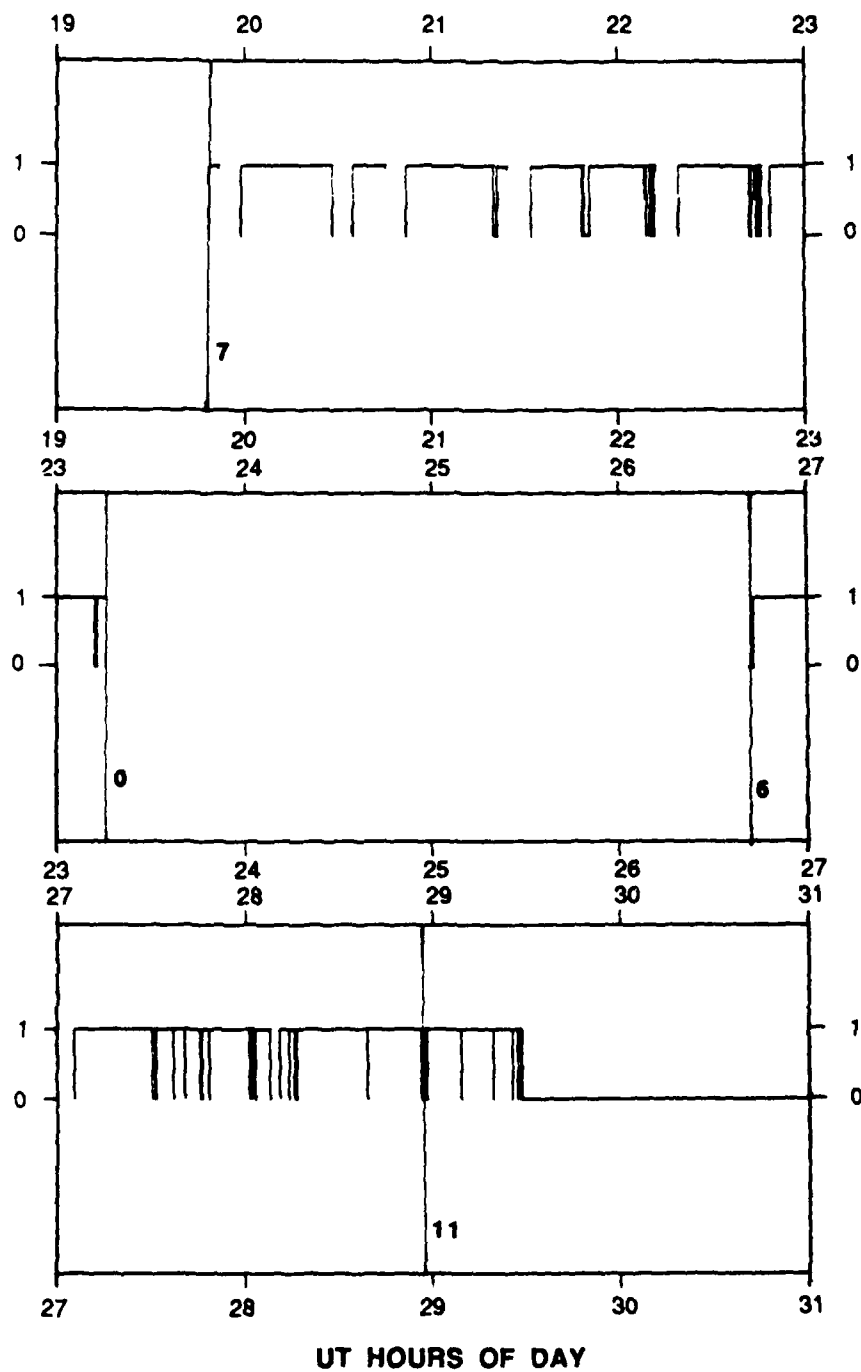


**FIGURE A10  
TRACKER 2  
PHASE REFERENCE RESET TIMES**



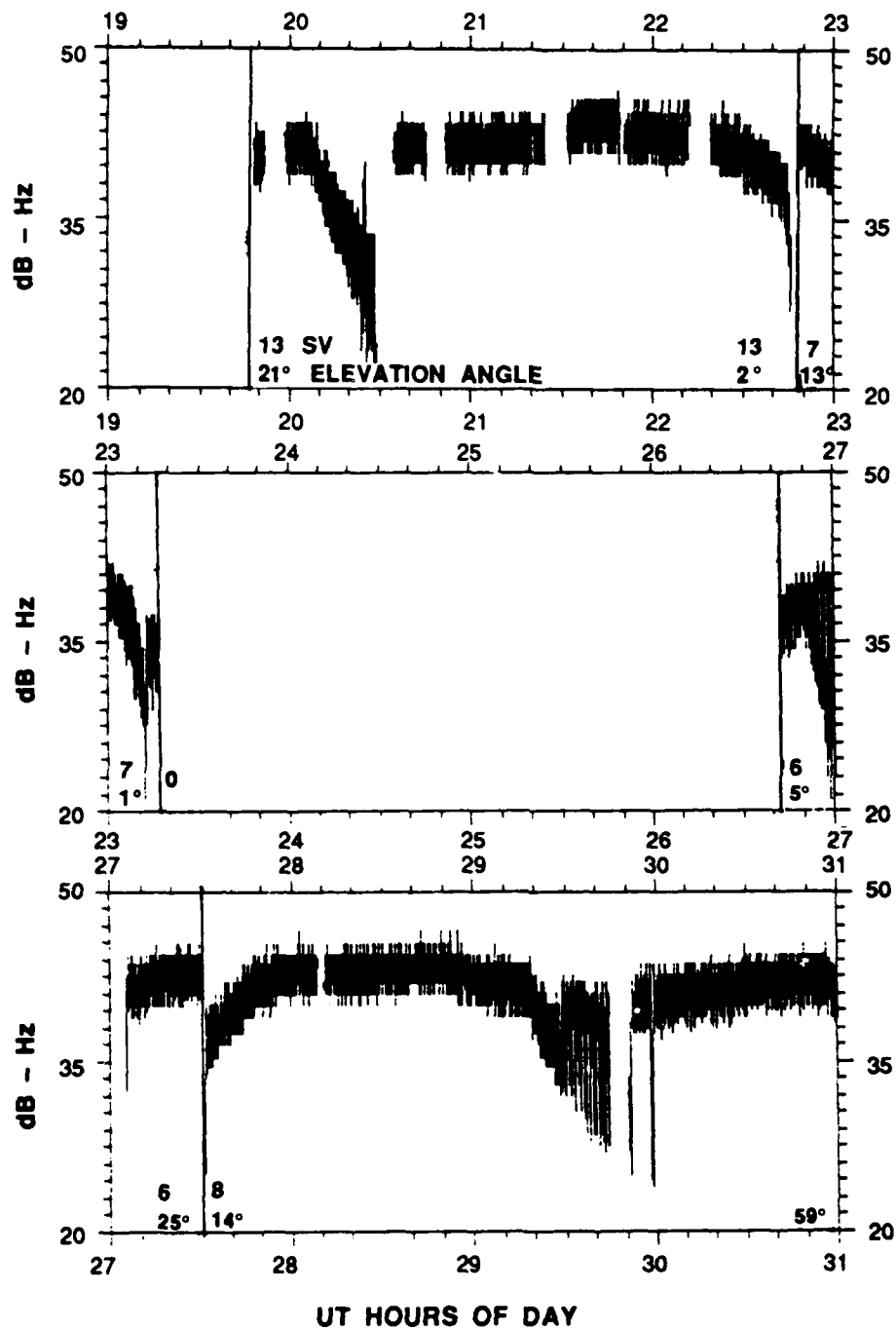


**FIGURE A11**  
**TRACKER 3**  
**L2 C/N0 versus TIME**

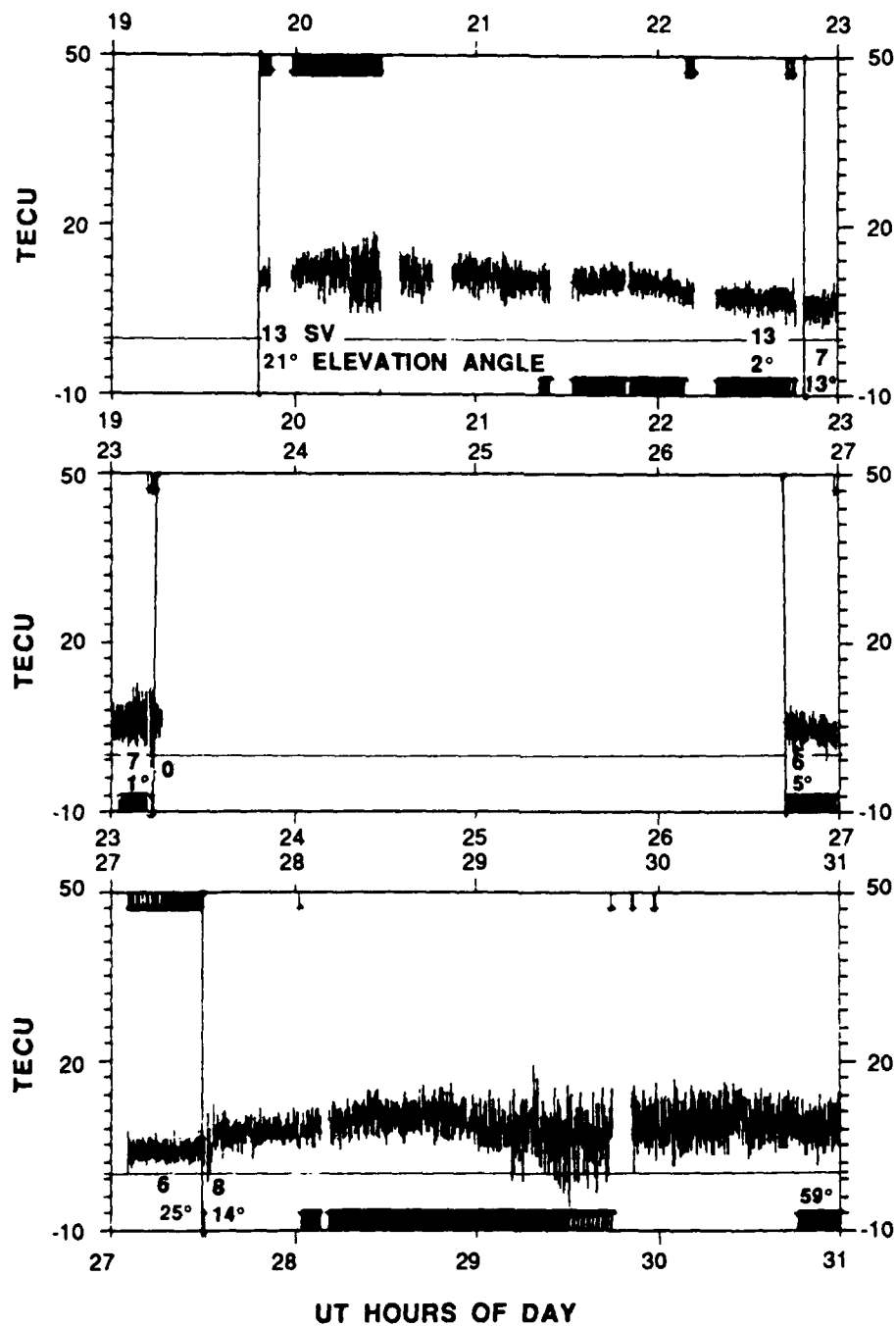


FIGURE A12  
TRACKER 3  
VERTICAL TEC versus TIME

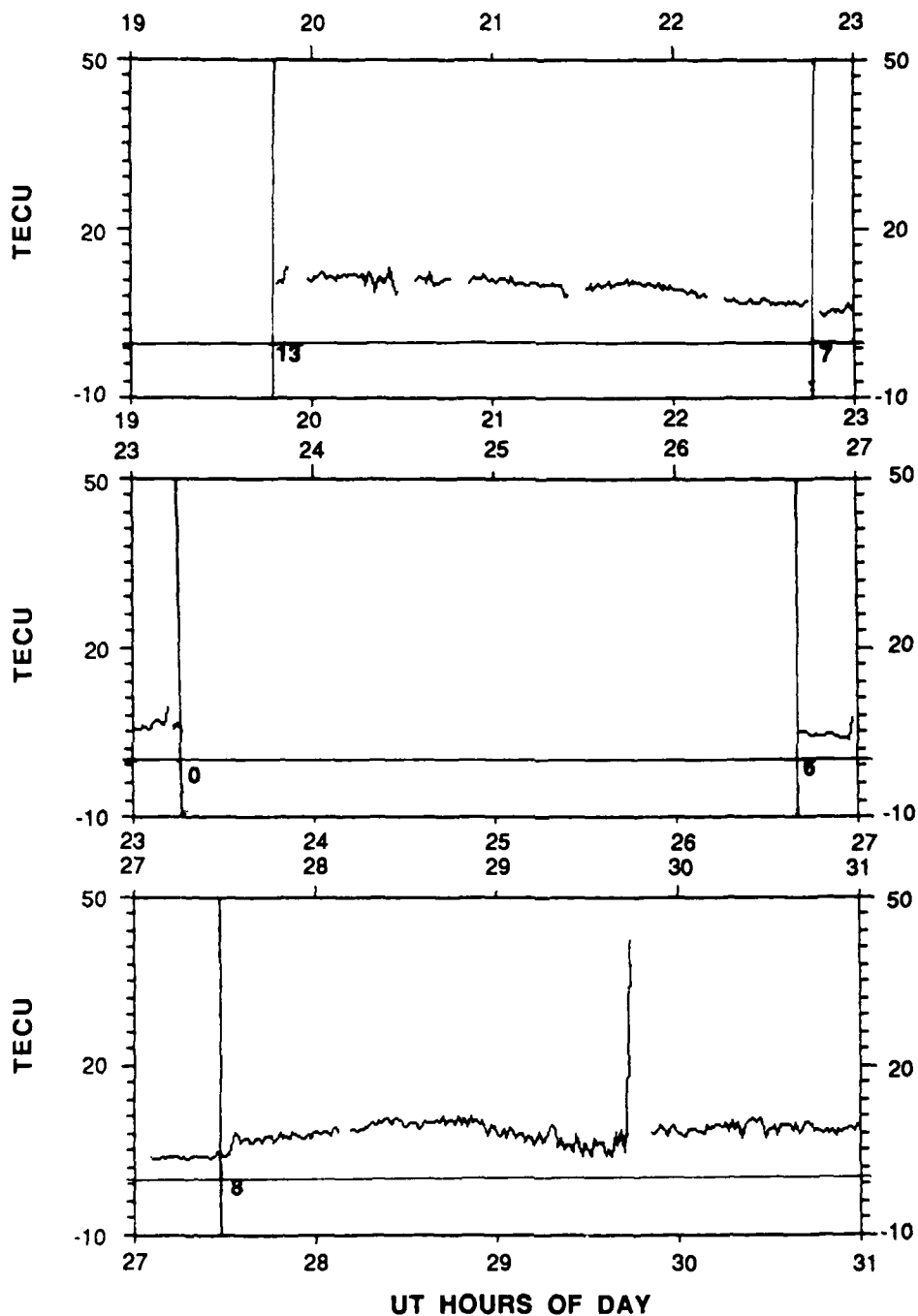
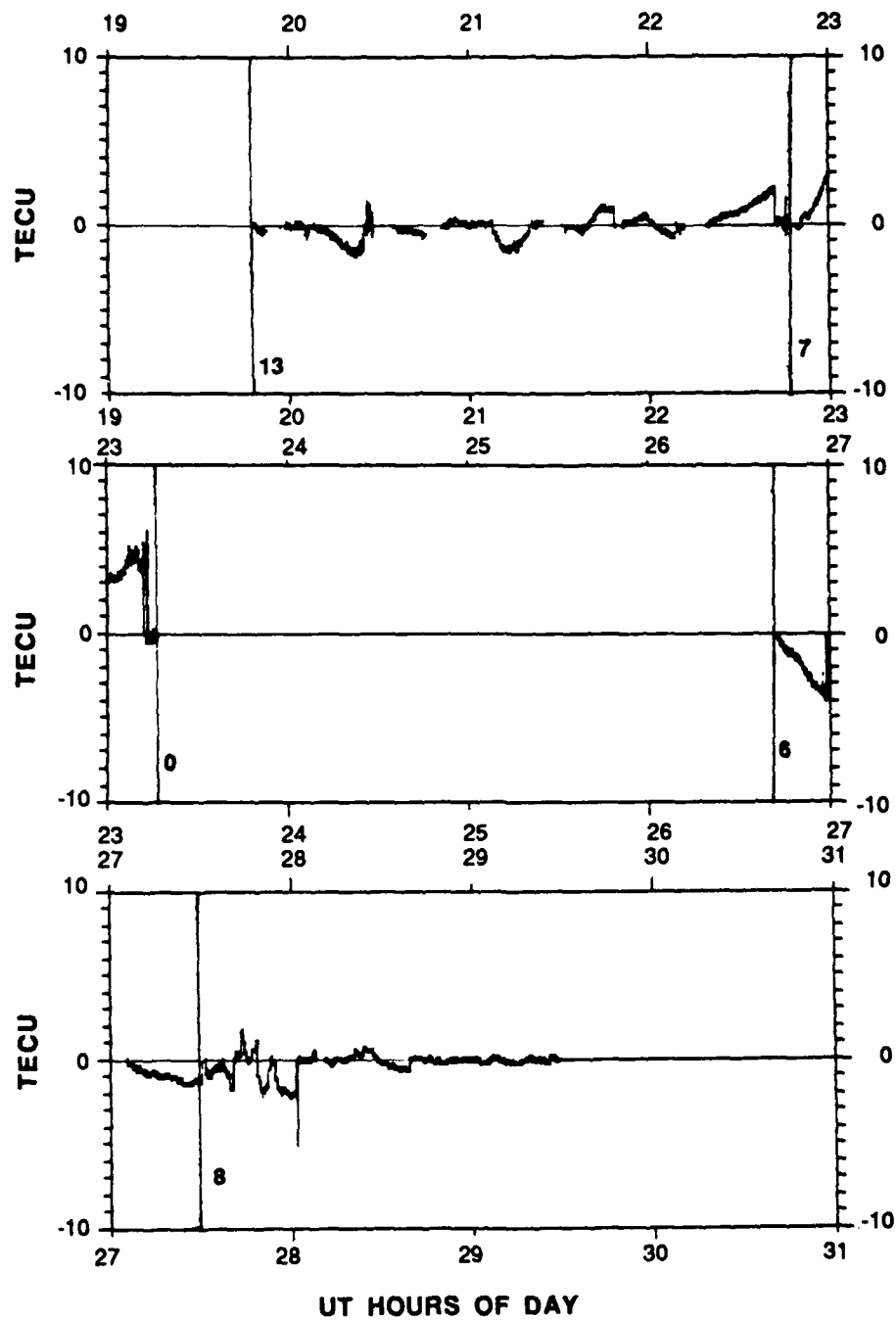
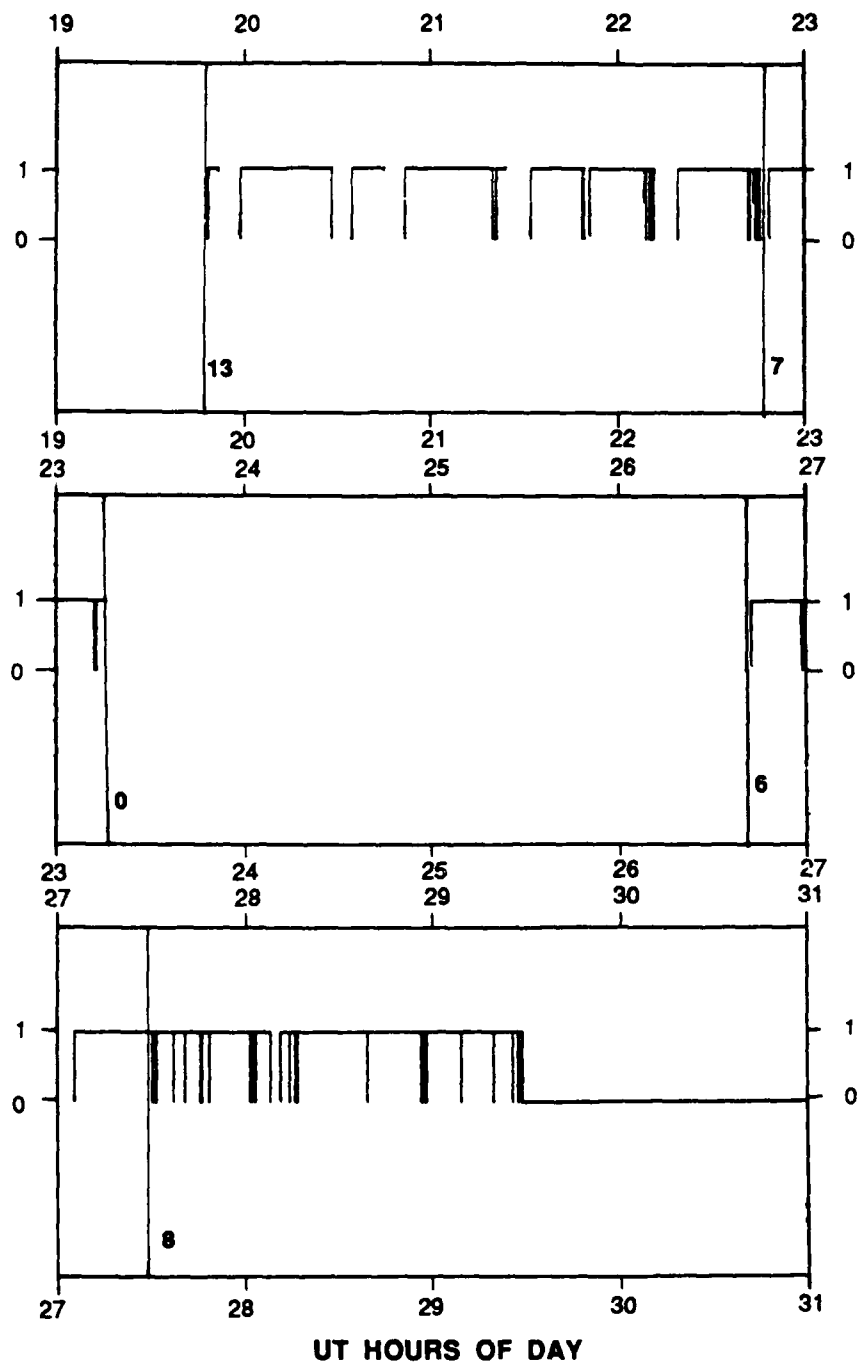


FIGURE A13  
TRACKER 3  
VERTICAL TEC versus TIME  
SMOOTHED DATA

ARL:UT  
AS-88-24  
CC - GA  
1-19-88



**FIGURE A14**  
**TRACKER 3**  
**RELATIVE TEC - CUMULATIVE versus TIME**



**FIGURE A15  
TRACKER 3  
PHASE REFERENCE RESET TIMES**

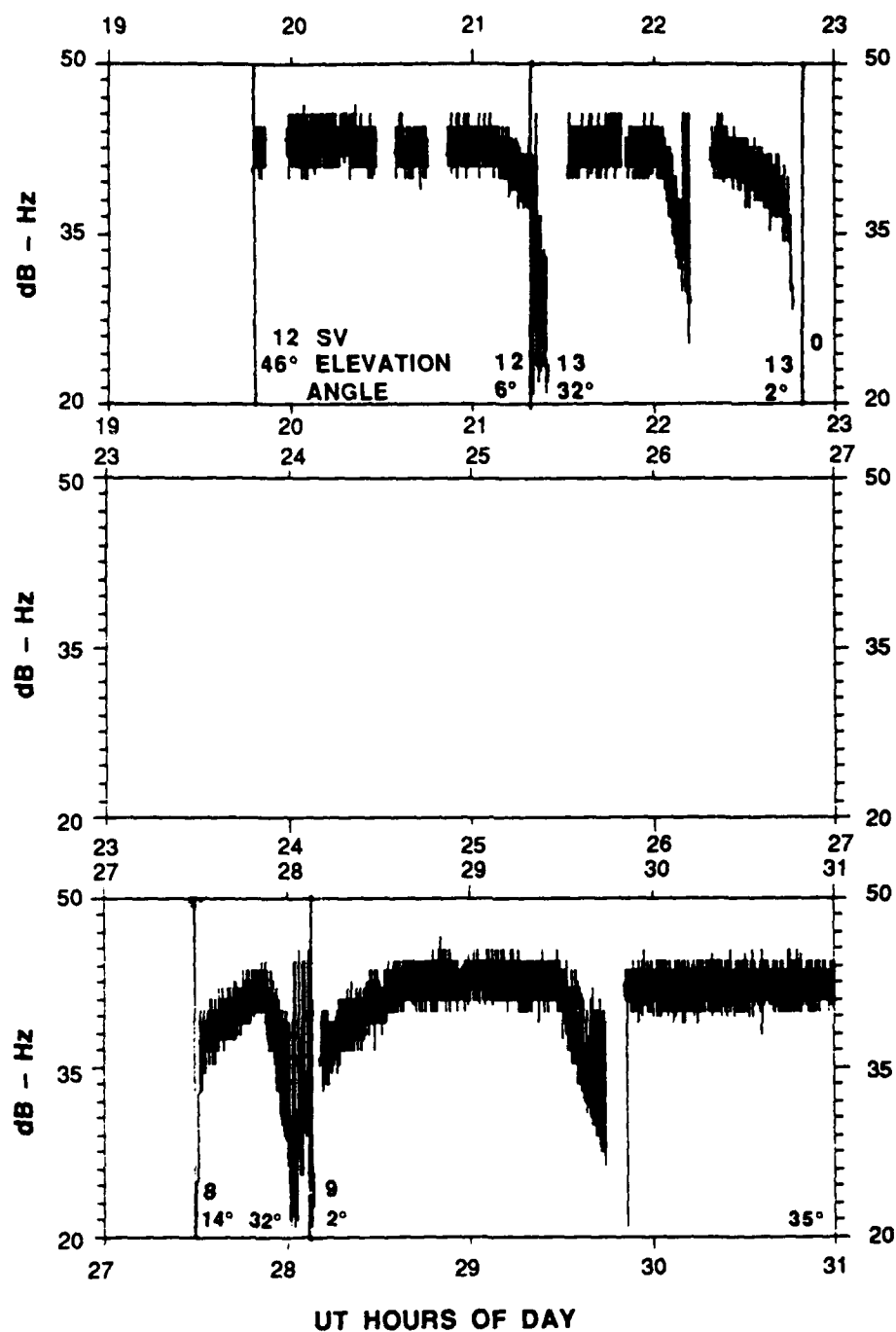


**FIGURE A16**  
**TRACKER 4**  
**L2 C/NO versus TIME**

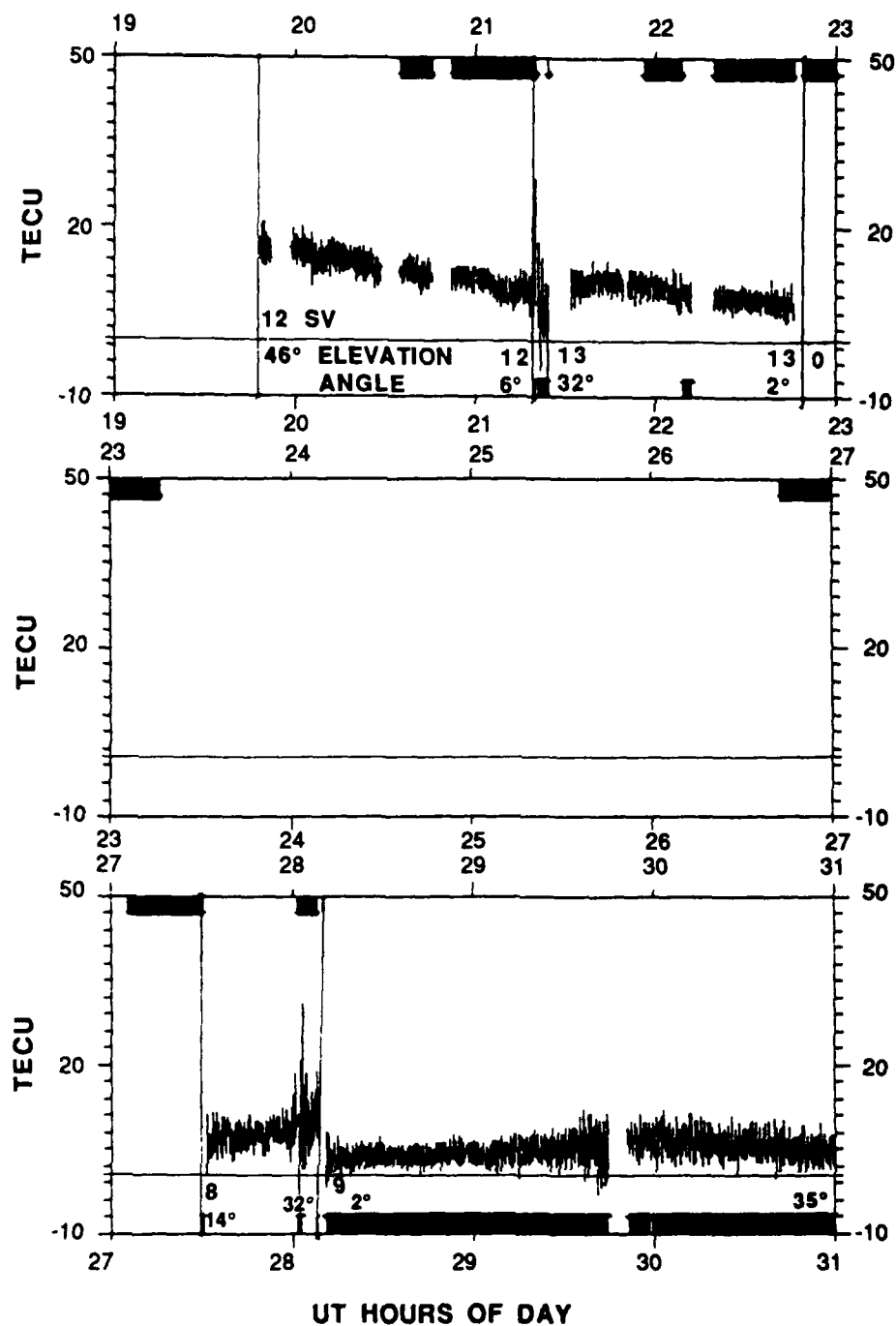


**FIGURE A17**  
**TRACKER 4**  
**VERTICAL TEC versus TIME**

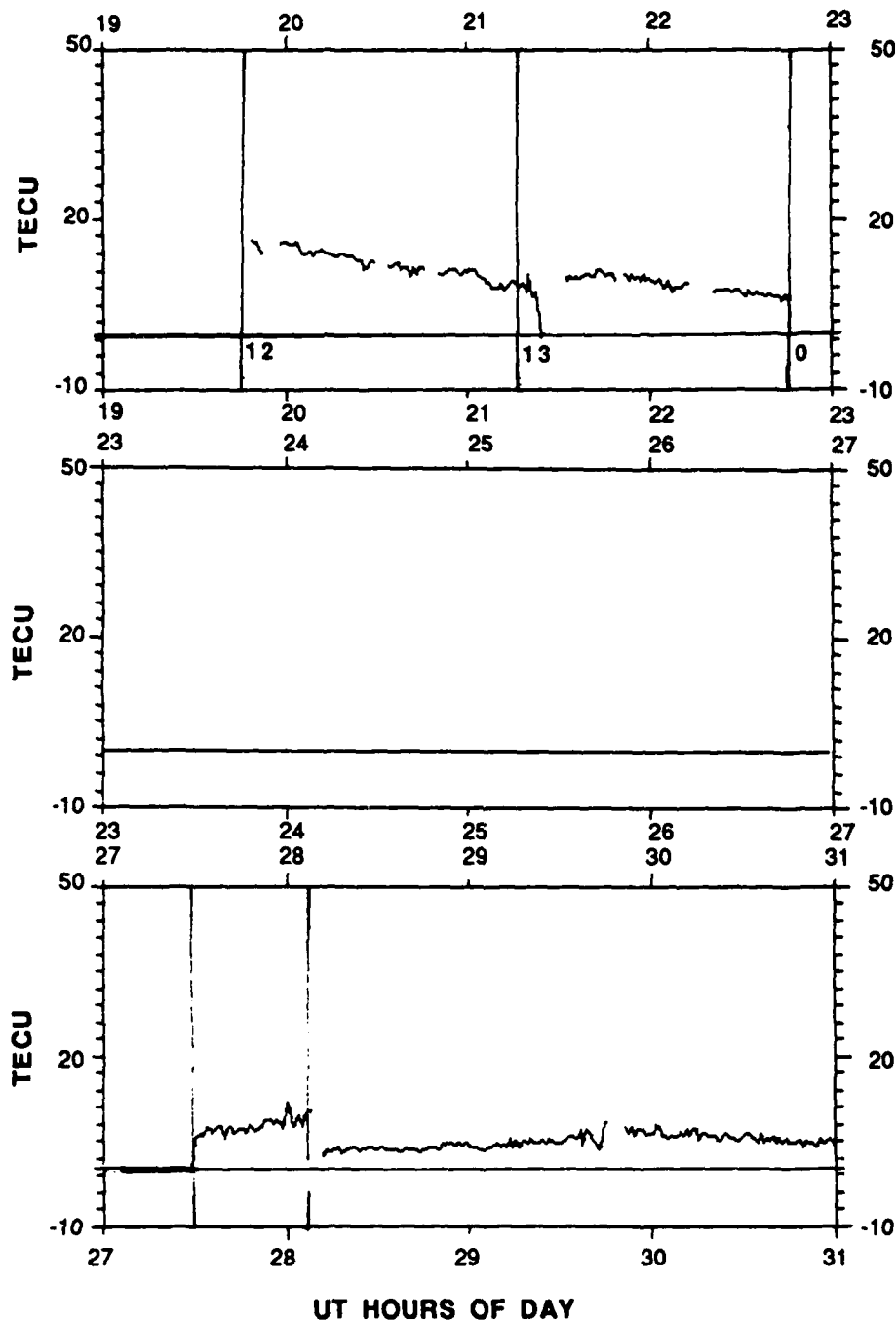


**FIGURE A18**  
**TRACKER 4**  
**VERTICAL TEC versus TIME**  
**SMOOTHED DATA**



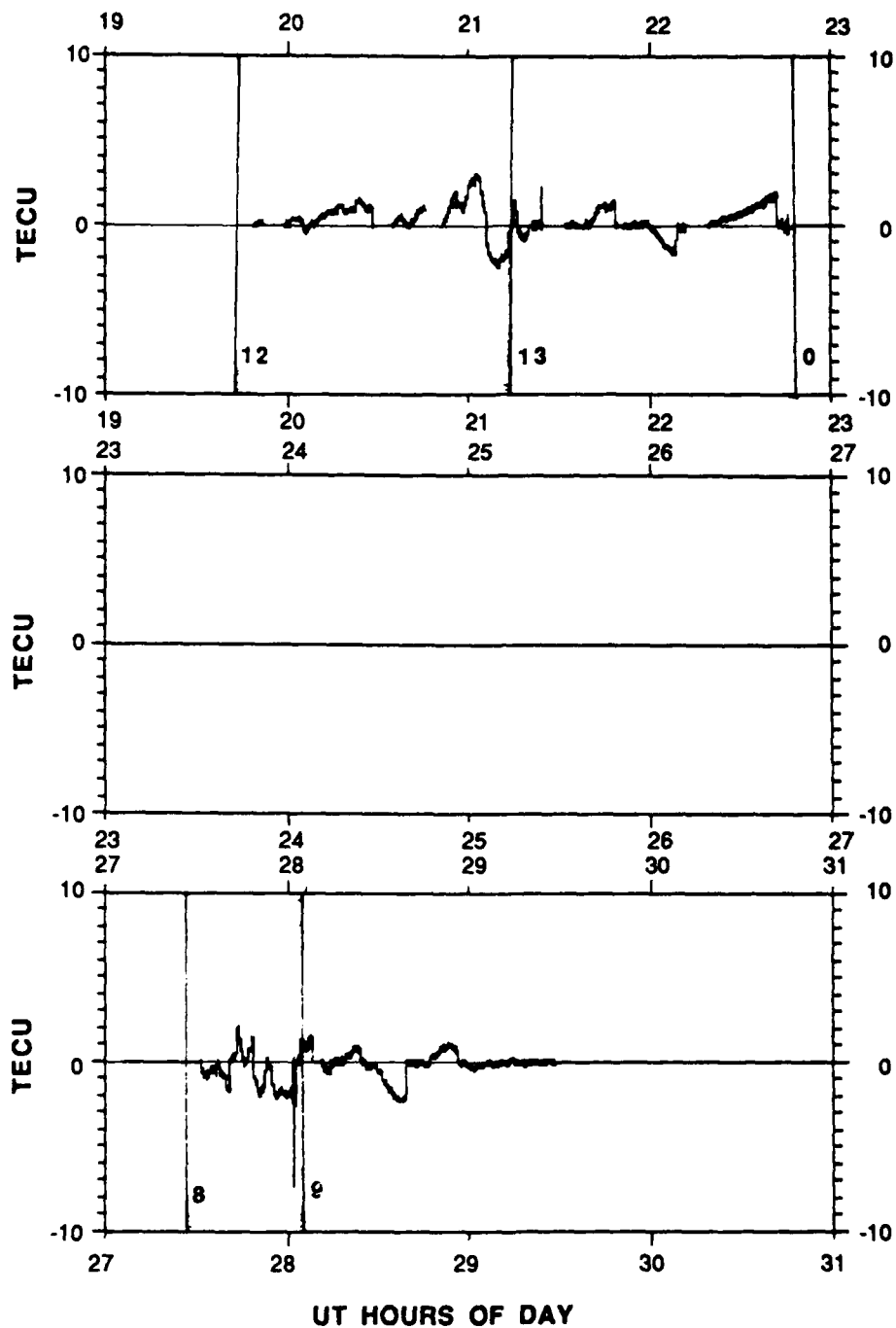


**FIGURE A19**  
**TRACKER 4**  
**RELATIVE TEC - CUMULATIVE versus TIME**

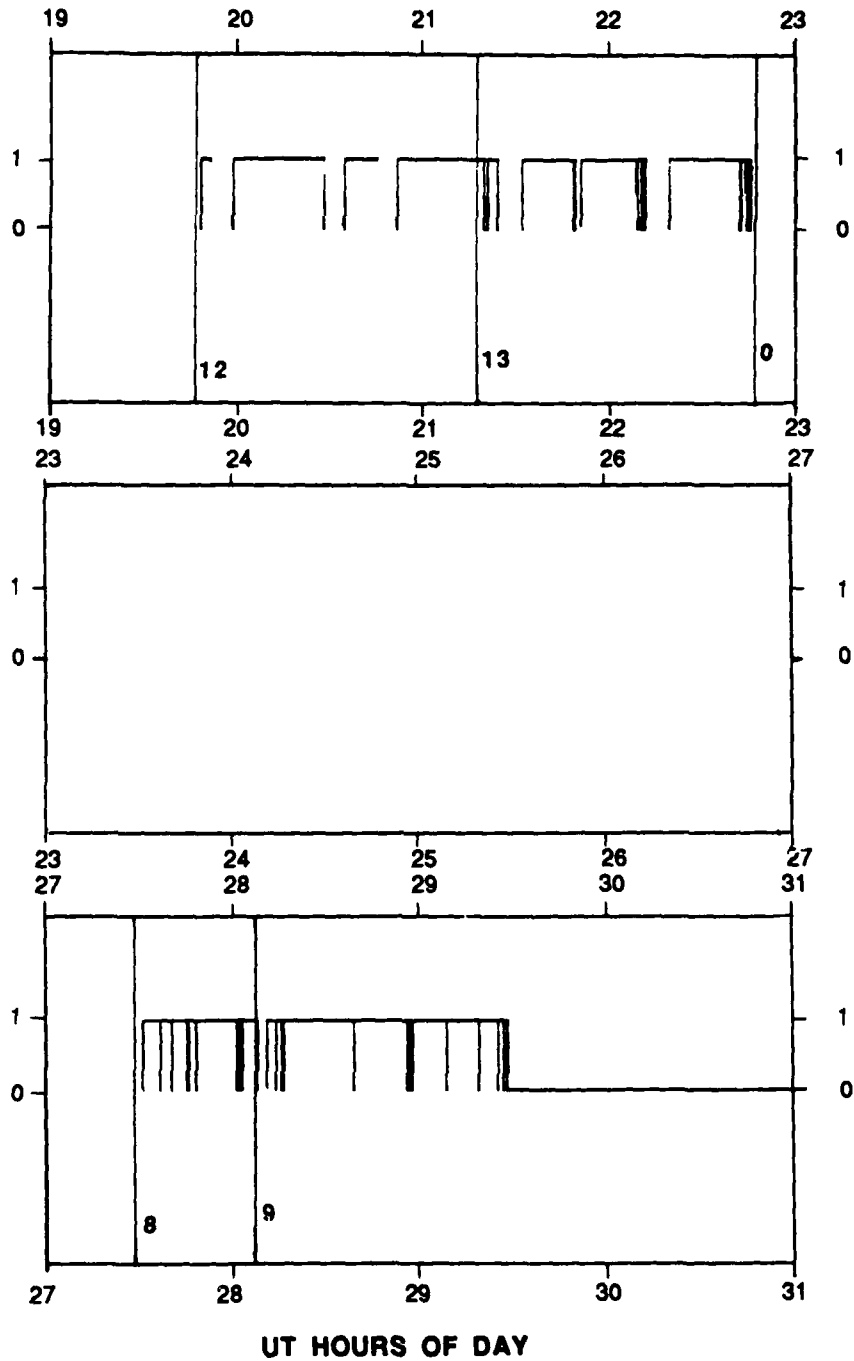


**FIGURE A20  
TRACKER 4  
PHASE REFERENCE RESET TIMES**

## REFERENCES

1. G. J. Bishop, J. A. Klobuchar, and P. H. Doherty, "Multipath Effects on the Determination of Absolute Ionospheric Time Delay from GPS Signals," *Radio Sci.* 20, 388-396 (1985).
2. G. J. Bishop, J. A. Klobuchar, D. J. Jacavano, Jr., and C. Coker, "Some Observations and Mitigation of Multipath Effects on GPS Differential Group Delay Measurements," presented at the Fall AGU Meeting, San Francisco, California 7-11 December 1987.
3. B. H. Briggs, and I. A. Parkin, "On the Variation of Radio Star and Satellite Scintillations with Zenith Angle," *J. Atmos. Terr. Phys.* 25, 339-366 (1963).
4. D. S. Coco and J. R. Clynch, "System Performance Tests for the TI 4100 Geodetic Receiver," Proceedings of the Fourth International Geodetic Symposium on Satellite Positioning, Applied Research Laboratories, The University of Texas at Austin, Austin, Texas 28 April - 2 May 1986.
5. E. J. Fremouw, R. L. Leadabrand, R. C. Livingston, M. D. Cousins, C. L. Rino, B. C. Fair, and R. A. Long, "Early Results from the DNA Wideband Satellite Experiment--Complex-Signal Scintillation," *Radio Sci.* 13, 167-187 (1978).
4. E. J. Weber, J. A. Klobuchar, J. Buchau, and H. C. Carlson, Jr., "Polar Cap F Layer Patches: Structure and Dynamics," *J. Geophys. Res.* 91(A11), 12,121 - 12,129 (1986).